ISAS - INTERNATIONAL SCHOOL
FOR ADVANCED STUDIES

# Mutation Analysis Of The Hepatitis C Virus Internal Ribosome Entry Site And Its Implication In Translation Initiation

Thesis submitted for the Degree of

*Doctor Philosophiae*

Candidate: Federico E. Odreman Macchioli

Supervisor: Prof. Francisco E. Baralle

Dr. Emanuele Buratti

Academic Year 2000/2001

SISSA - SCUOLA
TERNAZIONALE
SUPERIORE
STUDI AVANZATI
TRIESTE
Via Beirut 2-4

TRIESTE

*a Pamela Jabes*

## ACKNOWLEDGMENTS

The work described in this thesis was carried out at the International Centre for Genetic Engineering and Biotechnology (ICGEB), at the Molecular Pathology group, Trieste.

I am very grateful to Prof. Francisco Baralle for given me the opportunity to work in his group and for support me in these years.

A very special mention to Emanuele Buratti for follow me and for his friendship, work with him have been an honour .

I would like also to thank all member of the molecular pathology group: Gabriela Pittis, Rodolfo Garcia, C. Asencio, J. Flo, P. Arrisi-Mercado, M. Baralle, A. Brindisi, A.K. Chauhan, G.Danek, L. Del Turco, A. Iaconcig, C. Marchetti, R. Marcucci, M. Marro, A.F. Muro, F. Pagani, F. Porro, M. Romano, C. Stuani, M. Zotti, E.Zuccato and Sergio Tisminetzky.

Special thanks to all the ICGEB personnel for their co-operation and friendship during these years. It has been a pleasure to work daily with them.

Last but by no means least, I want to thanks to Ivan Galindo and Rafael Rangel-Aldao for support me.

TABLA OF CONTENTS

# CHAPTER 1

# INTRODUCTION

## 1.1 Hepatitis C virus, a general view

The hepatitis C virus (HCV) was first identified in 1989 (Choo et al., 1989) and is the major causative agent of parenterally transmitted and community-acquired non-A, non-B hepatitis. It infects hepatocytes and leads to chronic hepatitis and cirrhosis and is associated with the development of hepatocellular carcinoma (Saito et al., 1990). Over the past few years considerable progress has been made in the molecular characterization of this virus. Chronic infection with HCV has become a global health problem. HCV is frequently persistent and its spread in the population is still poorly understood (Simmonds, 2001). However, it is known to be principally transmitted by blood contact and has targeted risk groups such as injecting drug users, recipients of blood transfusion, and blood products. HCV infection sets in train an inexorable course of slowly progressive liver disease and part of the difficulty in understanding the epidemiology of HCV is the lack of symptoms associated with both initial infection and prolonged periods of chronic infection (Seeff et al., 2000).

The viral particle consists of an envelope (derived from the host membranes) into which are inserted the virally encoded glycoproteins (E1 and E2). This envelope surrounds a nucleocapsid and a positive-sense, single-stranded, RNA genome of approximately 9,500 nucleotides (Fig.1). HCV possesses a similar genomic organization to that of the pesti- and flaviviruses and has now been classified as a separate genus in

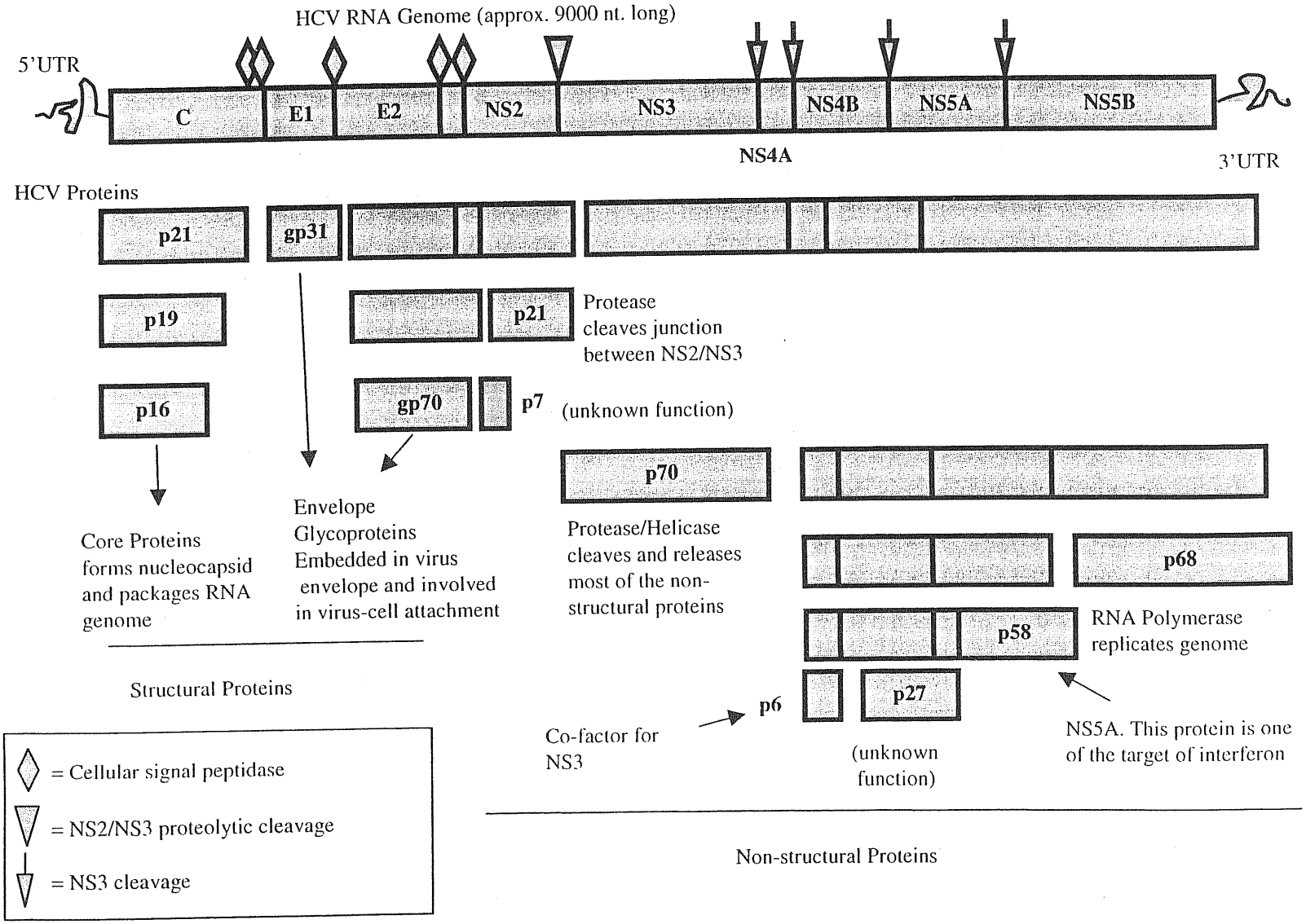


**Figure 1**. HCV genome. Proposed HCV genome showing regions coding for structural (core and envelope) proteins and nonstructural (helicase, protease, and RNA polymerase) proteins

the *Flaviviridae* family. A recent proposal for HCV nomenclature defined six major genotypes (numbered 1 to 6) based upon phylogenetic analyses of the 5'UTR, core, E1, and NS5 regions, and with further subdivisions into subtypes (1a, 1b, 2c, etc) (see section 1.10).

The viral genome contains two highly conserved untranslated regions (UTRs) at both the 5' and 3' termini which flank a large translational open reading frame encoding a polyprotein of ~3000 amino acids. Once translated, the polyprotein is processed by both cellular and viral proteases to yield the specific viral gene products (outlined in Fig.1). The structural proteins, core, E1 and E2, are located in the N-terminal quarter with the non-structural (NS) proteins (NS2, NS3, NS4A, NS4B, NS5A and NS5B) in the remaining portion of the polyprotein. Despite the lack of an efficient tissue culture system that could allow the analysis of viral replication (and gene function) a great deal of data have been accumulated through the use of expression systems. These studies have lead to the identification of functional regions and important interactions between viral products (see section 1.2).

At the 5' end of the virus there is an untranslated region (UTR) of about 341 nucleotides. This 5'UTR and the initial core region fold upon themselves to form several characteristic stem-loop domains (I, II, III, and IV), held together by a helical structure and a pseudoknot which are highly conserved in all virus isolates (Brown et al., 1992; Honda et al., 1996b). This is a fundamental region for the HCV life cycle because this region regulates HCV translation.

At the end of the carboxy-terminal region of the HCV ORF there is a short 3'UTR (Han et al., 1991) consisting of approximately of 50 nucleotides followed by a poly (U) tract, which in some isolates is replaced by a poly (A) tract (Han et al., 1991; Ito et al.,

1998). Recently, it has been discovered that these polynucleotide tracts do not represent the end of the HCV genome and that they are all followed by a highly conserved terminal sequence of approximately 100 nucleotides (Tanaka et al., 1996), which is believed to possess a complex and conserved secondary structure involved in protein binding (see section 1.9).

Very little is known concerning HCV-RNA replication but the similar genetic organization shared by HCV with flaviviruses and pestiviruses makes it likely that it includes the synthesis of negative stranded intermediates which in turn drive synthesis of new positive RNA genome (Fong et al., 1991; Bartenschlager R. and Lohmann V, 2000).

The structural region of HCV is shorter than that of flaviviruses and pestiviruses, and is organized in a similar fashion to pestiviruses: a basic N-terminal (p20) nucleocapsid Core protein (C) followed by two glycoproteins gp31 and gp70. The gp31 protein (E1) probably corresponds to a matrix/envelope glycoprotein in the virion whereas gp70 (E2) probably represents a second envelope glycoprotein (Selby et al., 1994). Both proteins are released from the precursor polyprotein by cellular proteases associated with the membranes of the endoplasmic reticulum (Hijikata et al., 1991). Although their exact function is unknown the fact that these two proteins are involved in the formation of complex protein-protein associations suggest a connection with the control of virus replication (Dubuisson et al., 1994; Lanford et al., 1993). Finally, E1 and E2 are important in terms of antigen variation studies, E2 being the most variable region of the HCV genome (Kato et al., 1992; Weiner et al., 1991). These variations are assumed to be caused by random mutations, raising the possibility that the selection of such mutants allows the virus to escape the neutralizing antibody response in the host.

Similarly to what has been observed for the structural proteins the non-structural proteins are released from the precursor by successive proteolytic cleavages. The exact number of these non structural proteins is unknown but by comparison with the organization of flaviviruses they have been divided in NS2, NS3, NS4(A/B), and NS5(A/B). The information currently available on the processing of the HCV encoded polyprotein suggests that it takes place in a fashion more closely resembling that of the pestiviruses than the flaviviruses. Specifically, the HCV NS5 protein domain is cleaved into two species as is the case of the pestiviruses (but not the flaviviruses) and also the processing of the NS4 and NS5 species is not dependent on the HCV NS2B protein. Together with the great primary sequence identity between HCV and pestiviruses (Choo et al., 1991) these data seem to indicate a closer evolutionary relationship between HCV and pestiviruses than between HCV and flaviviruses.

HCV is know to cause chronic hepatitis in 50% of cases and sensitive polymerase chain reaction (PCR) assays indicate that the virus persists in the vast majority of infected individuals (Alter, 1992). Conceivably, the extraordinary ability of HCV to cause persistent infections could be due to the lack of an immune response to this virus. However, experimental data indicate that nearly all HCV patients with chronic hepatitis have detectable levels of circulating antibodies to the envelope glycoprotein (Chien et al., 1993). In addition, patients with HCV infection have been shown to possess a wide $CD4^+$-T cells response to a variety of different HCV proteins (Botarelli et al., 1993). Furthermore, cytotoxic lymphocytes ($CD8^+$) specific for HCV have been isolated from the livers of many patients and chimpanzees with chronic HCV infection and it is now clear that there are many different HCV epitopes recognized by cytotoxic lymphocytes. Thus, these data suggest that HCV persists in the infected host despite the presence of a

significant humoral and cell-mediated immune response. However, there are a number of potential ways in which HCV could persist. Firstly, there is growing evidence that a hypervariable region at the N-terminus of the putative envelope glycoprotein E2 is under immune selection. Epitopes for potentially neutralising antibodies have been located to this region and the emergence of variants within the infected individuals has been well documented and the rapid creation of HCV variants that now escape such antibodies may well be an important factor in the persistence character of HCV (Kato et al., 1993; Taniguchi et al., 1993; Weiner et al., 1992). In addition, there is also growing evidence that HCV can replicate in peripheral lymphocytes (Zignego et al., 1992). If substantiated by further work, such a site of HCV replication could provide a reservoir of virus for continual reinfection of the liver. This also raises the interesting question of hepatitis C virus with different cellular tropisms which could be an important factor in both the natural history of HCV infection as well as the sensitivity to therapeutics such as interferon and ribavidin.

The next section will provide a brief overview of the HCV viral proteins and the role they play in the viral life cycle.

## 1.2 The viral proteins

As previously mentioned, the HCV proteins are generated from the polyprotein following co- and post-translational cleavage by cellular and viral proteases. Figure 1 reports the order and nomenclature of these products in the polyprotein and the sequence of their cleavage. Cellular signal peptidases, localized in the lumen of the endoplasmic reticulum (ER), catalyse the cleavage of the structural region (Grakoui et al., 1993b; Hijikata et al., 1991; Lin et al., 1994). The structural proteins are characterized by the presence of a hydrophobic domain at the C terminal which is important for membrane association and subsequent cleavage by the signal peptidases. Cleavage at the junction between NS2 and NS3 occurs autoproteolytically via an HCV protease encoded by NS2 and the N-terminal protein of NS3 (Grakoui et al., 1993b; Hijikata et al., 1993), while the cleavages of the other downstream NS proteins are mediated by a distinct, virally encoded serine protease located in the N-terminal third of NS3 (Hijikata et al., 1993; Tomei et al., 1993).

### 1.2.1 The core region

The first 191 amino acids of the HCV polyprotein were designated the putative nucleocapsid or core protein (p21) (Grakoui et al., 1993b; Hijikata et al., 1991). The core protein is highly conserved and immunogenic (Santolini et al., 1994). It is a highly basic protein with a hydrophobic region at the C-terminus which acts as a signal for translocation of E1 to the ER and is essential for membrane-dependent processing of the core protein itself. A core protein of 21 kDa (p21) has been identified in expression studies performed both *in vivo* and *in vitro*. In addition, a 19 kDa (p19) product was identified *in vitro* (Santolini et al., 1994) representing a C-terminally truncated form of

p21resulting in a protein associated with but not integrated into ER membrane (Santolini et al., 1994).

### 1.2.2. The envelope region

The glycoproteins E1 (gp31) and E2 (gp70) represent the putative viral envelope proteins and are N-glycosylated at 5, 6 or 11 sites, respectively (Miyamura and Matsuura, 1993). The sequence of cleavage events from the viral polyprotein is such that two possible precursors for E2 are produced: E2-NS2 and E2-p7 (Dubuisson et al., 1994; Mizushima et al., 1994; Selby et al., 1994). A hydrophobic sequence just upstream from the N-terminus of p7 probably directs translocation into the ER, allowing cleavage at the p7 site. However, this cleavage is inefficient, leading to the presence of two forms of E2: E2 and E2-p7 (Mizushima et al., 1994) differing only in their hydrophobic C-termini which may be important for membrane anchoring. This is supported by the observation that deletion of this region in E2 leads to the production of a secreted, soluble form, of the protein (Selby et al., 1994; Spaete et al., 1992). Neither the function of p7 nor the role of the E2-p7 protein in viral particle formation are known.

### 1.2.3 The NS2/NS3 region

The NS2 protein forms part of an HCV encoded protease which overlaps with the NS3 serine protease domain. The NS2-3 protease is believed to mediate autoproteolytic cleavage at the NS2/NS3 site (Grakoui et al., 1993a; Hijikata et al., 1993). It requires zinc and can function in *trans*, although inefficiently. (Grakoui et al., 1993a; Reed et al., 1995). The mechanism of cleavage at this site is poorly understood. The region required for processing at the NS2/NS3 site in mammalian cells has been shown

to lie between residues 827-1207 of the polyprotein. Santolini et al, (Santolini et al., 1994) provided evidence suggesting that NS2 is a transmembrane protein. However, these experiments were performed using constructs lacking the structural region sequences which may influence the membrane localization of NS2 (given that the NS2/NS3 cleavage is one of the earliest events in the polyprotein processing). (Tanji et al., 1994). The NS3 region was predicted to include serine protease, nucleotide triphosphatase (NTPase), and RNA helicase activities. These functions have now been confirmed by *in vitro* and *in vivo* analyses (Zemel et al., 2001). The serine protease activity has been particularly well characterized and probably plays an essential role in HCV processing. In fact, a flavivirus homologue has been previously shown to be indispensable for viral growth (Chambers et al., 1990). Therefore, the HCV serine protease presents an important target for antiviral therapy. The activity resides in the N-terminal third of the NS3 protein and functions independently in two sets of processing events. First, there is the cleavage of the NS2/3 site in conjunction with NS2 (Hijikata et al., 1993). This activity spans the two proteins and is located between aa 827-1207 of the polyprotein (Grakoui et al., 1993b) (see The NS2 Region). Second, the release of the remaining downstream NS proteins, mediating cleavage at the 3/4A, 4A/4B, 4B/5A, and 5A/5B sites. Each of the NS3-dependent cleavage sites contains certain residues that are conserved both between sites and genotypes, suggesting an importance for substrate specificity .(Komoda et al., 1994)

### 1.2.4 The NS4 region

The NS4 region encodes two viral proteins, designated NS4A and NS4B. The function of NS4B is unknown, while NS4A has been shown to act as a cofactor in NS3 protease activity. NS4 is 54 amino acids in length and has a hydrophobic N-terminal region followed by a hydrophobic C-terminus (Failla et al., 1994). This protein enhances cleavage *in cis* and *in trans* at the NS3/4A, NS4A/4B, NS4B/5A, and NS5A/5B sites, which are mediated by the NS3 serine protease (Failla et al., 1994).

### 1.2.5. The NS5 region

This region is processed into NS5A and NS5B. The primary function of NS5A is unknown. However, from comparative studies with other viruses it is predicted to be important for RNA replication (Frangeul et al., 1998). Epidemiological studies indicate that it may play a role in conferring sensitivity to interferon (INF) (Enomoto et al., 1995; Enomoto et al., 1996). Amino acid sequence variability was identified in the C-terminus of NS5A that correlates with IFN sensitivity, while patients containing the wild type 1b sequence in this region responded poorly to therapy, suggesting that INF treatment actually could select for resistant viral strains (Enomoto et al., 1996).

## Concluding remarks

It should be noted that production of all these proteins is preceded by a single translational event that is principally regulated by the presence of an internal ribosome entry site (IRES) principally located in the HCV 5'UTR region. The function of an IRES is that of recruiting 40S ribosomal subunits directly to an internal AUG initiation codon as opposed to the "scanning" mechanism employed by eukaryotic mRNAs. Because the aim of this study is represented by the functional dissection of HCV translation the remaining part of the introduction will be dedicated at providing an up to date overview of this process.

## 1.3 The Hepatitis C Virus 5′ Untranslated Region (5′UTR)

The complete 5′UTR of all HCV isolates consists of approximately 341 nucleotides (Simmonds, 1995; Smith et al., 1995). Interestingly, this length is longer than the average length of flavivirus 5′UTRs which consist of approximately 100 nucleotides (Brinton and Dispoto, 1988; Heinz, 1992). Indeed, it resembles more closely the 5′UTR of pestiviruses such as bovine viral diarrhoea (BVDB), border disease virus (BDV) and classical swine fever virus (CSFV) in terms of length, sequence, and secondary structure (Brown et al., 1992; Han et al., 1991; Honda et al., 1999a; Honda et al., 1996a; Zhao and Wimmer, 2001). In fact, the BVDV, BDV and CSFV 5′UTRs are 385, 372 and 372 nucleotides long, respectively. In addition, they contain several AUG triplets upstream of the initiation codon just like the HCV 5′UTR. Although the HCV 5′UTR differs from the BVDV and CSFV in over 50% of the base positions many of these nucleotide differences are covariant substitutions, indicative of conserved secondary and/or tertiary structure. In fact, it is now clear that the HCV 5′UTR folds upon itself to form highly conserved RNA secondary/tertiary structures (Kieft et al., 1999). The latest proposed secondary structure is shown in Fig. 2: four principal RNA domains (I-IV) are indicated together with the initial AUG for translation of the polyprotein (in bold). The presence of several AUG triplets before the authentic initiator codon have led to comparisons between the 5′UTR of HCV and that of picornaviruses and raised the question as to whether this region can act as an internal ribosome entry site (IRES) (Pelletier and Sonenberg, 1988). Such a feature, well characterized in picornaviruses, leads to the translation of the RNA genome through a mechanism of internal initiation of an uncapped message, rather than ribosome scanning from the 5′ end of a capped molecule (Jackson et al., 1990). In fact, Tsukiyama-Kohara et al (1992) showed for the

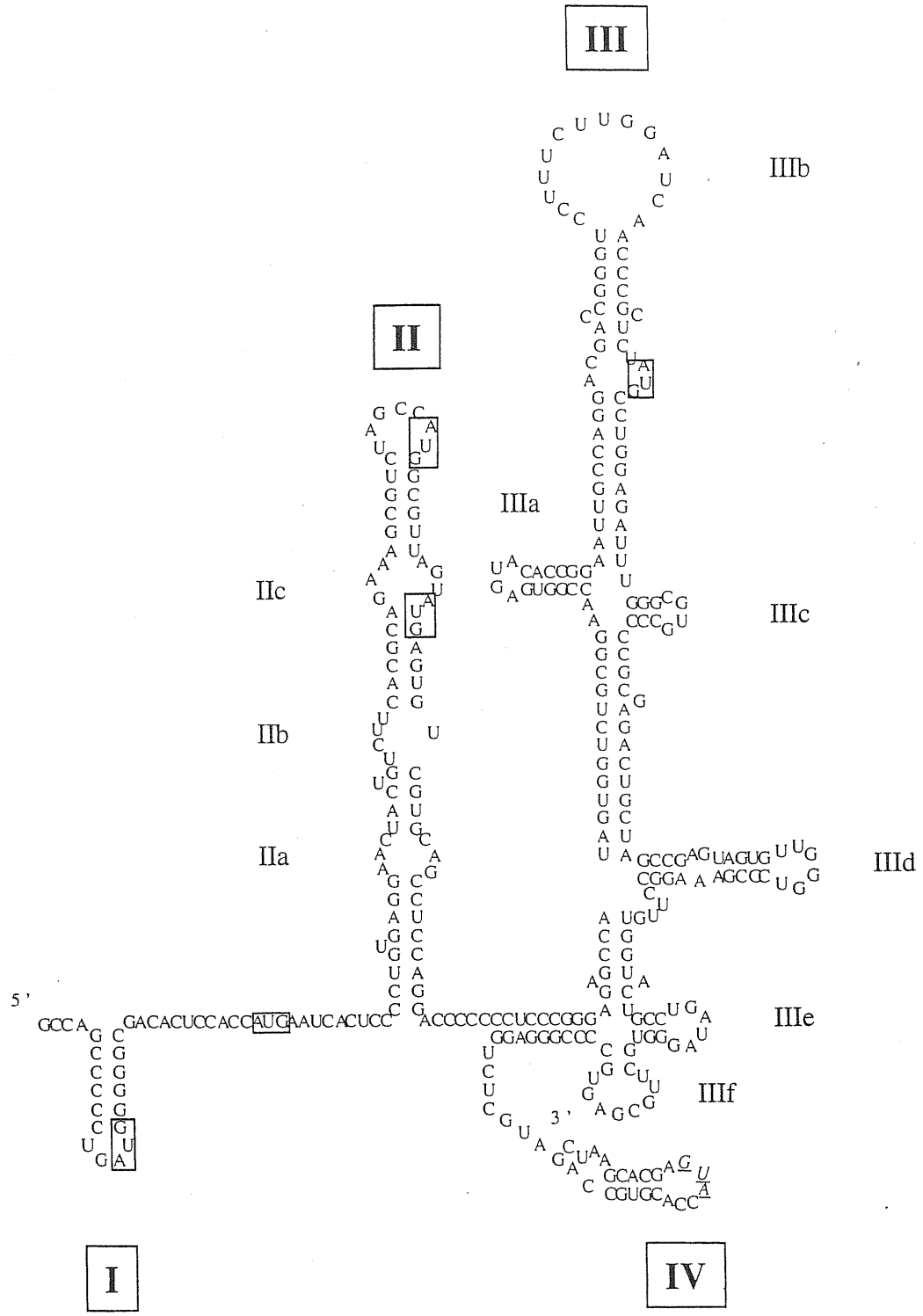


**Figure 2.** Sequence and predicted secodary structure of the HCV 5'UTR based on the model proposed by Honda et al, (1999a). Major predicted structural domains are labeled I to IV.Lightly shaded boxes represent AUG tripltes located within the 5'UTR, while underline AUG represent the polyprotein translation initiation site.

first time experimental evidence that this region could act as an IRES. More recent evidence has suggested that for IRES activity there exists unique requirement of HCV coding sequence from the core region, (Fukushi et al., 1994; Honda et al., 1996b; Reynolds et al., 1995). However, Tsukiyama-Kohara et al (1992) and Wang et al (1993) showed IRES activity using constructs containing reported genes placed immediately downstream of the HCV initiator AUG. To examine these discrepancies Honda et al (1996a) altered the stability of a proposed stem-loop IV in the HCV 5'UTR, which contains the initiator AUG and several nucleotides from the core region (Fig. 2). Translational activity was then measured for HCV core production and the results showed that mutations reducing the stability of this loop did not reduce translation. However, mutations stabilizing the stem-loop led to significant reduction in IRES activity, showing that is indeed part of the HCV IRES.

In conclusion, the minimal sequence required for IRES activity is believed to include nucleotides sequences spanning from nt 42 through 356 (Jubin et al., 2000; Kato et al., 1990; Tanaka et al., 1996). Within the minimal IRES sequence, three primary structural domains are known to participate (II, III, and IV) (Brown et al., 1992; Jubin et al., 2000; Kato et al., 1990) whilst stem-loop I had been shown not to be essential for IRES activity (Jubin et al., 2000; Wang et al., 1993; Yoo et al., 1992).

Each domains is also subdivided in subdomains: thus, domain II contains (Based on the last model from Honda et al, (1999a) three hairpins numbered IIa, IIb, and IIc and an apical loop IId. The biggest and most important domain III spanning from nucleotides 117 through 300 is subdivided in six subdomains numbered IIIa, IIIb, IIIc, IIId, IIIe and IIIf (Fukushi et al., 1994; Jubin et al., 2000; Pelletier and Sonenberg, 1988; Tanaka et al., 1996; Wang et al., 1993). In general, mutations altering double-stranded

helical regions can have deleterious effects on translation. However, when compensatory mutations are introduced to restore Watson-Crick base paring the translation efficiency can often be restored (Buratti et al., 1997). In contrast, mutational changes in loop regions appear to be more amenable and resulting mutant IRESs may retain activity (Buratti et al., 1998b; Hijikata et al., 1993; Jubin et al., 2000). Interestingly, several loop regions form a characteristic structure known as the "tetraloop", which often serves as a site for tertiary interactions, as recognition signal for RNA binding proteins, or as nucleation site for RNA folding (Psaridi et al., 1999). Tetraloops are formed by certain sequences, namely GNRA, UNCG, CUUG, which are found with a surprising frequency in large RNA molecules and are characterized by an exceptional high thermodynamic stability (Varani, 1995; Woese et al., 1990). These loops are very stable because of a striking base stacking and hydrogen bonding within the loop including an unusual base pair between the first and the last residues (Heus and Pardi, 1991). Interestingly, an interaction between the GNAR tetraloop and a receptor domain has been identified in the catalytic core of group I self-splicing introns and has been shown to be critical for the molecule's tertiary structure (Butcher et al., 1997; Heus and Pardi, 1991). Recently, a structural motif similar to the catalytic core structure of group I introns was identified at the 3' end of all viral IRES types (Le and Maizel, 1998; Le et al., 1996). This element includes the pseudoknot structure, two stems and in the case of flaviviral IRESs, an absolutely conserved tetraloop motif in the IIIe hairpin. In addition, a GNRA-type tetraloop has been identified at similar location (domain III) in all known picornavirus IRESs (Belsham and Sonenberg, 1996). Since invariant positions are often required for tertiary structure folding, this GNRA loop is considered to be a candidate

element for determining the tertiary structure of the 5'UTR of these RNAs (Psaridi et al., 1999).

## 1.4 Initiation of translation by internal ribosomal entry

Initiation of translation in most eukaryotic mRNAs is strongly dependent on the modified $m^7G$ 5′ terminal "CAP" and can be described in terms of the "scanning" model (Merrick, 1992). First, a 43S complex is formed by binding of eukaryotic initiation factor 3 (eIF3) and an [eIF2/GTP/Met-tRNA] complex to 40S ribosomal subunits. Next, eIF4F binds the capped 5′ end of the mRNA and together with eIF4A and eIF4B unwinds adjacent secondary structure to create a binding site for the 43S complex. Interactions between eIF4F and the cap, between eIF4F and eIF3, and between eIF3 and mRNA are thought to promote binding of the 43S complex near the 5′ terminal cap. The 43S complex then scans downstream from the 5′end of the mRNA and forms a stable 48S complex at the first AUG triplet that it encounters (which acts as the initiation codon). At this stage eIF5 stimulates GTP hydrolysis, initiation factors are released and the initiation tRNA is left in the P site of the 40S subunit. The 60S ribosomal subunit then joins the 40S subunits to form the 80S complex and protein synthesis can start. Although the first AUG is usually the starting site, it is also dependent on its local sequence context. In fact, (Kozak, 1989) has determined a consensus context for an initiation codon to be A/GXXAUGG (for detailed review consult (Hershey et al., 1996; Merrick, 1992) (Fig. 3).

Translation of mRNAs can also occur by internal initiation which involves direct ribosomal attachment to an AUG initiation codon in the RNA (Fig. 4). The RNA structures that are responsible for this process are called "IRES" for Internal Ribosome Entry Site. IRESs were first identified in picornaviruses, such as encephalomyocarditis virus (EMCV) and have subsequently been identified in various cellular and viral mRNAs (Jackson and Kaminski, 1995). However, internal initiation can also occur as a

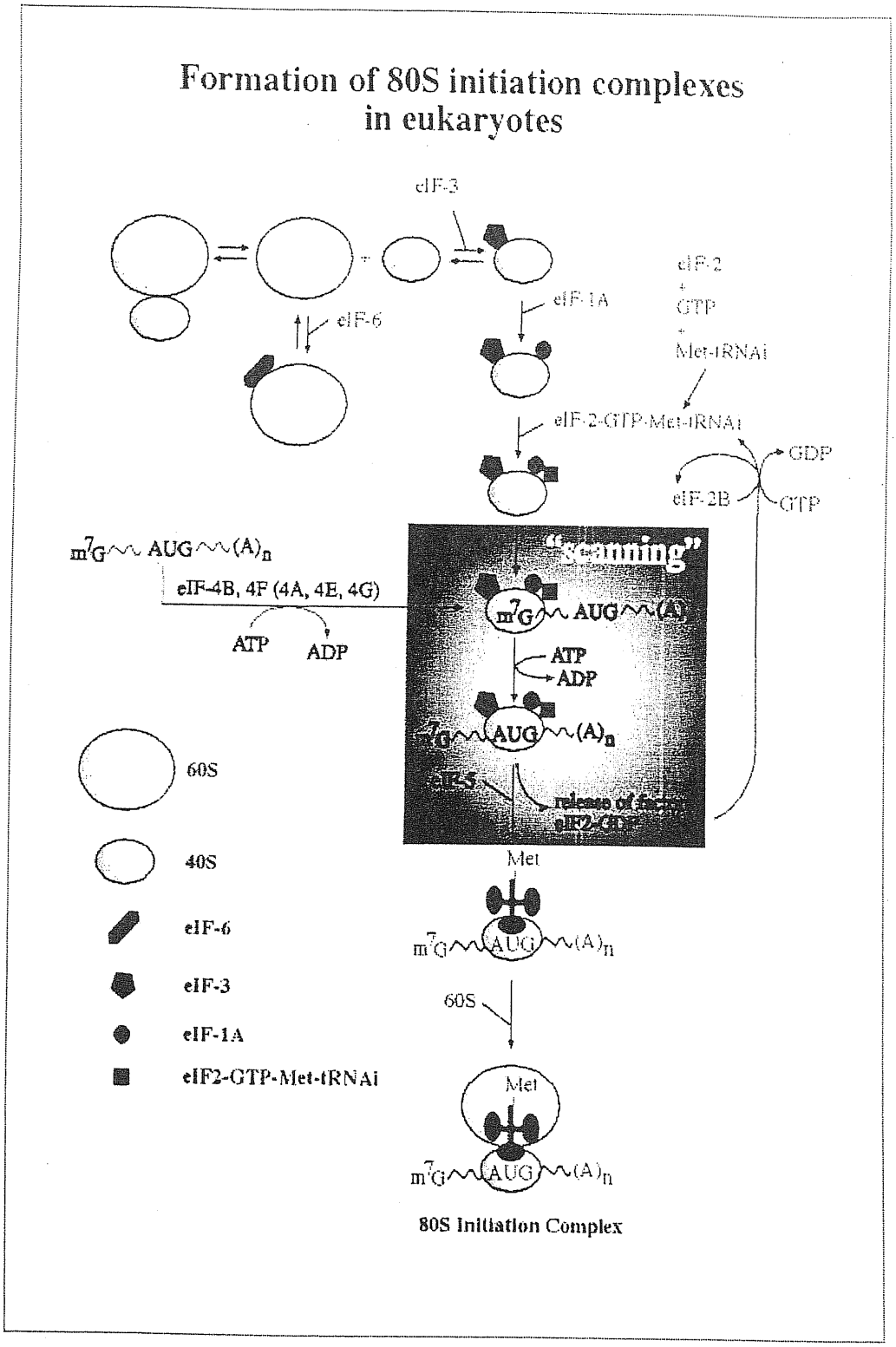


**Figure 3**. Schematic representation of the 80S complex formation and translation initiation in eukaryotes. This model is based on the study made by Kozak, 1989. In the dark box is hightlighted the process by which the 40S subunits, after have bound the "cap" structure, perform a scanning along the mRNA till the first AUG is reached. Then, the 60S ribosomal subunit joins the 40S subunit forming the 80S complex. After this event the tranlation elongation can start.

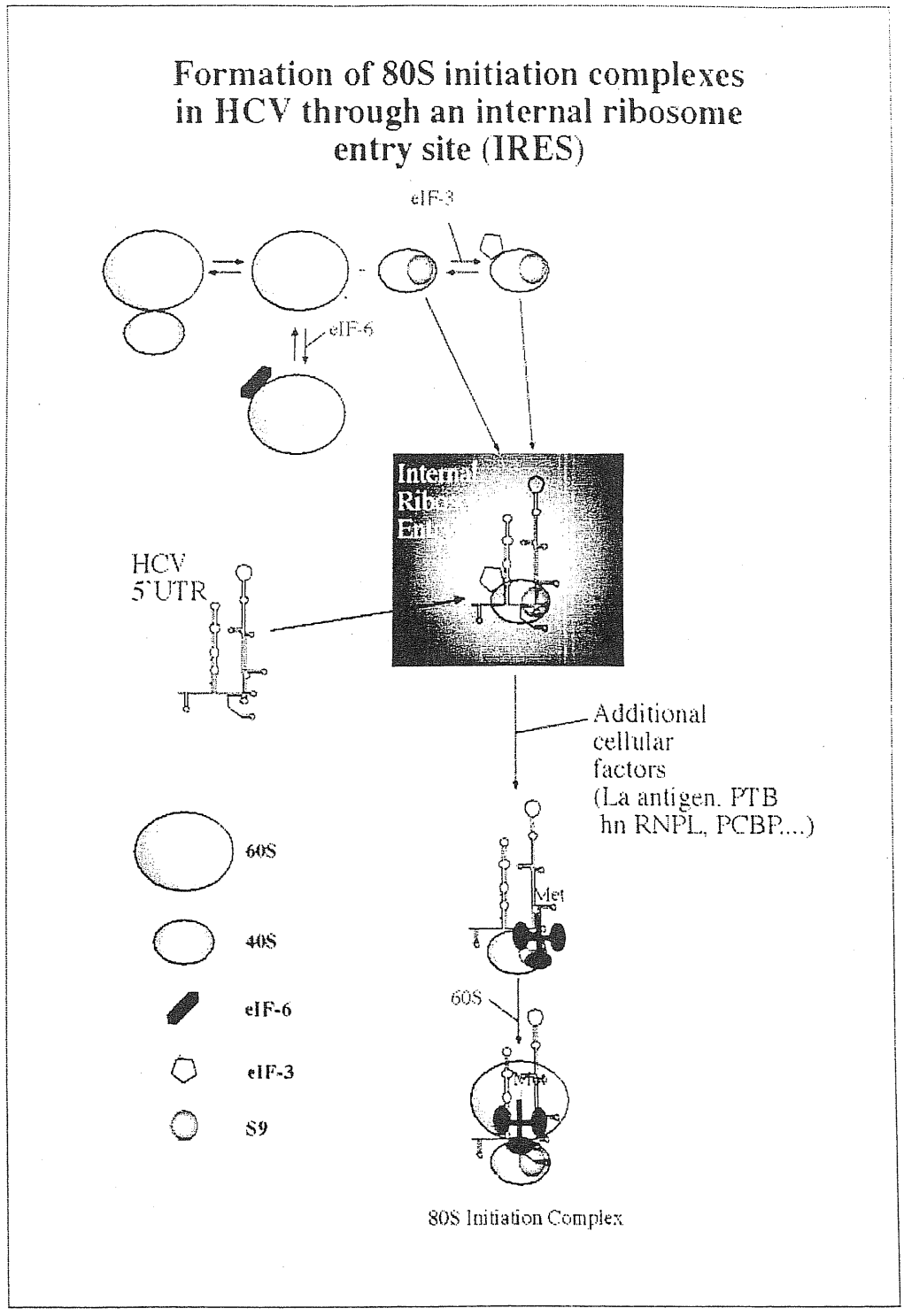


**Figure 4.** Schematic representation of the HCV IRES translation initiation. Unlike eukaryotes, the 40S ribosomal subunit is positioned upon the AUG start codon. This process is allowed because the complex secondary stracture of the IRES that act as a doking platform. The attachment of the 40S ribosomal subunit does not need the assistant of cellular factors.

result of leaky scanning or of reinitiation. The most decisive test to differentiate these two mechanisms of initiation is by the insertion of the putative IRES into the intercistronic spacer of a dicistronic construct. In order to rule out leaky scanning and reinitiation several conditions must be present. Firstly, insertion of a stable hairpin near the 5′ end of a mRNA must prevent translation of the upstream cistron without affecting translation of the downstream cistron. Second, although the size and structure of different IRES elements may vary considerably a common property is that their activity is often impaired by minor sequences changes, including deletion, insertion and substitution. These different assays have shown unambiguously that HCV, BVDB and CSFV 5′UTRs all contain IRES elements (Poole et al., 1995; Rijnbrand et al., 1996; Tsukiyama-Kohara et al., 1992; Wang et al., 1993).

## 1.5 Mapping the HCV IRES

The 3′ and 5′ boundaries of the HCV IRES have been mapped using bicistronic system mRNAs to assay the effects of progressive deletion on IRES activity. Deletion of domain I enhances HCV IRES-mediated initiation *in vitro* and *in vivo* (Honda et al., 1996a; Kamoshita et al., 1997; Rijnbrand et al., 1995; Wang et al., 1993). The physical basis for this effect is not known. IRES activity is strongly reduced by deletion that surround the basal helix of domain II which is therefore considered to be the 5′ boundary of the IRES even though residual activity can be detected after complete removal of this domain (Fukushi et al., 1994; Reynolds et al., 1996)

AUG triplets introduced as little as seven nucleotides upstream of the initiator codon or eight nucleotides downstream of an inactive initiation codon are not recognized by the translation apparatus (Reynolds et al., 1996; Rijnbrand et al., 1996). The 3′ boundary of the IRES must therefore be downstream of nucleotide 335. This conclusion is supported by the observation that truncation of the HCV 5′UTR to nucleotide 332 abrogates IRES activity (Wang et al., 1993). Insertion between the pseudoknot and the initiation codon also strongly reduce IRES activity (Yoo et al., 1992). These observations indicate that the ribosome is directed by the IRES to bind precisely in the vicinity of the initiation codon and is unable to scan downstream from this position. This model is strongly supported by the observation that substitution of the initiation codon $AUG_{342}$ by several different non-AUG triplets has little effect on initiation efficiency (Reynolds et al., 1995).

Most importantly, there is a strong bias against synonymous nucleotide substitution in the 5′ proximal core protein coding sequence (Ina et al., 1994) which may therefore function in more than just a protein-coding capacity. One possibility is that

the first 30 nucleotide of the HCV coding region are part of the IRES: direct replacement of the HCV ORF by some heterogeneous reporter genes strongly impaired IRES activity (Lu and Wimmer, 1996; Reynolds et al., 1995). However, not every heterologous reporter gene had this effect (Wang et al., 1993). The core protein coding sequence *per se* is therefore not essential for IRES activity but sequences placed downstream of the HCV initiation codon nevertheless influence internal ribosomal entry. Toeprinting analysis indicated that ribosomal complexes assembled on the HCV IRES interact with it slightly differently, depending on the nature of the reporter gene (Pestova et al., 1998b). The HCV IRES therefore comprises domain II, III and IV. Even small deletion within HCV and CSFV domain II and III substantially reduce or even abrogate IRES activity (Honda et al., 1996b; Pestova et al., 1998b).

## 1.6 Interaction of canonical initiation factors and HCV IRES

The components of the translation machinery required for translation initiation on HCV have been identified by reconstituting this process *in vitro.* (Pestova et al., 1998b) These studies have revealed several remarkable and unique aspects of the initiation process on this RNA.

First of all, 40S ribosomal subunits bind directly and specifically to the HCV IRES in the absence of initiation factors in such a way that the initiation codon is placed in the immediate vicinity of the ribosomal P site. Ribosomal attachment does not require any initiation factors, including those (eIFs 4A, 4B and 4F) that are required for ribosomal attachment to capped mRNAs (e.g. α-globin) or to the EMCV IRES (Pestova et al., 1996). In fact, HCV is unlike these mRNAs in that it is resistant to the inhibitory effects on translation of a *trans*-dominant mutant eIF4A (R362Q) (Pause et al., 1994; Pestova et al., 1998b). Thus, 43S complexes bind the HCV IRES directly to form 48S complexes in which the initiation codon and the anticodon of initiator tRNA are base paired. This 48S complex is competent to complete the remaining stage in initiation. Assembly of 48S complexes is enhanced by (but does not require) eIF3, so eIF2 is the only essential initiation factor up to this stage. However, in the final stage of initiation eIF3 is absolutely required for subsequent joining of the 60S subunit to the 48S complex to form 80S ribosomal complexes capable of polypeptide synthesis (Pestova et al., 1998b) (Fig 4).

Therefore the initiation process on the HCV IRES has very simple factor requirement although we will see that several cellular proteins, including the La autoantigen, PTB, hnRNP L, etc., can influence this process.

Direct ribosomal attachment to eukaryotic mRNAs without a requirement for initiation factors is unprecedented in eukaryotes but is a characteristic of the prokaryotic translational process. In fact, prokaryotic mRNAs bind the small (30S) ribosomal subunits as a result of base paring between the Shine-Delgarno (SD) sequence and complementary anti-SD sequences in the 16S rRNA (Shine and Dalgarno, 1974). The exact sequences in the HCV IRES that are recognized by the 40S ribosomal subunits have not yet been identified. However, nucleotides 1-39, 26-67, 172-227, 229-238 and 332-331 of the 5'UTR and all of the coding sequence can be deleted without preventing binary 40S subunit-IRES complex formation, so these sequences do not contain primary determinant of ribosomal binding.

In conclusion, HCV translation initiation appears to involve sequential IRES-40S subunit interactions: a primary binding step is followed by interaction(s) that promote entry and accurate orientation of the initiation codon and flanking sequences in the mRNA-binding-cleft. In contrast to the attachment of prokaryotic ribosomes to the linear S-D sequence, attachment of eukaryotic ribosomes to the HCV IRES is therefore likely to involve interactions with multiple discontinuous sites on this highly structured RNA. The strongly conserved loops in domains II and III are candidate ribosomal-binding sites (see results section).

Recently, Spahn et al (2001) using cryo-electron microscopy have accurately analysed the interaction between the 40S ribosomal subunits and the HCV IRES. They found that the IRES RNA is bound to the solvent side of the 40S subunits in a position that is consistent with the proposal path of the mRNA through the subunit. From this experiment they deduced that the 40S binding requirements are contained in domain IIId/e/f stem-loops and junctions, whereas the remaining density extending away from

the 40S subunit surface corresponding to IIIb, IIIa and IIIc (Fig 5). Interestingly, 40S/HCV IRES contacts also take place with the apical loop of domain II. However, these contacts are not critical for binding to occur and their significance is still the subject of studies.

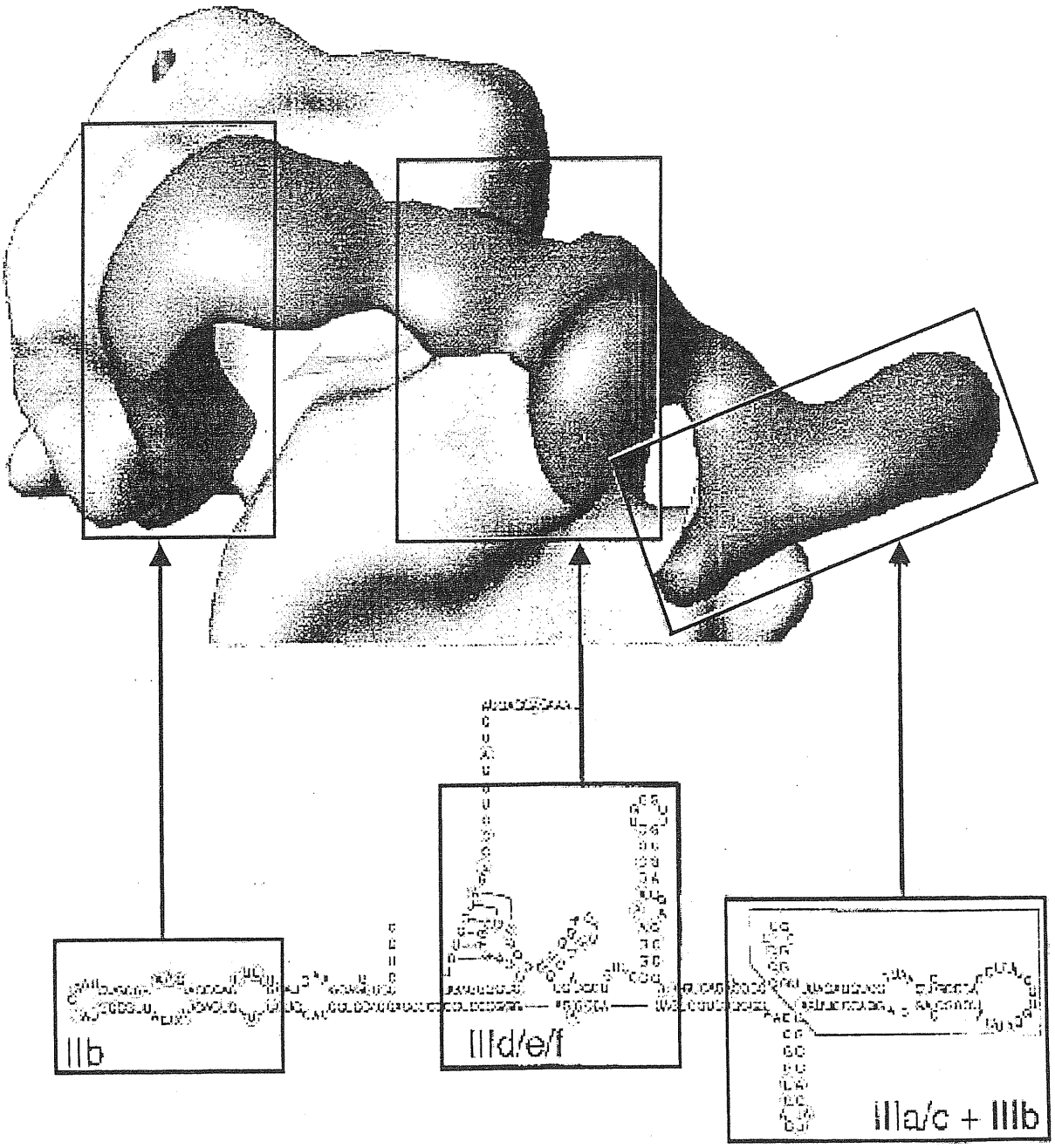


**Figure 5.** Cryo-electron microscopy structure of the HCV IRES RNA-40S subunits complex. The three IRES RNA tertiary structural elements are boxed within the secondary structure. Arrows link the tertiary structure domains to the corresponding elements within the IRES RNA cryo-EM (taken from Spahn et al, 2001).

## 1.7 Interaction between cellular factors and the HCV-IRES RNA

In general, the ability of an IRES sequence to direct translation initiation depends on its ability to interact with the translational machinery/cellular factors. Interestingly, the variety of IRES found in viruses suggests that different sets of *trans*-acting cellular factors are required for individual IRES. In fact, the translation of poliovirus does not occur efficiently in a cell-free translation system prepared from rabbit reticulocyte lysates (RRL). The poor translation in RRL, however, is markedly improved by the addition of factors from HeLa cells. On the other hand, other IRESs such as the IRES of encephalomyocarditis virus (EMCV) RNA (Jang et al., 1988) and HCV RNA (Tsukiyama-Kohara et al., 1992) are highly functional in RRL systems.

Nevertheless, several cellular proteins that do not take part in the canonical translation process have been described to affect HCV translation (Fig 6):

### 1.7.1. Binding of the La autoantigen to the HCV IRES

La antigen (p52 or SS-B) is a cytoplasmic phosphoprotein that was originally identified as an autoantigen in patients with autoimmune disorders (Tan, 1989) and several studies have provided evidence that it functions as a helicase (Craig et al., 1997; Goodier et al., 1997; Xiao et al., 1994). The human La antigen contains three putative RNA recognition motifs (RRM) and a basic region followed by a stretch of acidic residues at the C-terminus (Goodier et al., 1997). Through these motifs the La antigen can bind to a variety of RNA structures (Kenan et al., 1991) and its targets include the 5'UTR regions of picornaviruses, influenza virus, sindbis virus, and the HIV TAR element.

PCBP

Spangberg K. and Schwartz S.
J. Gen. Virol. 1999 80: 1371-6

FukushiS. et al.
Virus Res. 2001 73: 67-69

La antigen

Ali N. et al.
J.Biol.Chem. 2000 275: 27531-40

Isoyama T. et al.
J. Gen. Virol. 1999 80: 2319-2317

hnRNP L

Hahm B. et al.
J. Virol. 1998 72: 8782-8

PTB

Anwar A. et al.
J. Biol. Chem. 2000 275: 34231-5

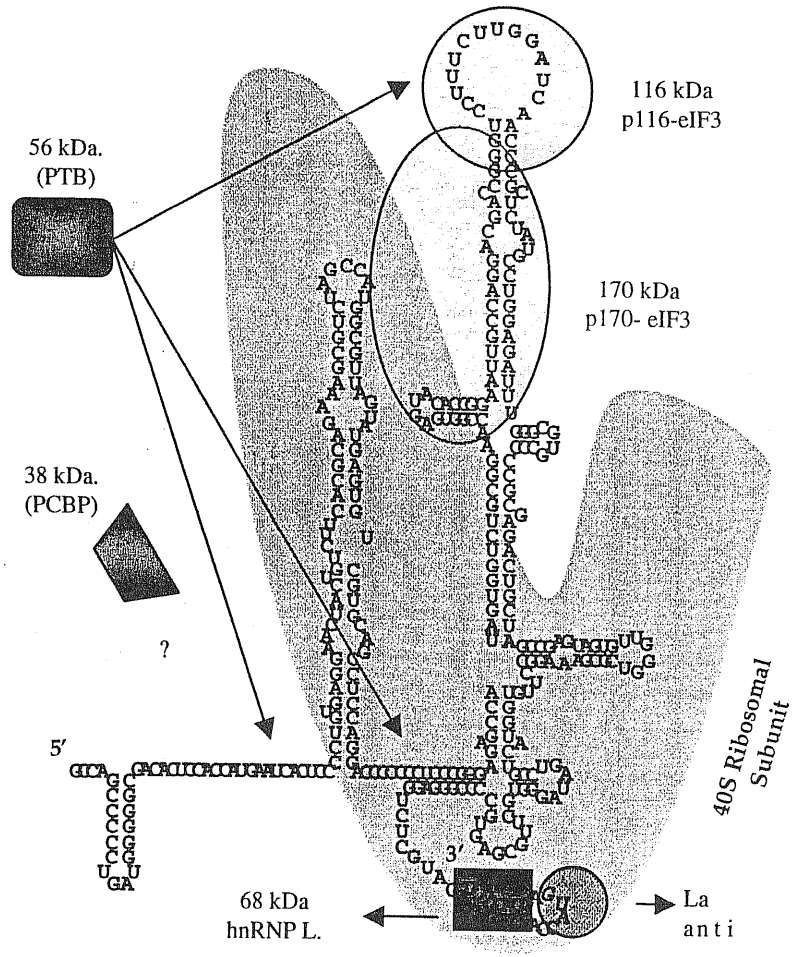


**Figure 6.** Proteins binding to the HCV IRES (an overview)

The aberrant translation initiation of poliovirus IRES-mediated RNA is corrected in the presence of La antigen that is also accompanied by modest stimulation of translation (Meerovitch et al., 1993; Svitkin et al., 1994). In a recent work Ali et al, 2000, have characterized additional contact between La antigen and the HCV-IRES, indicating that this interaction appears to be responsible for La-dependent translation initiation of the HCV RNA. Binding of La HCV appears to be dependent on the integrity of the higher-order of the HCV 5'UTR in the immediate vicinity of the initiator AUG (Ali and Siddiqui, 1997; Wang et al., 1995; Wang et al., 1994). Although, the reason for this stimulation in the HCV context is unknown La autoantigen may function as a chaperon in stabilizing higher-order RNA structure and may also be involved in protein-protein interaction. Recently, Spangberg et all, 2001 have presented evidence that indicates that La proteins is able to bind at the 3'UTR of HCV and its function may be to prevent premature degradation of the HCV RNA.

### 1.7.2. Polypyrimidine-Tract-Binding protein (PTB) binds both 5' and 3'UTR in the HCV RNA

Polypirimidine tract-binding protein (PTB, [p57 or hnRNP-1]) has been shown to exist as a homodimer in solution and contains an oligomeric array of eight RNA recognition motifs (four in each monomer) (Perez et al., 1997) with unusual features (Conte et al., 2000). This protein binds polypyrimidine rich region near the splice site of many introns and can act as a repressor of splicing (Singh et al., 1995). In the cytoplasm, PTB has been shown to physically interact with viral and cellular 5'-UTRs (Ali et al., 1995; Belsham and Sonenberg, 1996; Hellen et al., 1993; Kaminski et al., 1995; Sickinger and Schweizer, 1999). Furthermore, it has been shown to facilitate translation of

picornaviral IRES elements in the rabbit reticulocyte translation system (Belsham and Sonenberg, 1996). The overexpression of PTB has been recently shown to have a considerable stimulatory effect on translation directed by IRES elements derived from hepatitis A virus, poliovirus, and HCV in different types of cells (Gosert et al., 2000). Ali and co-workers, (1997) have previously shown interaction of PTB with the HCV 5'UTR at multiple sites using a UV cross-linking assay. Interestingly, Ito et al, (1999) have demonstrated an additional PTB-binding site at the end of the core coding region that appears to have a regulatory effect on the HCV IRES activity.

In conclusion, the available evidence suggests a physical interaction of PTB with HCV in the following regions: 1) multiple Py-tracts in the 5'UTR, 2) an internal Py-rich motif at the 3' end of the core coding sequence, and 3) near the end of the HCV genome (within the 3'UTR). Interestingly, these viral elements appear to bind PTB with different affinities and the different kinetics may play critical role(s) in regulating the HCV IRES activity (Ali et al., 2000). Another important feature of PTB is its intrinsic ability to homodimerize and/or multimerize in solution. Because of these unusual features, PTB could have a role in establishing a connection between the 5' and 3'UTR by bringing the ends in close proximity. Anwar et al, (2000) have also proposed a possible chaperon activity of the PTB because of its ability to bind multiple domains within the 5'UTR.

### 1.7.3. Heterogeneous Nuclear Ribonucleoprotein L (hnRNP L) Interacts with the 3′ border of the IRES of the HCV

hnRNP L has an apparent molecular mass of 68 kDa. It has been shown to interact with PTB in a yeast two-hybrid system and by co-immuno precipitation. The binding of hnRNP L to the HCV IRES has been shown to correlate well with the translation efficiency of corresponding mRNAs, suggesting that this protein may also play a role in the translation of HCV mRNA. Interestingly, for maximum binding efficiency hnRNP L needs the first 33 aminoacids of the coding region, a finding that is consistent with the fact that the initial coding region of IRES HCV is an important feature for efficient translation initiation.

Because, hnRNP L was reported to be localized mainly in the nucleus (Pinol-Roma et al., 1989) it is not clear how this protein may affect HCV translation in the cytoplasm. However, hnRNP L was found in the cytoplasm as well as the nucleus when transcription of cellular mRNA was blocked by poliovirus infection or treatment with actinomycin D (Hahm et al., 1998). These data suggest that hnRNP L may shuttle between the nucleus and the cytoplasm in a transcription-sensitive manner similar to that of some other hnRNP proteins (e.g. hnRNP A1, E, and I).

### 1.7.4 Interaction of the Poly(C)-binding protein (PCBP2) with the HCV 5′UTR

The human cellular protein PCBP2 was identified in RSW of HeLa cells by RNA affinity column chromatography using PV stem-loop IV RNA (Blyn et al., 1997). PCBP2 is present in most mammalian tissues and it is related to a class of RNA binding proteins which contain three internal RNA-binding regions corresponding to K-homologous (KH) domains, originally identified in heterogeneous nuclear

ribonucleoprotein K (Leffers et al., 1995; Siomi et al., 1993). PCBP2 does not contain any other known nucleic acid binding motifs and therefore the KH domain is believed to be the only determinant of its RNA binding activity. Previous demonstration of PCBP binding to homopolymeric RNA sequences showed strong binding to poly(rC) sequences in vitro and lesser binding to poly(rG) and poly(U) sequences (Leffers et al., 1995). Preliminary data from competition assays showed that the IRES elements of different picornaviruses such as coxsackievirus B3, human rhinovirus 14, EMCV, and HAV were able to compete with PV RNA for binding of PCBP2 (Dildine and Semler, 1992). Spangberg et al, 1999 have recently found that PCBP-2 is also able to bind HCV IRES and speculate that PCBPs binding to the HCV 5'UTR could be involved in initiation of translation at the HCV IRES. Its binding site on the HCV IRES has not yet been mapped.

### 1.7.5 Binding of the S9 ribosomal protein

The S9 ribosomal protein is a 25 kDa protein that belongs to the 40S ribosomal subunits. Incubation of purified 40S with a radiolabelled full-length HCV IRES results in its specific labelling of ribosomal protein S9 (Fukushi et al., 1997; Odreman-Macchioli et al., 2000; Pestova et al., 1998b). This protein is located on the surface of the 40S ribosomal subunits on the entry side of the mRNA binding cleft in contact with the solvent (Spahn et al., 2001) and electron microscopy of antibody labelled 40S subunits located S9 at the back of the shoulder, below helix 16, near the mRNA binding cleft entry site (Lutsch et al., 1983). The results of Spahn et al, 2001 indicate that the IRES RNA-S9 crosslinking occurs to the coding part of the IRES RNA just 3' of the start

codon. The significance of the S9/HCV IRES binding is still unknown (see results for a more detailed discussion of this interaction).

### 1.7.6 Interaction between HCV 5'UTR and eukaryotic initiation factor 3 (eIF3)

Mammalian eIF3 is a multisubunits complex of about 600 kDa that has been implicated in several aspect of 48S complex formation (Kozak, 1992; Maitra et al., 1982). Purified eIF3 promotes dissociation of 80S ribosomes into 40S and 60S subunits. Using different domain III mutants (Buratti et al., 1998b) and chemical and enzymatic footprinting analysis (Kolupaeva et al., 2000; Pestova et al., 1998b), the binding site this factor was determined to be the apical half of the domain III. Footprinting analysis show that eIF3 protects both unpaired and base paired residues in the central helix from chemical modification and enzymatic cleavage involving hairpins (IIIa, IIIb and IIIc (Kolupaeva et al., 1998)). Deletion of these regions from the HCV IRES abrogates the binding of eIF3 to this RNA and results in abrogation of HCV translation activity (Buratti et al., 1998b). eIF3 is absolutely required for 80S complex formation and abolition of its binding results in HCV IRES inactivation (Buratti et al., 1998b; Pestova et al., 1998b). (see results for a more detailed discussion of this interaction)

## 1.8 Possible involvement of the 3'UTR in the translation process

Early analyses of the 3'UTR resulted in conflicting data regarding its exact sequence content. Most studies indicated that the genome terminated with a poly (U) tract (Ito et al., 1998; Okamoto et al., 1991) while one group reported a poly (A) (Han et al., 1991). These difference in the 3'UTR were consider unusual given the importance of these generally well-conserved untranslated regions in the RNA replication of other positive-stranded viruses. Recently, three independent groups employing different experimental strategies have identified similar elements in the 3'UTR of HCV suggesting that these represent the real HCV 3'UTR sequences (Kolykhalov et al., 1996; Tanaka et al., 1995; Yamada et al., 1996). The 3'UTR characterized by these investigators contains a region of approximately 30 nt following the stop codon of the ORF followed by a poly (U) tract of variable length, a polypyrimidine C(U)n stretch plus a conserved X region (Kolykhalov et al., 1996; Tanaka et al., 1996). The X region interestingly, forms a three-stem-loop structure and binds polipyrimidine tract-binding protein (PTB) (Ito and Lai, 1997). Recently, Ito et al, (1998) have demonstrated that the X region in the 3'UTR enhanced translation in rabbit reticulocyte lysates and in intact mammalian cells binds PTB and enhance translation. This enhancement was not due to RNA stabilization by the X region, since mutation in this region affect binding of PTB but did not completely abolish the translation enhancement, suggesting that the PTB-3'UTR interaction may be at least partially involved in the regulation of HCV translation. Furthermore, this region also enhanced translation from another IRES derived from EMCV RNA, but did not affect the 5'-end-dependent translation of α-globin mRNA. Bicistronic RNAs which contain an IRES between two reporter genes confirmed that the X region enhanced only IRES-dependent translation. Thus, the X region in HCV 3'-UTR very likely regulates HCV RNA translation in natural infection (Ito et al., 1998).

## 1.9 Genetic variability of HCV

The majority of HCV isolates identified so far can be classified into six major group, designated genotypes 1 to 6, with subdivision within each (a, b, c, etc.) (Fig. 7) in order of discovery (Chamberlain et al., 1997; Simmonds et al., 2000). Therefore, the sequence cloned by Chiron is assigned type 1a, HCV-J and –BK are 1b, HCJ6 is type 2a and HC-J8 is 2b.

Owing to its high conservation in all viral isolates it is the 5′ UTR that has been used in most laboratories to develop sensitive detection assays for HCV RNA (Hijikata et al., 1991) and to differentiated between the different genotypes.

Interestingly, epimediological analysis have suggested biological differences between genotypes 1 and 2, in terms of quantity of virus in serum or sensitivity to interferon (Kohara et al., 1995; Zein and Persing, 1996) and in the distribution of type 1 and type 2 HCV infections, which may correlate with initiation of protein translation.

Indeed, previous studies have reported differences in the IRES efficiency when comparing 5′UTR sequences from two or three different HCV genotypes *in vitro* or *in vivo* (Tsukiyama-Kohara et al., 1992; Buratti *et al*., 1997; Kamoshita et al., 1997). In particular Collier et al (1998), extended these studies to representatives of the six major genotypes of HCV using different cells lines. These results provide a starting point for such structure function analysis, but mapping the important domains may prove difficult. In fact, as Kamoshita et al. (1997) were unable to identify regions influencing activity in chimeric IRES elements derived from genotypes 1b and 2b.

Recently, Honda et al, (1999b) have studied the translation efficiency of the genotype 1a and 1b. They compared the complete 5′UTR sequences of 25 different genotype 1a and 1b viruses from GenBank . The most frequent differences between the

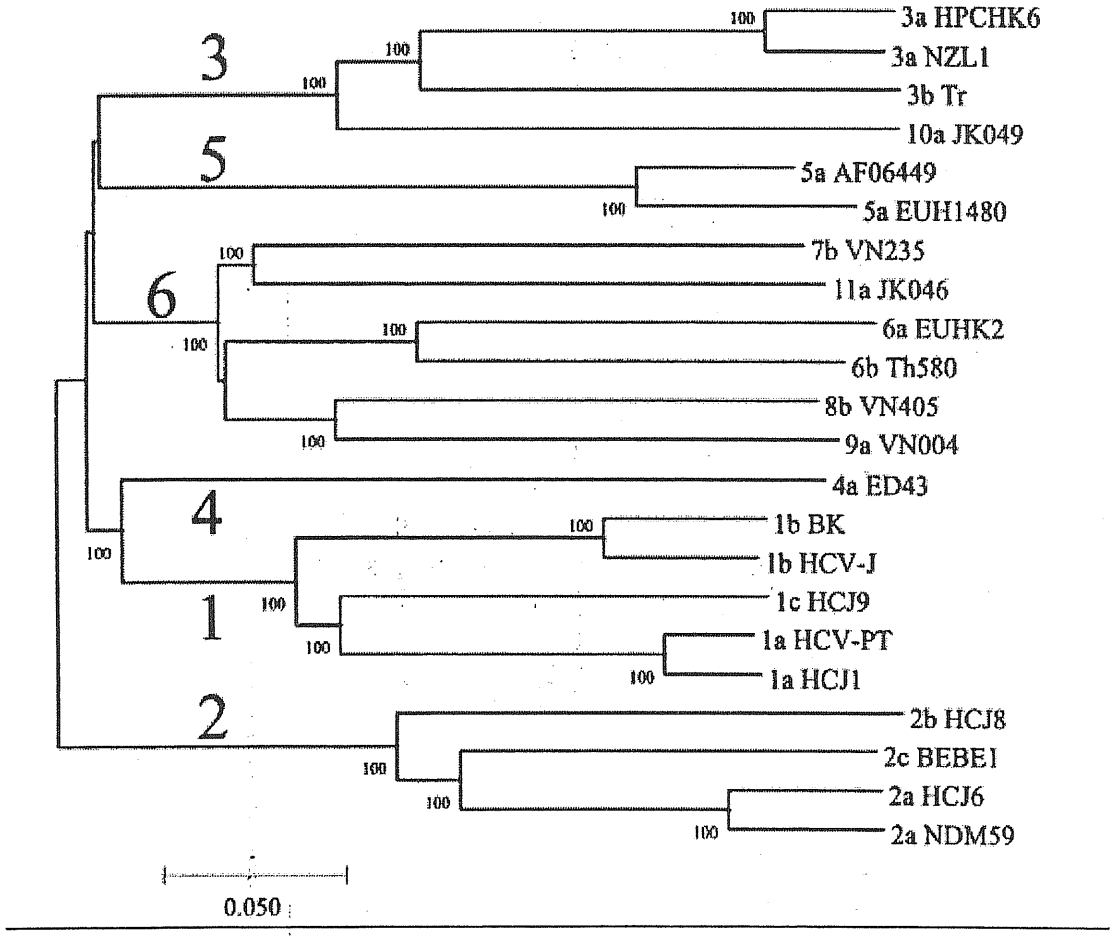


**Figure 7.** Sequence relationships of currently available complete genomic sequences of HCV (listed in Chamberlain*et al*., 1997), and their classification into six genotypes (first tier) and subtypes a, b etc. (second tier). The nomenclature of the HCV genotypes follows the consensus proposal for classification of HCV (Simmonds *et al*., 1994), i.e. the prototype sequence cloned by Chiron is assigned type 1a, HCV-J and -BK are 1b,HC-J6 is type 2a and HC-J8 is 2b, although note the anomalous genotype assignations of types 7b, 8b, 9a and 11a which cluster with types 6a and 6b, and type 10a, which clusters within genotype 3 sequences.

1a and 1b strains were those which distinguish the HCV-H and HCV-N strains, at nucleotide 11 to 13 (UGA versus GAU in 1a and 1b, respectively), nucleotide 34 and 35 (GA versus AG), nucleotide 204 (A versus C), and nucleotide 243 (A versus G). Importantly, all 17 genotype 1b sequences contained the AG dinucleotide sequence at nucleotide 34 and 35, whilst this sequence was present in only 1 of 8 genotype 1a strains. Thus, the differences that was found in the translational activities of the HCV-H and HCV-N 5'UTRs likely typify differences between most genotype 1a and 1b viruses. However, this difference was expressed only when transcripts contained the complete HCV capsid coding sequence (nucleotide 1 to 929) indicating that the determinants of the greater translational activity of the genotype 1a 5'UTR are also located outside the minimal essential IRES sequence.

## Aim of the project

The translation of the HCV viral proteins represents a key step in the life-cycle of this virus. In recent years, the available experimental evidence has conclusively determined that the translation initiation process of HCV is principally controlled by the viral 5′ Untranslated Region (5′UTR). The principal characteristic of this region is represented by the fact that it can fold upon itself to form a complex RNA secondary/tertiary structure (known as IRES). This structure acts as an internal docking site for selected elements of the eukaryotic translational machinery, such as eIF3 and the 40S ribosomal subunit, allowing the assembly of a correct initiation complex on an internal AUG codon. The different RNA secondary structures that bind these elements are known as domain II, III, and IV. Integrity of these structures is essential for translation to occur and the aim of this project is to identify and characterize selected RNA-protein interactions that are essential for this process. The characterization of these interactions will hopefully provide not only a better knowledge of the translation processes driven by IRES elements but also novel targets for the development of specific HCV translation inhibitors.

# CHAPTER 2

# MATERIAL AND METHODS

## 1.1 General reagents

General chemicals were purchased from Sigma Chemical Co., or Merck FR, Germany.

## 2.2 Enzymes

(A) Restriction enzymes were purchased from Pharmacia Biotech (Sweden) or New England Biolabs, Inc (USA).

(B) DNA modifying enzymes: Taq Polymerase, Klenow fragment of *E.coli*, DNA Polymerase I, T4 DNA Polymerase and T4 DNA ligase were obtained from Boehringer Manheim (Germany). The T4 polynucleotide Kinase was from New England Biolabs, Inc. and Calf Intestinal Alkaline Phosphatase was from Pharmacia Biotech (Sweden)

(C) Exonucleases: RNAse A was purchased from Sigma Chemicals Ltd. The 10 mg/ml stock solution of RNAse A was prepared in 5mM EDTA and boiled for 10 minutes to destroy trace amounts of DNase activity. DNase I was purchased from Boehringer Mannheim (Germany).

(D) Proteinase K was purchased from Sigma chemicals Ltd. and stocks prepared at 10 mg/ml.

All enzymes were used following the manufacturers instructions.

## 2.3 Synthetic oligonucleotides

Synthetic DNA oligonucleotides were purchased from Primm s.r.l. (Milan, Italy).

## 2.4 Radioactive isotopes

$\alpha$-$^{32}$P dCTP, $\gamma$-$^{32}$P dATP and $\alpha$-$^{32}$P UTP were supplied by Amersham UK. Ltd.

## 2.5 Bacterial culture media and strain

The *E. coli* K12 strain, DH5$\alpha$, was transformed with the plasmids described in this study and used for their amplification. Plasmids were maintained in the short term as single colonies on agar plates at 4°C but for longer periods of time as glycerol stocks, made by adding sterile glycerol to a final 30% v/v concentration to liquid bacterial cultures. Glycerol stocks were stored at -20°C. When necessary, from the glycerol stocks or agar plates an overnight culture of bacteria was grown in Luria-Bertani medium (LB medium: per litre: Difco Bactotryptone 10 g, Oxoid yeast extract 5 g, NaCl 10 g, pH 7.5). Bacterial growth media were sterilized before use by autoclaving. Where appropriate, ampicillin was added to the media at a final concentration of 200 mg/ml.

## 2.6 Standard solutions

All solutions are identified in the text where used except for the following:

a) TE: 10mM Tris-HCL pH 7.4, 1 mM EDTA pH 7.4

b) PBS: NaCl 137 mM, KCl 2.7 mM, Na2HPO4 10 mM, KH2PO4 1.8 mM, pH 7.4

c) 10X TBE: 108g/l Tris, 55g/l Boric acid, 9.5g/l EDTA

d) MOPS: 200 mM MOPS, 50mM CH3COONa, 10mM EDTA pH 7

e) 10X RNA sample buffer: 500µl deionised formamide, 100µl 10X MOPS, 167µl foramaldehyde 37%, 233µl H2O, 5µl ethidum bromide (EtBr)

f) 5X Ficoll loading buffer: 0.25% w/v bromophenol blue, 15% w/v Ficoll type 4000 in water

g) Sequencing gel loading buffer: 98% deionised formamide, 10mM EDTA, 0.025% Xylene cyanol FF, 0.025% bromophenol blue

h) 2X SDS sample buffer: 100mM Tris-HCl (ph 6.8), 200 mM dithiothreitol, 4 % SDS, 0.2% bromophenol blue, 20% glycerol.

## 2.7 Nucleic acids preparations

### 2.7.1 Small scale preparation of plasmid DNA from bacterial cultures

Rapid purification of small amounts of recombinant plasmid DNA was basically performed with the method described in Sambrook et al., 1989), section 1.25. Briefly, alkaline lysis of recombinant bacteria was performed by resuspending the bacterial pellet in 100µl of solution I (50mM glucose, 25mM Tris.Cl (pH 8), 10mM EDTA (pH 8). 200µl of solution II (0.2 M NaOH, 1% SDS) was then added and the contents mixed by inversion. This was followed by the addition of 150µl of solution III (3M sodium acetate) and the contents were again mixed by inversion. The bacterial lysate is then centrifuged in an Eppendorf table top centrifuge at maximum speed and the supernatant transferred to a new tube. An equal volume of 1:1 v/v phenol:choloroform solution was added to the supernatant. The tube was then vortexed and centrifuged as above. The aqueous phase containing the DNA is then recovered and the DNA pelleted by ethanol precipitation. The final pellet was resuspended in 59µl of $dH_2O$ and 1µl of

RNase. 5µl of such preparations were routinely taken for analysis by restriction enzyme digests.

### 2.7.2 Large scale preparations of plasmid DNA from bacterial cultures

Large scale preparations of plasmid DNA were carried out with the use of JetStar DNA purification columns (Genomed), following the manufactures instruction. This material was used mainly in transfection experiments.

### 2.7.3 Precipitation with ethanol or isopropanol

This was performed by the addition of NaCl to the DNA or RNA solution to a final concentration of 0.2 M. The DNA precipitate can then recovered by centrifugation at 12000g for 10 minutes. This was washed in 70% ethanol and the DNA redissolved in an appropriate buffer, quantified with the spectrophotometer technique and brought to the desired concentration.

## 2.8 Estimation of nucleic acid concentration

### 2.8.1 Spectrophotometric

An optical density of 1.0 at 260nm was taken to be equivalent to a concentration of 50mg/ml for double stranded DNA, 33mg/ml for single stranded DNA and 40 mg/ml for RNA samples. The ratio of values for optical densities measured at 260nm and 280nm is 1.8 for pure sample of DNA and 2 for RNA, these are reduced by protein contaminants and therefore the values were used to assess both the concentration and the purity of the samples.

### 2.8.2 UV fluorescence of intercalated ethidium bromide

Nucleic acids, size-fractionated on agarose gels, can be visualized after staining with ethidium bromide (0.5mg/ml) since fluorescence of ethidium bromide is enhanced by intercalation between bases in the nucleic acid helix. It is therefore possible to estimate the quantity of nucleic acid on a gel by comparing the intensity of UV-induced fluorescence of the sample with that of a known standard sample. This procedure was mostly performed by eye and utilized in estimations of amounts of DNA to be utilized in subsequent cloning reactions.

## 2.9 Electrophoresis of nucleic acids

### 2.9.1 Agarose gel

DNA or DNA restriction fragments were size fractionated by electrophoresis in agarose gels ranging in concentrations from 0.6% for larger fragments to 1.5% w/v for smaller fragments. The gels contained ethidium bromide and 1X TBE. Horizontal 10 X 8 mini gels were routinely used for fast analysis of DNA restriction enzyme digests, estimation of DNA, or DNA fragment separation prior to elution from the gel. Samples of 20µl containing 1X Ficoll dye were loaded into submerged wells. These were electrophoresed at 50-80mA for a time depending on the fragment length expected and gel concentration, in a running buffer of 1X TBE. DNA was visualised by UV transillumination (lower limit 5-10ng DNA) and the result recorded by digital photography.

RNA was visualized/fractionated in 1% agarose gels containing 1X MOPS and formadlehdye (37%). Samples containing 1X RNA loading buffer were loaded into submerged wells. These were electrophoresed at 50-80mA for approximately 2-4 hours

in a running buffer 1X MOPS, 1/10 v formaldehyde 37%. The total-RNA quality was deduced from the ribosomal 28S and 18S RNA bands that are clearly visible while the mRNA is not.

### 2.9.2 Elution and purification of DNA fragments from agarose gels

This protocol was used to purify small amounts (less than 1 mg) of DNA for subcloning or for use in the production of radioactive probes. The DNA samples were loaded onto an agarose minigel and electrophoresed as described. The DNA was visualized with UV light and the required DNA fragment excised from the gel. This slab was put into the minimum length of dialysis tubing with as little gel running buffer as possible and was electrophoresed in a minigel apparatus at 150 V, the time required for the DNA sample to migrate out of the gel slice. At this stage the current was reversed for 30 seconds to elute any bound DNA from the dialysis tubing. Buffer containing DNA was passed to a microcentrifuge tube and the tubing was washed twice with 100µl of gel running buffer. Aliquots were pooled and DNA recovered by ethanol precipitation preceded by a phenol/chloroform extraction. The amount of DNA recovered was approximately calculated by UV fluorescence of intercalated ethidium bromide.

### 2.10 Sequence analysis

The sequence analysis of plasmid DNA were performed either manually by the dideoxynucleotyde chain termination method or with a Beckman CEQ 2000 Dye terminator Cycle sequencer.

The dideoxynucleotyde chain termination method (Sanger et al., 1977) was performed using a T7-based DNA sequencing kit (Pharmacia), following the manufacturers instructions. Approximately 100 ng of the plasmid DNA of interest was subjected to the sequencing reaction. Prior to the sequencing reaction samples are denatured by the addition of NaOH to a final concentration of 0.4 M and then passed through a spun column (Pharmacia), removing the NaOH and further purifying the sample from bacterial RNA and protein. The samples are then loaded onto an polyacrylamide gel and or onto a gradient sequencing polyacrylamide gel and run at 50W. The gel is then dried onto to 3mm Whatmann paper and autoradiographed overnight using Kodak X-OMAT film. Sequencing samples run on the Beckman CEQ 2000 Dye terminator Cycle sequenator were prepared by amplification of plasmid DNA samples with dideoxy nucleotide terminators which were labelled with specific dyes. The sample was then fractionated by capillary electrophoresis with automated fluorescent reading.

## 2.11 Enzymatic modification of DNA

### 2.11.1 Restriction enzymes

Restriction endonuclease cleavage is accomplished simply by incubating the enzyme(s) with the DNA in appropriate reaction conditions. The amounts of enzymes and DNA, the buffer and ionic concentration, and the temperature and duration of the reaction will vary depending of the suppliers. A standard reaction consist in adding restriction endonuclease (1 to 5 U/ug DNA) and incubating the reaction mixture (1 to 3 hr) at the recommended temperature (in general, 37 °C). In principle, 1 U restriction endonuclease completely digests 1 ug of purified DNA in 1 hr using the recommended

assay conditions. However, crude DNA preparations, such as those made by rapid procedures, often require more enzyme and or more time for complete digestion. The volume of restriction endonuclease added should be less than 1/10 the volume of the final reaction mixture, because glycerol in the enzyme storage buffer may interfere with the reaction. The reaction is stopped and prepared it for agarose gel electrophoresis by adding 1/10 of 10X loading buffer. The reaction can also be stopped by chelating Mg2+ with 0.5 ul of 0.5 M EDTA (12.5 mM final concentration). If the digested DNA is to be used in subsequent enzymatic reactions (e.g., ligation or filling-in reaction), addition of EDTA should be avoided. Alternatively, many enzymes can be irreversible inactivated by incubating 10 minutes at 65 °C or purified from the reaction mixture by extraction with phenol/chloroform and then precipitation in ethanol.

### 2.11.2 Large fragment of E. Coli DNA Polymerase I (Klenow)

This enzyme is used for creating compatible ends for blunt ended ligation during construction of recombinant plasmids and to digest aspecific residues added by Taq DNA polymerase during P.C.R amplification at the 5′ terminus. The Klenow polymerase was used with the appropriate buffer supplied at a final concentration of 5U per µg of DNA. When a "fill-in" was required (DNA fragments with protruding 5′ ends) dNTP for a final concentration of 0.5 mM were added. The mixture was incubated at 37 °C for 20 minutes.

### 2.11.3 Dephosphorylation of DNA 5′ termini

Used to reduce self-ligation of vector DNA during generation of recombinant clones, this procedure was performed with the use of Calf intestinal phosphatase (CIP).

This reaction was carried out in a final volume of 50-100µl using 1U of enzyme per 0.5 µg DNA, incubating at 37°C for 1 hour. The enzyme can be inactivated by adding 1mM EDTA and incubating for 20 minutes at 75°C. When purification of the DNA of interest via agarose gel elution was required, this latter procedure was not performed.

### 2.11.4 T4 DNA ligase

T4 DNA ligase catalyses the formation of a phosphodiester bond between adjacent 3' hydroxyl and 5' phosphoryl termini in DNA, requiring ATP as a cofactor in this reaction. This enzyme was used to join double stranded DNA fragments with compatible ("sticky" or "blunt") ends during the generation of recombinant plasmid DNAs. The amount of DNA used in the ligation reaction depended on the length of the vector used. If this was 3000bp; 15-30ng of DNA was used, If 7000bp; 25-50ng DNA. During the ligation the molar ratio of the insert to vector ratio was kept as close as possible to 5:1. In some reactions synthetic oligonucleotide were included, in these cases the amounts added to each reaction to obtain inclusion of oligonucleotides in the resulting plasmid were about 100 fold molar excess over the DNA vector.

The final volume of ligation depended on the volume of the insert (X1) and vector (X2). If X1+X2 < 2µl; reaction volume 10µl, if X1+X2 < 3.5µl; reaction volume 15µl and if X1+X2 > 3.5µl; reaction volume 20µl. O.1 units of DNA Ligase were used if the DNA fragments to be ligated had 5' overhangs (sticky) and 2 units if the DNA fragments to be ligated were blunt or had been blunt ended by the use of Klenow DNA polymerase.

## 2.12 Transformation of Bacteria

### 2.12.1 Preparation of competent cells

E.coli strains were grown overnight in a 200 ml volume of LB at 37°C. The cells were then incubated in ice for 15 minutes and centrifuged. The pellet was resuspended in 20 ml of a solution consisting in: K-acetate 30 mM, KCl 100 mM, $CaCl_2$ 10 mM, $MnCl_2$ 50 mM, glycerol 15%, pH 5.8. The solution was then incubated in ice for 5 minutes and centrifuged. The pellet was resuspended in 2 ml of a solution of: MOPS 10 mM, $CaCl_2$ 75 mM, KCl 10 mM, glycerol 15%, pH 6.5. The cells were aliquoted and stored at -80°C. Competence was determined by transformation with 0.1ng of PUC 18, and was deemed satisfactory if this procedure resulted in more than 100 colonies.

### 2.12.2 Transformation

Transformation of ligation reactions were performed using a third or a half (sticky or blunt respectively) of the reaction volume. Transformation of clones were carried out using 1ng of the plasmid DNA. In both cases the DNA was incubated with 60 µl of competent cells for 30 minutes on ice, followed by 90 seconds at 42°C. At this point 60µl of LB were added and the bacteria allowed to recover for 10 minutes at 37°C. The cells were then spread on agarose plates containing the appropriate antibiotic required for selection. The plates were then incubated for 12-15 hours. If virgin plasmid vectors were used, 30µl of IPTG 100 mM and 20µl of X-Gal (4% in dimethylformamide) were spread onto the surface of the agarose prior to the plating to facilitate screening of positive clone through identification of galactosidase activity.

## 2.13 Amplification of selected DNA fragments (PCR)

The polymerase chain reaction was performed on genomic or plasmid DNA following the basic protocols furnished with the Boehringer Taq DNA polymerase. The volume of the reaction was 50-100µl with 1x Taq buffer, dNTP mix 200µM each, appropriate sense and antisense oligonucleotide primers (10µM final concentration, each), and 2.5-5 U of Taq DNA Polymerase (Boehringer). In general, 0.1 ng for plasmid and 100-500ng of genomic DNA were used for amplification. The cyclic conditions employed, unless described otherwise, consisted in 94°C 1 minute, 56°C 1 minute, 72°C 1 minute for a total of 33 cycles and then a soak at 4°C. These were performed on a Perkin Elmer Cetus DNA Thermo Cycler. The fragments to be subsequently cloned were treated with Klenow DNA polymerase and phophorylated with polynucleotide kinase. These were then gel purified and eluted.

## 2.14 Densitometric analysis and Phosphoimager quantification

When required densitometric analysis was carried out using Macintosh version of the public domain National Institutes of Health (NIH) Image 1.62 program (developed at the U.S. National Institutes of Health and available on the Internet at http://rsb.info.nih.gov/nih-image).

Quantification of radioactive CAT assays, Southern and Northern blots was performed, following the manufacturers instructions using an Instant Imager, Packard Instrument Co., Meriden, CT machine. Alternatively, a Canberra Packard Instant Imager was used for the same purpose.

## 2.15 Plasmid construction of HCV 5′ UTR mutants

The strategy used to swap the positions of different domains of HCV 5′UTR using a template sequence has already been described in detail elsewhere (Buratti et al 1998b). The domain II region missing from 5′MscStu (nt. 23 to 102) was amplified and inserted back in the MscI site of this plasmid (obtaining plasmid 5′domII) using two sense and antisense primers (5′**gggcga**cactccacc3′ and 3′oligo: 5′**aggctgcacga**cact3′). In the StuI site we then inserted the amplified sequences of domain III using the following 5′ and 3′ primers: 5′**acccccccctcccgggggtctgcgg3′**, 5′cagtctcgcgggggca3′ for mutant 5′domIII (145-248), 5′**acccccccctcccggg**aattgccagga3′, 5′caatctccaggcata3′ for mutant 5′domIII (172-227), 5′**acccccccctcccgggg**accgggtc3′, 5′cgagcgggttgatccaa3′ for mutant 5′domIII (184-213) (see Fig.9A for a schematic diagram of each mutant). All these primers contained a 5′ leader sequences (in bold lettering) aimed at restoring the nucleotides deleted during the formation of the MscI and StuI site. All these different mutants were inserted in the pSV GH bicistronic expression system for transfection experiments in COS-1 cells as already described (Buratti et al, 1998a) and in the XbaI/HindIII restriction enzyme sites of pBluescript II KS+ (Pharmacia). An *in vitro* transcription and translation assay (Novagen) was performed according to manufacturer's instructions using 2 μg of each Bluescript plasmid. Mutant 5′S/L, 5′MscStu, and the wild type 5′UTR sequence (5′wt) have already been described in detail elsewhere (Buratti et al, 1998b).

All mutants described in this study were constructed by polymerase chain reaction (PCR), and the primer sequences are shown in Table I. All mutants were amplified from a template plasmid containing nt 1 to 920. All mutants were prepared in a pBluescript II

**TABLE I**

Primers used for PCR amplification

| Primer | Sequence (5'⟶ 3') |
|---|---|
| domIIaS | CCCTGTGAGGTACTGTCTTC |
| domIIaAS | GTCCTGGAGGCACGACACTC |
| domIIbS | GGATCTACTGCACGCAGAAA |
| domIIbAS | AGGCTGCACGCACTCATACT |
| domIIcS | TCTTCACGCAAGCGTCTAGC |
| domIIcAS | ACGACACTCATACTAACGCC |
| domII76S | GCAGAAAGCCGCTAGCCATG |
| domII76AS | CATGGCTAGCGGCTTTCTGC |
| domII82S | AGCGTCTAAAAATGGCGTTA |
| domII82AS | TAACGCCATTTTTAGACGCT |
| domIII260S | AGTAGTGTTGCGTCGCGAAA |
| domIII260AS | TTTCGCGTCGCAACACTACT |
| domIII290S | ACTGCCTGATGGGGTGCTTG |
| domIII290AS | CAAGCACCCCATCAGGCAGT |
| AUG339S | ACCGATGACCAAAAGCACGA |
| AUG339AS | TCGTGCTTTTGGTCATCGGT |
| AUG345S | ACCGTGCACCAAAAGCatgA |
| AUG345AS | TCATGCTTTTGGTGCACGGT |

KS+ (Pharmacia) using the primers in the following combination: 1. for mutants Δ54-56 and Δ108-110, domIIaS/reverse and domIIaAS/Universal primer, 2. for mutants Δ62-65 and Δ103, domIIbS/reverse primer, and domIIbAS/Universal primer, 3. for mutants Δ72-75 and Δ93-95, domIIcS/Reverse and domIIcAS/Universal primer. Both amplification products were mixed in the same molar proportion and subjected to a second round of amplification using the universal and reverse primers. To obtain the double mutants, the same group of primers were used on single deletion mutants rather than the original template. To prepare the different set of AUG mutants we used the primers described in Table I using the same strategy described above using the 5'wt and the Δ72-74 mutant as template.

**2.16 Enzymatic analysis of RNA secondary structure**

In order to investigate the secondary structure of the domain III mutants we used single- and double-strand specific RNAses. RNA was transcribed using T7 RNA polymerase (Stratagene) from the Bls KS+ domIII(145-248), domIII(172-227), domIII(184-213), 5'wt, and 5'S/L mutants with HindIII. Reaction mixes (100 µl final volume) contained 1 µg of RNA and 0.02 U of RNAse V1 (Pharmacia Biotech), or 0.5 U of RNAse T1 (Sigma) in buffer A (10 mM Tris pH=7.5, 10 mM $MgCl_2$, 50 mM KCl), or 20 U of S1 nuclease (Pharmacia Biotech) in buffer B (buffer A plus 1 mM $ZnSO_4$). The RNA was digested at 30°C for 15 minutes in a water bath and a control aliquot of RNA without the addition of RNAses was processed simultaneously with the digested samples. Reactions were stopped by extraction with phenol/chloroform and ethanol precipitated in 0.3M sodium acetate pH=5.2. The pellet was resuspended in 3µl of water and RNAse cleavage sites were

identified by primer extension with a domain IV specific end-labelled oligonucleotide primer (5'ggtgcacggtctacgaga3'). In a total volume of 5µl, 10ng of $^{32}$P-labelled primer was hybridized to the resuspended RNA in RT buffer (50 mM Tris, pH=8.3, 3 mM $MgCl_2$, 75 mM KCl). The solution was heated at 65°C for five minutes and allowed to cool for five minutes at room temperature. To each reaction we then added 15µl of a solution in RT buffer containing 0.2 U of M-MLV reverse transcriptase (Gibco-BRL), 2µl of dNTP mix 5mM, and 2µl of 0.1M DTT. The mixture was held at 42°C for 30 minutes and then 2µg of RNAse A were added and the mixture incubated a further 30 minutes at 37°C. It was then phenol/chloroform extracted and ethanol precipitated in 0.3M sodium acetate pH=5.2. The samples (enzymatically digested RNA, control reaction, and a sequencing reaction using the same primer used for the RT reaction) were loaded on a 6% polyacrylamide gel which was subsequently dried and exposed to Kodak X-Omat AR films for 12 to 24 hours.

**2.17 Sucrose density gradients of binary IRES-40S complexes**

Ribosomal complexes were assembled on 1 ug of HCV RNA labelled with $^{32}$P-UTP in 100 ul reaction volume in binding buffer (20 mM Tris.Cl pH 7.5, 2.5 mM magnesium acetate, 100 mM KCl, 2 mM DTT) by incubation for 10 min at 30°C. The 40S-IRES complex was then loaded on a 10 to 30% sucrose gradient and centrifugated for 16 hr at 4°C and 22.000 rpm in a Beckman SW28 rotor. 1 ml fraction were colected and the radioactivity of each one was determined by Cerenkov counting.

## 2.18 Footprinting analysis

The enzymatic footprinting analysis was performed basically as described by Kolupaeva et al, 2000. The assembly of binary IRES-40S ribosomal complexes were performed essentially as described by Odreman-Macchioli et al, (2000). The IRES-40S ribosomal complex were assembled in 20 µl reaction volumes. Free or 40S/IRES RNA complexes were digested in binding buffer (20 mM Tris.Cl pH 7.5, 2.5 mM magnesium acetate, 100 mM KCl, 2 mM DTT) by incubation for 10 min at 30°C with RNase T1 (Sigma) at a final concentration of 0.02 U/µl (in the absence or presence of the 40S ribosomal subunit). The end-labelled primer 5'TTCGTGCTCATGGTGCACGGT-3' (complementary to HCV nt 332 to 352) was annealed to RNA and the extended cDNA products (using M-MLV RT according to standard protocols) were analysed by electrophoresis on a 8% polyacrilamide-7M urea gels and after dry exposed to X-Omax film (Kodak).

## 2.19 In vitro transcription and translation

Transcription and translation reaction were carried out in rabbit reticulocyte lysates RRL (Novagene). The Single Tube Protein™ System 3 (STP3) is designed for *in vitro* synthesis of proteins directly from supercoiled or linear DNA templates containing a bacteriophage T7 or SP6 RNA polymerase promoter. The system is based in a unique two-step protocol in which transcription with T7 or SP6 RNA polymerase is directly followed by translation in an optimized RRL. In the standard reaction, the DNA template (typically 0.5 ug plasmid or 2 ul amplified reaction was transcribed in 10 ul at 30°C for 15 minutes, followed by the addition of 40 ul of translation mixture and continued incubation for 60 minutes.

This second step was carried out in the presence of $^{35}$S-methionine (40 uCi) that was incorporated in the protein. The products were analyzed by 15% SDS-PAGE, dried and X-ray exposed at –80°C overnight using a X-OMAT film (Kodak)

### 2.20 Trasnfection of COS-1 cells with the pSV GH mutants

The different 5'UTR sequences inserted into the pSV GH expression vector were used to transfect COS-1 cells using DOTAP liposomal transfection reagent (Boehringer Mannheim) that is a liposome formulation of the cationic lipid DOTAP. The DNA plasmid (1ug/ul) was mixed with 30 ul of DOTAB reagent in a reaction volume of 150 ul in PBS and were incubate for 15 minutes at room temperature. This mixture results in spontaneously formed stable complexes that can be added directly to the cells. The cells were incubated for 4 hr in presence of DOTAB/DNA, then the media was replaced with fresh culture medium and further incubated cells for 48hr.

### 2.21 Transcription of the pBluescript II KS+ plasmids

All plasmids described in this study were linearized by digestion with Hind III and transcription was performed with T7 RNA polymerase (Stratagene) in the presence of [$^{32}$P] UTP and purified on a Nick column (Pharmacia) according to manufacturers' instructions. The labelled RNAs were then precipitated and resuspended in RNAse-free water. The specific activities of labelled RNA preparations were in the range of $4x10^6$ cpm/µg of RNA. Ribosomal salt wash extract from COS-1 and the binding conditions for the UV crosslinking assay using

[$^{32}$P]UTP labelled RNA probes (1x$10^6$ cpm per incubation) have already been described in detail in a previous work (Buratti et al, 1998a).

### 2.22 UV-crosslinking assay

The UV crosslinking assay was performed by adding [$^{32}$P]UTP-labelled RNA probes (1 x $10^6$ c.p.m.) per incubation in a water bath for 15 minutes at 30°C with 20 ug of the different protein extracts in a 30 ul final volume. Final binding conditions were 20 mM HEPES pH 7.9, 72 mM KCl, 1.5 mM $MgCl_2$, 0.78 mM magnesium acetate, 0.52 mM DTT, 3.8% glycerol, 0.75 mM ATP and 1 mM GTP and 2 ug of *Escherichia coli* tRNA as an aspecific competitor. In the competition experiments cold RNA was also added as a competitor 5 minutes before addition of the labelled RNAs (the amount used for the data point was from 1 to 5 ug). Samples were then transferred in the wells of an HLA plates (Nunc, InterMed) and irradiated with UV light on ice (800.000 kJ, ~5 minutes) using a UV Stratalinker 1800 (Stratagene). Unbound RNA was then digested with 30 ug of RNAse A (Sigma) and 6 U of RNAse T1 (sigma) by incubating at 37°C for 30 min in a water bath. Samples were then analysed by 12% SDS-PAGE followed by autoradiography.

### 2.23 Ribosomal Salt wash preparation (RSW)

RSW from COS-1 and HeLa cells was prepared by resuspending the cells in 4 volumes of lysis buffer (HEPES 10 mM pH 7.9, KCl 10 mM, $MgCl_2$ 1.5 mM, 0.5 mM DTT). They were broken in ice with 50 strokes of a Dounce homogenizer (tight pestle). This suspention was centrifuged at 4500 g for 10 minutes at 4°C. The supernatant was

centrifuged at 100.000 g per 1 hr. The pellet was resuspended in 0.25 M sucrose, 1 mM DTT and 0.1 mM EDTA. 4 M KCl was then slowly added to a final concentration of 0.5 M. After 1 hr on ice this suspension was centrifuged per 2 hr at 100.000 at 4°C. The supernatant was dialyzed overnight against buffer A (20 mM HEPES pH 7.9, 1.1 mM $MgCl_2$, 0.37 mM DTT, 0.2 mM EDTA, 0.1 M KCl). The supernatant (RSW) was frozen at –80°C in small aliquots.

**2.24 SDS polyacrylamide gel electrophoresis**

One-dimentional gel electrophoresis under denaturing conditions (e.g., in the presence of 0.1% SDS) separates proteins based on molecular size as they move through a polyacrilamide gel matrix toward the anode. The polyacrilamide gel is cast as a separating gel (sometimes called resolving or running gel) topped by a stacking gel and secured in an electrophoresis apparatus. Conventional slab gel SDS PAGE was performed in 20 X 20 cm vertical gels with 15% w/v polyacrylamide, running at 200 Volts per 3 hr and stained with Coomassie Blue R250 in methanol-water-acetic acid 45:45:10 (v/v/v) or dried and X-ray exposed.

**2.25 40S ribosomal purification**

The 40S ribosomal purification was performed basically as described by Pestova et al, 1996. 40S ribosomal subunits were prepared from HeLa cells. After disrupted the cells with about 50 strokes of the tight pestle, the homogenate was centrifuged in a precooled rotor at 4500 g for 15 minutes. The supernatant was collected and the ribosomes were precipitated by centrifugation for 4 hr at 4°C and 30.000 rpm in a Beckman 60Ti rotor and resuspended in buffer A (20 mM Tris-HCl [pH 7.6], 2 mM DTT,

6 mM $MgCl_2$, with 0.25 M sucrose and 150 mM KCl to a concentration of 50 to 150 $A_{260}$ U/ml. This suspention was incubated with 1 mM puromycin for 10 minutes at 0°C and then for 10 minutes at 37°C before addition of KCl to 0.5 M. Ribosomal subunits were resolved by centrifugation of 1 ml aliquots of this suspension through a 10 to 30% sucrose gradient in buffer A with 0.5 M KCl for 17 hr at 4°C and 22.000 rpm, using a Beckman SW 28 rotor. 40S ribosomal subunits were precipitated from 2 ml gradient fraction by centrifugation for 18 hr at 4°C and 50.000 rpm using a Beckman 60Ti rotor. Pellets were resuspended in buffer in buffer B (20 mM Tris-HCl [pH 7.6], 0.2 mM EDTA, 10 mM KCl, 1 mM DTT, 1 mM $MgCl_2$, 0.25 M sucrose) to a concentration of 60 to 80 $A_{260}$.

**2.26 Wester blot (inmunoblot) analysis**

Transfected COS-1 cells were disrupted by sonication and a defined amount of total proteins were loaded in a SDS-PAGE. This gel was blotted on a nitrocellulose membrane at 200 mA for 2h. The membrane was prehybridised in PBS-5% low fat dry milk for 1 hr at room temperature. After 3 washes with PBS (5 minutes each one) the membrane was hybridised for 2 hr in the presence of the primary monoclonal antibody MAb B12.F8 kindly provided by prof. M.U. mondelli (University of Pavia, Italy). The appropriated horse radish peroxidase conjugated second antibody was added a 1:1000 dilution in PBS 2% non fat dry milk for 1 hr. The membrane was washed 3 times with PBS and then evidentiated on Kodak autoradiographic film by ECL chemioluminescence analysis (Amersham Life Science) according to the manufacturer's instruction. The film was subsequently scanned using an Imaging Densitometre GS-670

(Bio-Rad) and each band was quantified using the molecular Analyst program for Macintosh computer. Each transfection was repeated three times and standard deviation values.

# CHAPTER 3

# RESULTS

## 3.1 Construction of HCV IRES mutants of the major domain III

Structural studies have shown that the HCV IRES forms a complex secondary structure with several domains (numbered from I to IV), a helical structure, and a pseudoknot. As expected the integrity of some of these features has been observed to be critical for the ability of HCV RNA to promote internal initiation and/or its control. Up to now, mutational analysis performed on most of the HCV IRES has allowed to shed considerable insight on the relationship between the ability of this IRES to drive efficiency translation and its ability to recognize cellular factors that improve or help to start HCV proteins translation.

It has been previously shown that an isolated domain III sequence RNA (nt. 134 to 290) binds two eIF3 subunits (Fig. 8) (Buratti et al., 1998b) even when transcribed apart from the rest of the entire HCV 5'UTR sequence. This result is in agreement with a recent study showing that a binary complex between the entire eIF3 complex and the full HCV IRES sequence protects from footprinting analysis only stem-loops IIIa, IIIb, and IIIc of this domain (Sizova et al., 1998). Taken together, these data were indicative that the apical portion of domain III is the only HCV 5'UTR region involved with eIF3 binding to the IRES. Therefore, in order to better define these observations, three additional mutants were prepared which carry selected portions of this domain: nt. 145 to 248, nt. 172 to 227, and nt. 184-213 (Fig.9A). First of all, considering that all these sequences were inserted back in the exact position of the original wild type domain III (nt. 134 to 290) it was interesting to measure if any of these mutants had retained some IRES activity. Fig.9B shows that in an *in vitro* transcription and translation assay and in a transfection assay in COS-1 cells using a bicistronic system all three mutants failed to stimulate IRES activity, as estimated by production of a reporter HCV core protein. In

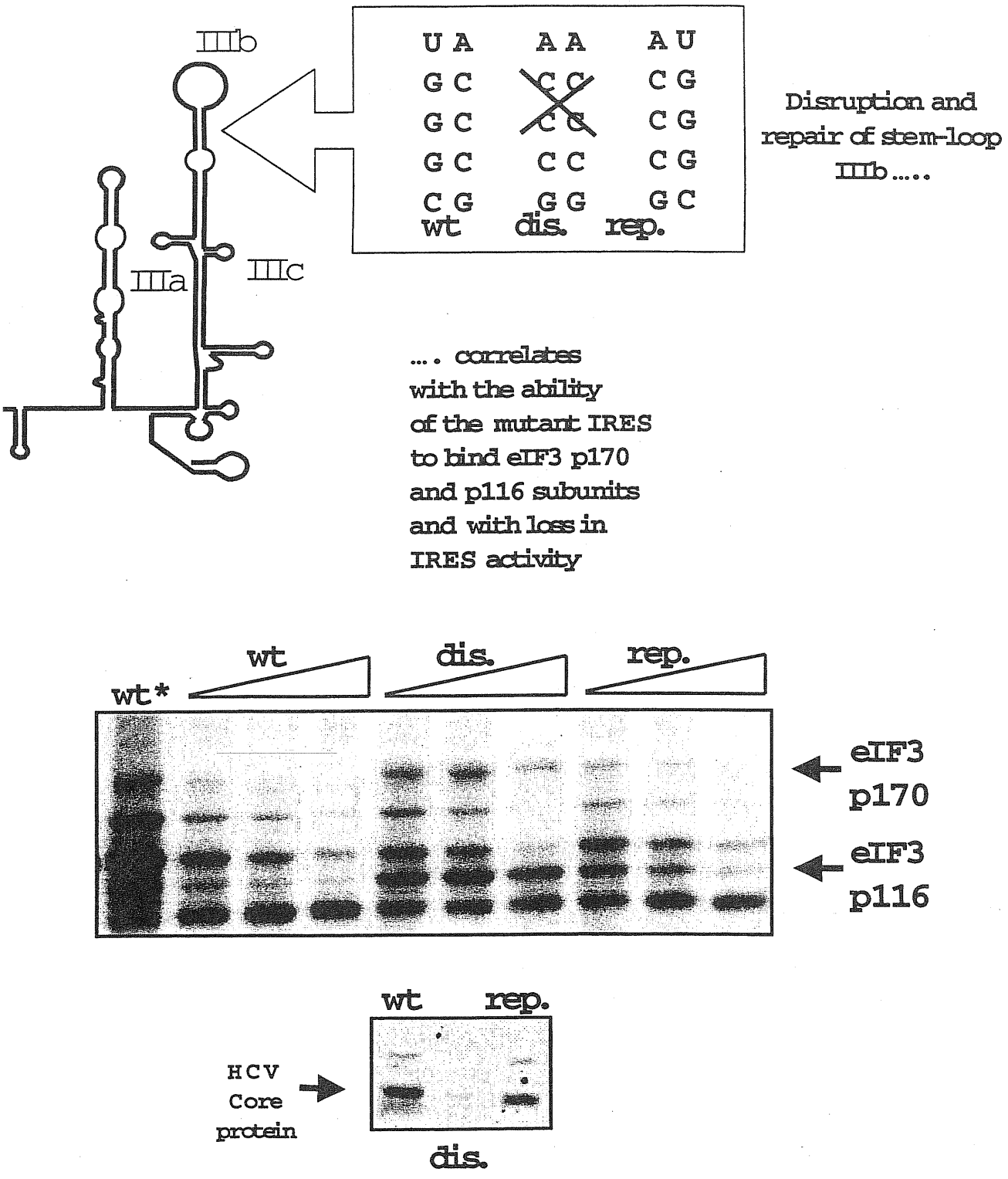


**Figure 8.** Binding of eIF3. Two proteins (p170 and p116)which belong to eIF3 recognize the upper portion of the major domain III. Disruption of the subdomain IIIb abolishes the binding of both proteins and inhibits the ability of the IRES to initiate protein translation. Invertion of the stem portion in IIIb restored the ability to recognize both protein, as shown in a competition assay

addition, it should be noted that transfection efficiencies in Fig.9C, as measured by growth hormone production from the first cistron, were all similar, indicating that all RNAs were equally stable. As positive controls we used both the wild type sequence (5'wt) and the previously described mutant (5'S/L) in which the apical region sequence (IIIb) had been inverted without occurring in a loss of IRES activity (Buratti et al., 1998a). It should be noted that in the *in vitro* assay only the unprocessed form of the core protein can be detected and that in both assays the molecular weight of this protein is slightly higher than the HCV native core protein (25 kDa as opposed to 23 kDa) due to the addition in our constructs of a C-terminal tag sequence (Buratti et al., 1998b).

### 3.2 Secondary structure analysis of the domain III mutants

A necessary control to understand the inability of these mutants to drive IRES translation is represented by the analysis of their secondary structure (and comparing it with the wild type structure). Although the secondary structure of HCV 5'UTR wild-type domain III (shown in Fig. 10) has already been extensively validated based on computer predictions and confirmed by mutational analysis/RNAse probing (Brown et al, 1992; Honda et al, 1996b), this analysis was repeated in order to obtain a reference pattern to compare it with that of the mutants. As shown in Fig. 10 (right panel) the cleavage data obtained in the domain III region (nt.134-290) are in very good agreement with the already existing model (Fig. 10, left panel). In particular, strong T1 and S1 cleavages (indicating single-stranded regions) can be detected in correspondence to the apical loop (IIIb) and the lateral IIIa and IIId loops, with the exception of the proposed loop IIIc. Interestingly, a prominent S1 cleavage can also be detected in the lateral bulge which was described to be protected in footprinting experiments using the entire eIF3 complex (Sizova et al., 1998). Furthermore, all the V1 cleavages (indicating double-stranded regions) detected in this analysis are entirely consistent with the proposed stem structures.

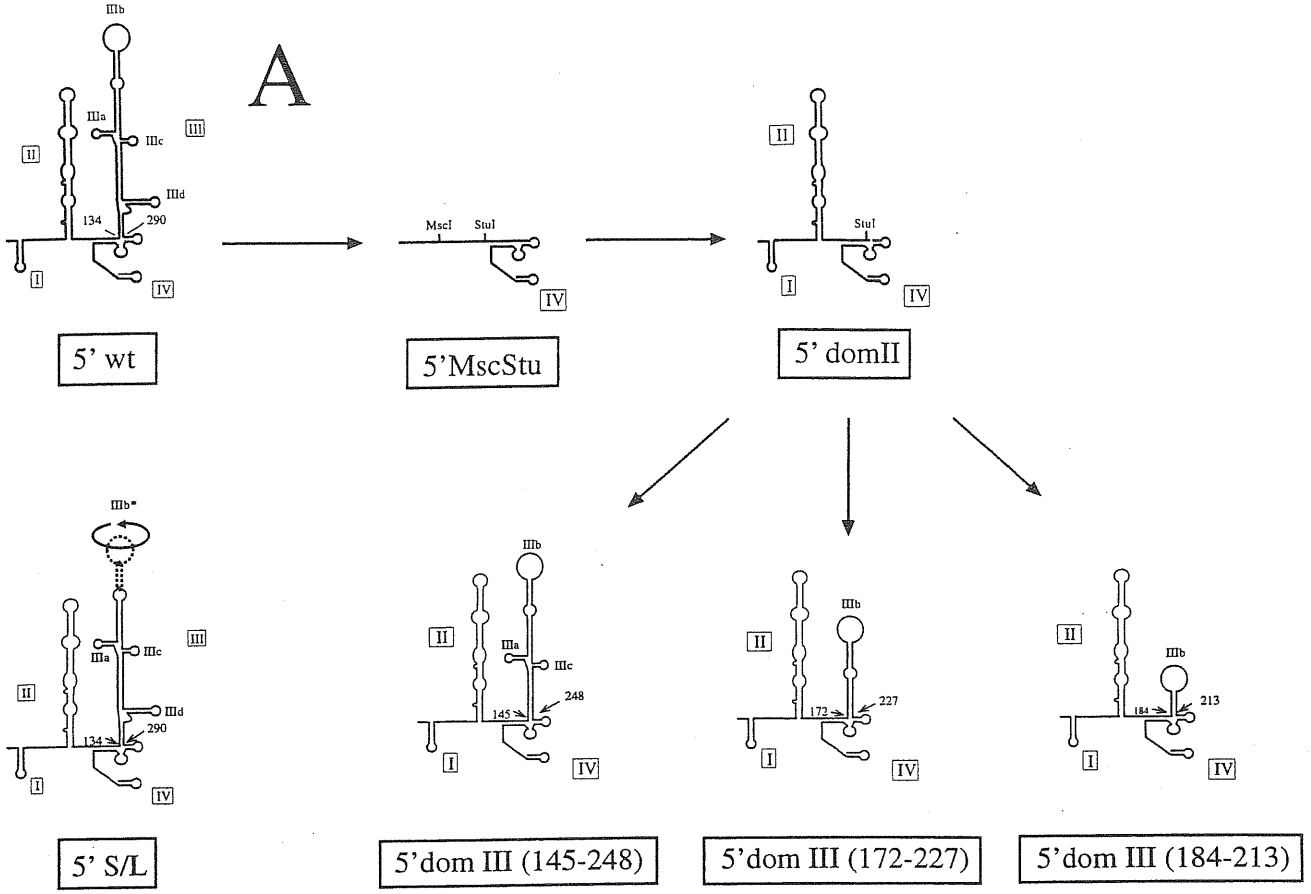


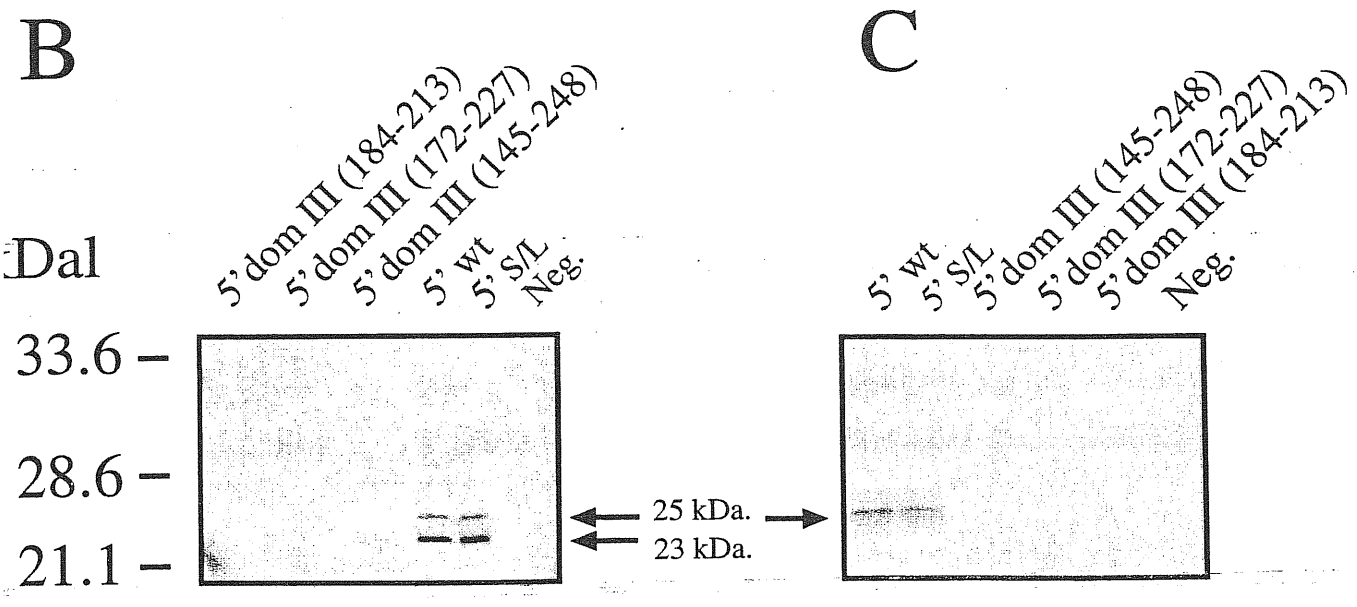


Fig.9A shows a schematic representation of the different domain III mutants. The arrows indicate how each mutant was obtained from the original 5'wt and template sequence (5'MscStu). The three novel mutants contain different regions of domain III: 145-248, 172-227, 184-213. Fig.9B shows the IRES activity of each mutant as assayed in transfection in COS-1 cells. The arrows indicate the position of the processed (23kdal) and unprocessed (25kdal) HCV core protein. The HCV core protein was recognized using MAb B12.F8 (35) and visualised by ECL staining. Fig.9C shows an *in vitro* transcription and translation assay of all three mutants including 5'wt and mutant 5'S/L. The arrow indicates the unprocessed $^{35}$S-labelled HCV core protein (visualised by autoradiography).

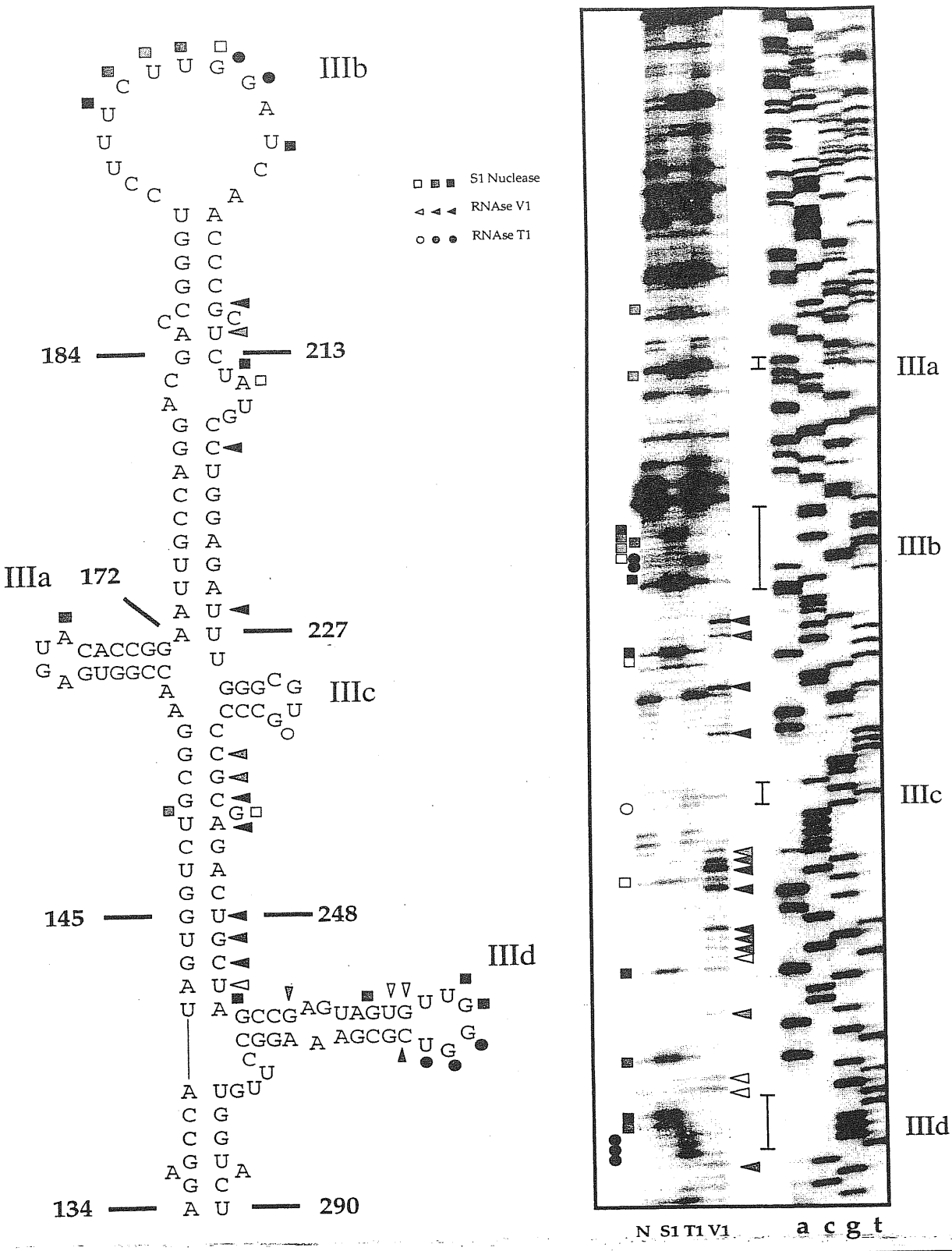


**Figure 10.** Enzymatic determination of the RNA secondary structure of HCV 5'UTR domain III. In vitro transcribed RNA was enzymatically digested with S1 nuclease, T1 and V1 RNAses and reversly transcribed. The RT products were then separated on a 6% polyacrylamide sequencing gel and a sequencing reaction performed with the same primer used for the RT reaction was run in parallel to precisely determine the cleavage sites. Squares, circles, and triangles indicate S1 nuclease, RNAse T1 and V1 cleavage sites respectively. Black, shaded, and white symbols indicate high, medium, and low cleavage intensities. The vertical bars indicate the proposed loop regions of IIIa, IIIb, IIIc and IIId. No enzyme was added to the reaction mixture in lane N. The observed cleavage sites (panel on the right) are reported on the proposed schematic diagram of domain III (panel on the left). Reported on this panel are also the portions of domain III inserted on the template sequence to obtain the three novel mutants.

The same procedure was then used to map the secondary structure of each mutant and the results of this analysis is shown in Fig. 11. Only mutant 5'domIII (145-248) shows an apical cleavage pattern very similar to that of the wild-type RNA. Indeed, not only the single strand cleavages in the loop are conserved but also the V1 specific cleavages in the stem immediately underneath. On the other hand, the apical loop region in mutants 5'domIII (172-227) and 5'domIII (184-213) shows very few, if any, single-strand specific cleavages, showing that a conformational change had occurred. Interestingly, the structure of the 5'S/L mutant shows that in the IIIb mutated region the two G residues in the loop IIIb (present in inverted positions with respect to 5'wt) were recognized by RNAse T1 and that even the mutated stem region presented V1 cleavages, confirming the maintenance of a stem-loop structure similar (but not identical) to 5'wt. Therefore, although the 5'S/L mutant presents a very extensive primary sequence mutation its conformation resembles more the wild type pattern than the two 5'domIII (172-227) and 5'domIII (184-213) mutants.

### 3.3 UV-crosslinking and protein identification using the domain III mutants

It was then of interest to determine how the variation in secondary structure of these mutants was reflected in their ability to bind the previously described p170 and p116/p110 subunits. Fig. 12A shows the UV crosslinking assay of each $^{32}P$ labelled RNA with a ribosomal salt wash extract from COS-1 cells loaded on a 8% SDS-PAGE gel to better visualise high molecular weight proteins. This analysis shows that, as expected, mutant 5'domIII (145-248) was capable of binding both p170, p116/p110 (although with lower efficiency than 5'wt) whilst no binding could be detected for the other two mutants 5'domIII (172-227) and 5'domIII (184-213). The fact that mutant 5'domain III (145-248) showed a structure and binding pattern identical to that of the wild type sequence but was completely incapable of IRES activity made it an ideal target to identify essential cellular factors that bind to (or whose binding is affected by)

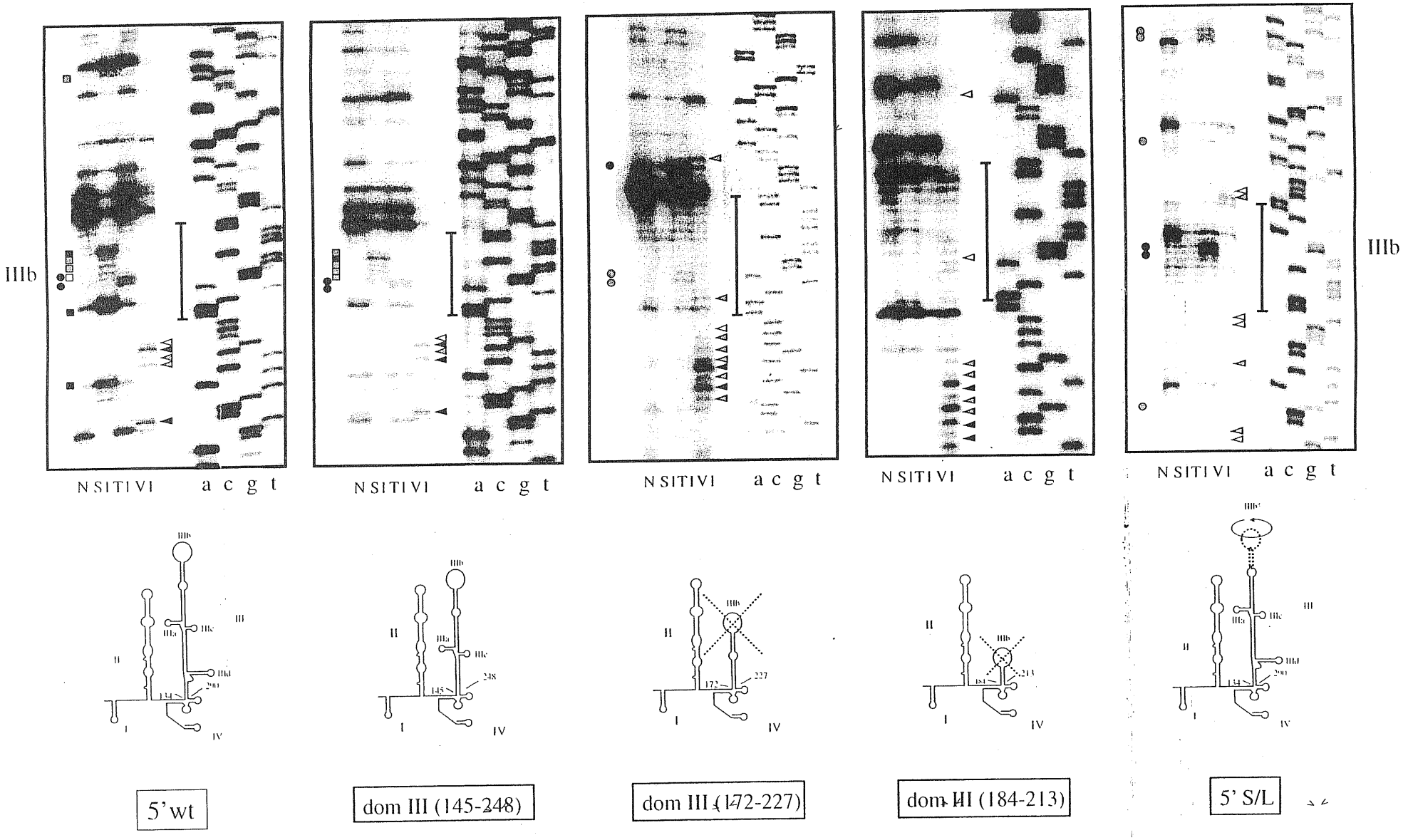


**Figure 11.** RNA secondary structure of the apical portion of each domain III mutants with respect to the wild type and 5'S/L sequence. In vitro transcribed RNAs were enzymatically analyzed as described in the legend to Fig.2. Only the apical stem loop region of domain III is shown and the putative IIIb loop portion is indicated by the vertical bar. The structure of mutants 5'domIII(172-227) and 5'domIII(184-213) are crossed to indicate that the stem loop configuration is not consistent with the RNAse analysis. In addition this figure shows the RNA secondary structure of domain

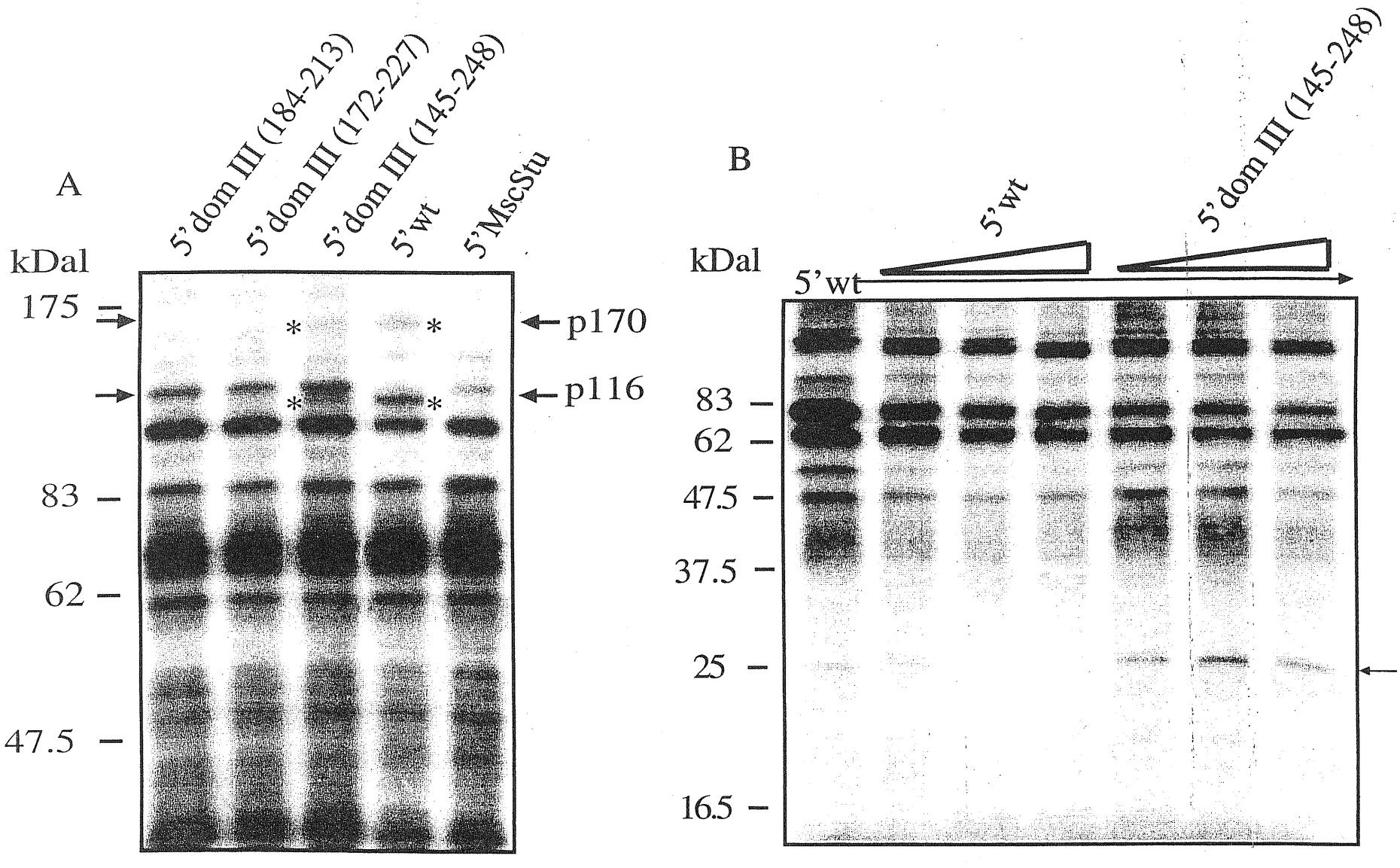


**Figure 12.** UV crosslinking analysis used to identify proteins binding to the wild type HCV RNA and the domain III mutants. Fig.12A shows a UV-crosslinking assay (loaded on a 8% SDS-PAGE gel) using a COS-1 ribosomal salt wash extract with all the mutant UTRs carrying different portions of domain III. The arrow indicates the position of p170 and p116/p110. To better visualise the binding of these subunits we used 5 µg of cold 5'MscStu template RNA as competitor (which had already been reported not to bind p170, p116/p110). Fig.12B shows a competition analysis (loaded on an 12% SDS-PAGE gel) of the proteins bound by labelled 5'wt with cold 5'wt and 5'domIII(145-248) RNA. The arrow indicates the 25 kDal protein that binds labelled 5'wt

the lower missing portion of domain III (principally stem-loop IIId) and which could account for this loss. This possibility was enhanced by the fact that, in addition to eIF3, ribosomal protein S9 had also been detected as binding to domain III (Pestova et al., 1998b; Sizova et al., 1998). In particular, binding of this protein was reported to be reduced by deletions of hairpins IIa and IIIc but not by deletion of hairpin IIIb (Pestova et al., 1998a). Fig. 12B shows a competition analysis performed on the 5'wt labelled RNA using a ribosomal salt wash extract with 5'wt and 5'domIII (145-248) cold RNA as competitor (in 2, 5 and 10 molar excess). and loaded on a 12% SDS-PAGE gel to visualise low molecular weight proteins. In this analysis, a protein of 25kDal apparent molecular weight, consistent with the reported S9 ribosomal protein molecular weight observed in previous studies (Pestova et al., 1998a), was found to bind the 5'wt sequence and could be competed away by cold 5'wt RNA but not by cold 5'domIII (145-248) RNA.

### 3.4 Construction of sub-domain IIId mutants

In order to better investigate the binding requirements for this protein a set of mutants (Fig. 13A) was then prepared which involved inversion of stem-loop IIId sequence (5'IIId S/L), disruption of the principal stem (5'IIId disr.), and its compensatory mutation (5'IIId rep.). Analogously to the apical stem loop mutants these mutants were analyzed for IRES activity both *in vivo* and *in vitro* (Fig. 13B). The results show that none of these mutants displayed IRES activity, including the one bearing the intended compensatory mutation.

### 3.5 Secondary structure study on the sub-domain IIId mutants

Analysis of the secondary structure of each mutant is shown in Fig. 14 and in keeping with the loss in IRES activity both the conformation of the disrupted mutant

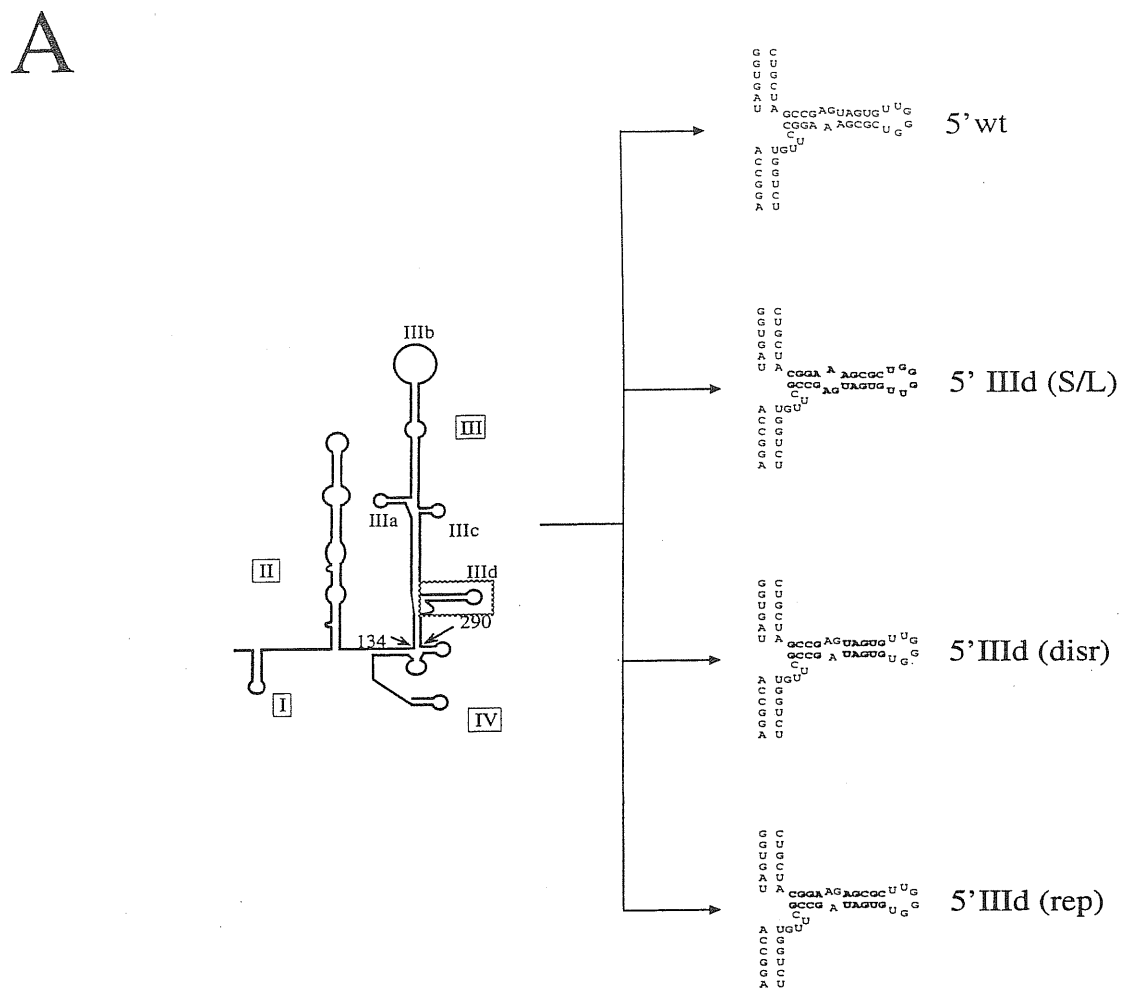


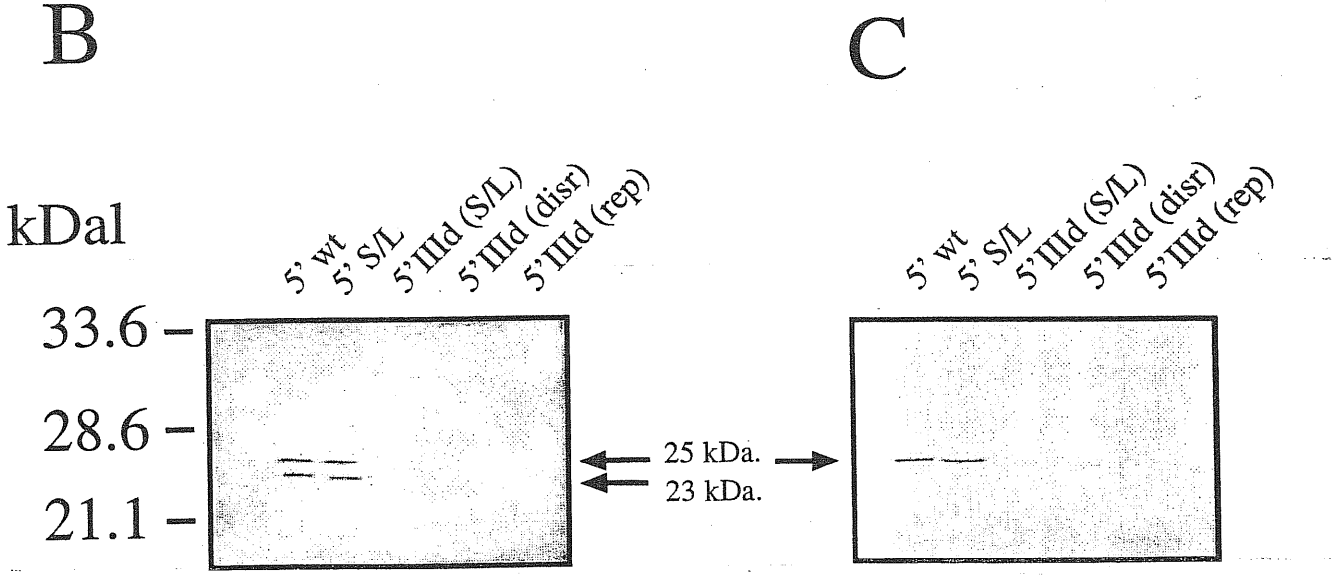


**Figure 13.** Fig 13A shows a schematic representation of the stem-loop IIId mutants 5'domIIId(disr.) 5'domIIId(rep.), and 5'domIIId S/L. Fig.13B shows the transfection in COS-1 cells of these mutant 5'UTRs and the arrows indicate the position of the processed (23kdal) and unprocessed (25kdal) HCV core protein. The HCV core protein was recognized using MAb B12.F8 and visualised by ECL staining. Fig.13C shows an *in vitro* transcription and translation assay of all mutants. The arrow indicates the unprocessed $^{35}$S-labelled HCV core protein (visualised by autoradiography).

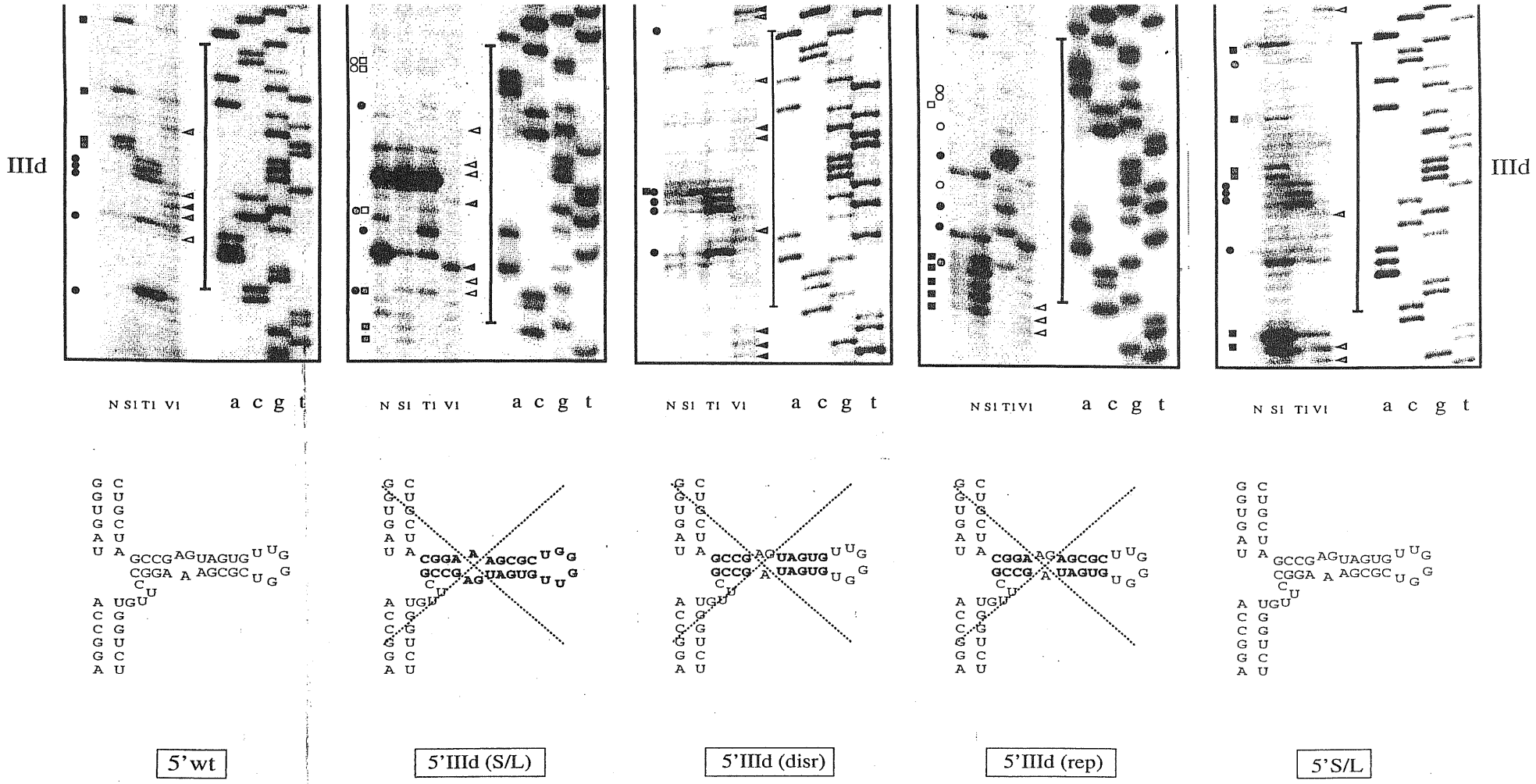


**Figure 14.** RNA secondary structure of the stem-loop IIId mutants with respect to the wild type sequence 5'wt and the 5'S/L mutant. In vitro transcribed RNAs were enzymatically analyzed as described in the legend to Fig.10. Only the lower region of domain III is shown and the putative IIId loop is indicated by a vertical bar. The structure of mutants 5'domIIId(disr.), 5'domIIId(rep.), 5'domIIId S/L are crossed to indicate that the original stem-loop configuration is not consistent with the RNAse analysis.

and that of the putatively repaired mutant fail to mimic that of the wild type sequence or the 5'S/L mutant. The fact that even the supposedly repaired mutant fails to fold again correctly highlights the fact that it is very difficult to predict beforehand the effect of engineered mutations. Fig.14 also shows that the secondary structure of the IIId stem-loop of mutant 5'S/L is identical to that of 5'wt (although this was an expected result considering that the engineered mutation was located in the apical IIIb stem-loop).

### 3.6 UV-crosslinking analysis of the sub-domain IIId mutants

The results of the structural analysis were reflected in the UV-crosslinking assay, as shown in Fig.15: only 5'wt and 5'S/L bind the 25 kDa protein, whilst none of the IIId mutants is capable of doing so. Binding of S9 to the 5'S/L (whose mutation involved only hairpin IIIb) is in keeping with published data that report a reduction of p25 UV-crosslinking following deletion of hairpins IIa and IIIc but not by deletion of hairpin IIIb (Pestova et al, 1998b). These results thus provide a likely reason for the loss in IRES activity experienced by the correctly folded 5'domIII (145-248) mutant and also report for the first time that stem-loop IIId actively participates in the binding of S9 ribosomal protein to HCV 5'UTR.

The fact that distant stem-loops (IIa, IIIc, and in the present work IIId) have been found to affect S9 ribosomal protein binding suggests that, unlike p170 and p116/p110, the binding requirements for this protein might not be present on a single domain. A simple experiment to test this hypothesis was then to see if S9 ribosomal protein binding can still be detected on a HCV 5'UTR in which the sequences of hairpins IIa, IIIc and IIId are present (and unmutated) but in different orientations with respect to the wild type. Therefore, the mutants already described in a previous paper were used in this experiment (Buratti et al., 1998b). In these mutants the position of domain II and domain III on the HCV 5'UTR had been inverted (Fig. 16A) and they did not possess

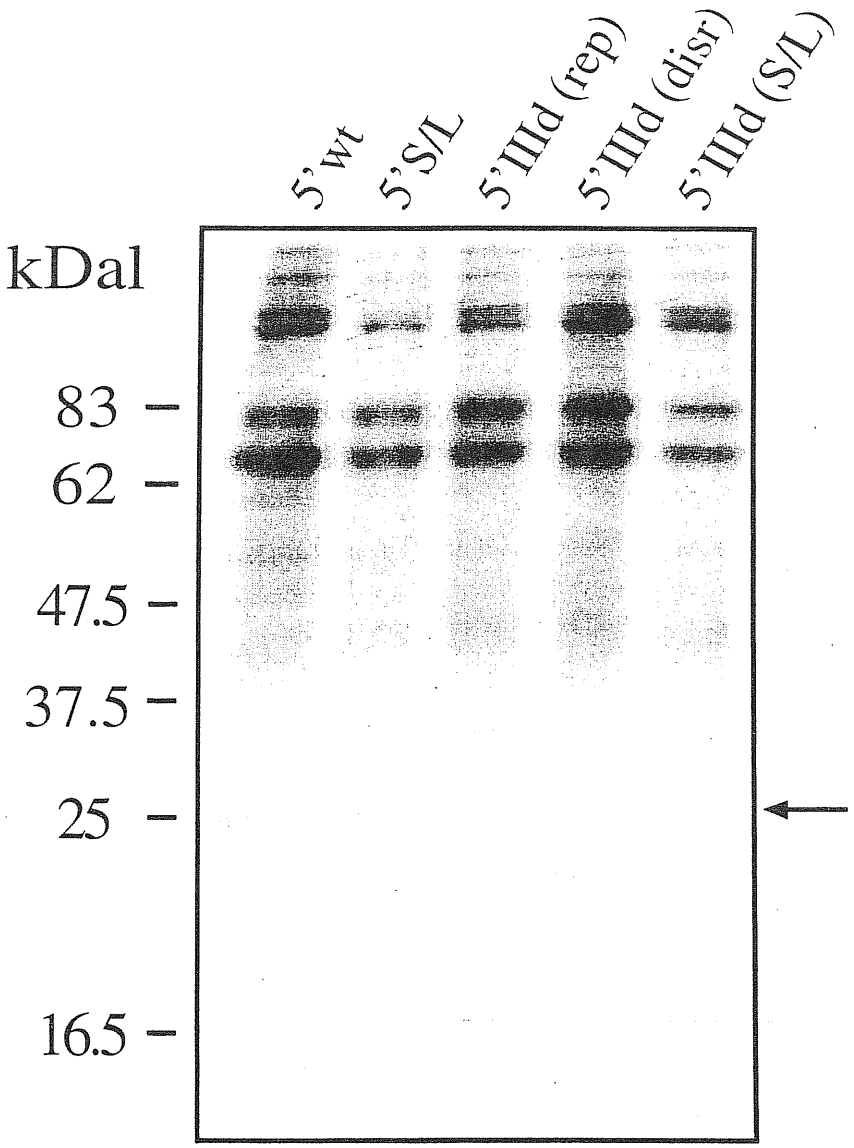


**Figure 15.** This Fig. shows a UV-crosslinking assay (loaded on a 12% SDS-PAGE gel) using a COS-1 ribosomal salt wash extract with all the mutant UTRs carrying different mutations in stem-loop IIId. Binding of the 25kDal protein (indicated by an arrow) could be detected only for the wild type sequence (5'wt) and for mutant 5'S/L. No binding could be observed with the 5'domIIId(disr.), 5'domIIId(rep.), and 5'domIIId S/L mutant. To better visualise this binding we used 5 µg of cold 5'MscStu template RNA as competitor.

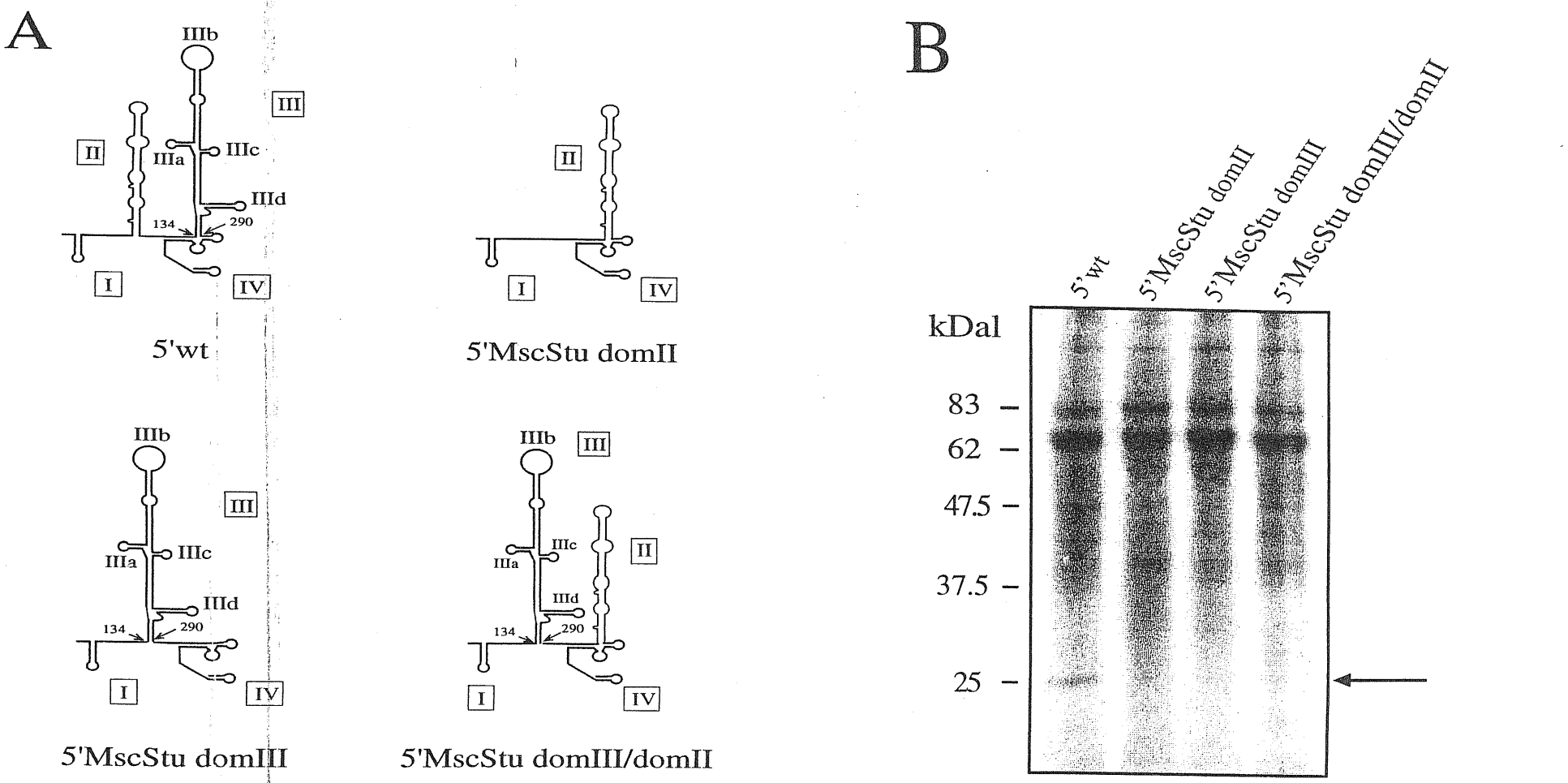


**figure 16.** Fig 16A shows the mutated UTRs used in the part of the study concerning the effect of swapping the positions of domain II and III on the binding of protein S9. The arrows indicate how the different mutants were obtained from the original sequence. Major structural domains are indicated by Roman numerals I-IV. Fig.16B shows a a UV cross-linking assay using a COS-1 ribosomal salt wash extract with all the mutant UTRs carrying different combinations of domain II or III in swapped positions. The arrow indicates the 25kDal protein observed to bind only to 5'wt. No binding could be observed with 5'MscStu dom II, 5'MscStu domIII, and 5'MscStu domIII/domII.

any IRES activity. The results of the UV-crosslinking analysis performed on these mutants (Fig. 16B) shows that only the wild type sequence (5'wt) can bind S9 whilst mutants 5'MscStu domII, 5'MscStu domIII, and 5'MscStu domIII/domII do not bind this protein. It is important to note that both 5'MscStu domIII and 5'MscStu domIII/domII have already been reported (Buratti et al, 1998a) to bind both p170 and p116/p110, and that a secondary structure analysis of their domain IIId structure showed that this hairpin presented cleavage pattern identical to that of the wild type structure (data not shown).

### 3.7 Sucrose gradient analysis of the sub-domain IIId mutants

Finally, the failure to detect UV cross-linking of the S9 protein in these previous mutants could be due to two reasons: the first and simpler explanation is that the 40S ribosomal subunit does not actually bind to the mutant RNAs. Alternatively, the mutant RNAs might be able to bind to the 40S ribosomal subunit but in a different orientation compared to the wild type RNA. In order to differentiate between these two possibilities sucrose-density gradient analysis was performed of the wild type RNA and of representative mutants in the presence of purified 40S subunits. Previous studies have already shown that in order to obtain binding of the 40S ribosomal subunit to the HCV IRES no additional initiation factors are required (Buratti et al., 1998b). The results shown in Fig. 17 demonstrate that a ribosomal complex can only be detected with the wild-type HCV IRES, whilst mutant 5'domIII(145-248) and mutant 5'IIId rep. do not bind to the 40S ribosomal subunit.

### 3.8 Construction of single point mutation on the domain II

As shown, mutation/deletion studies performed on the lower portions of HCV 5'UTR domain III have highlighted the existence of a very close relationship between RNA structure and IRES translational ability. Indeed, even single nucleotide changes in

A

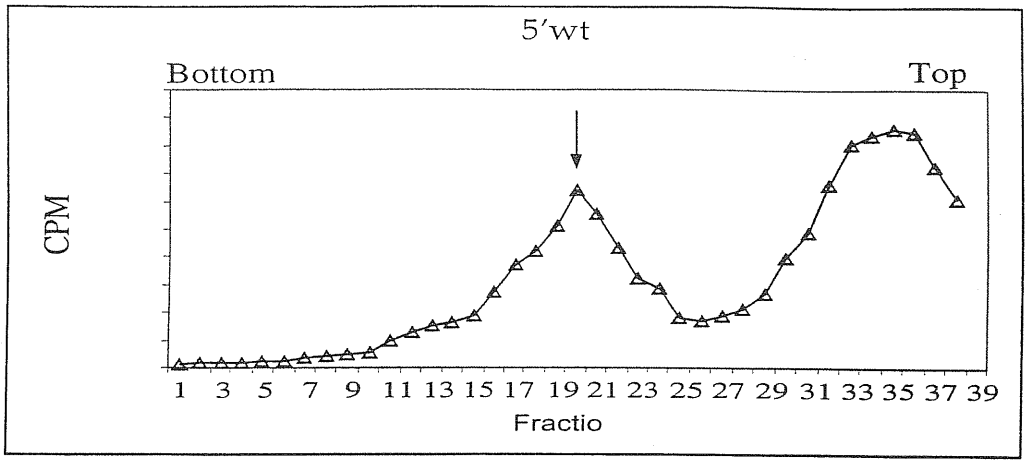


B

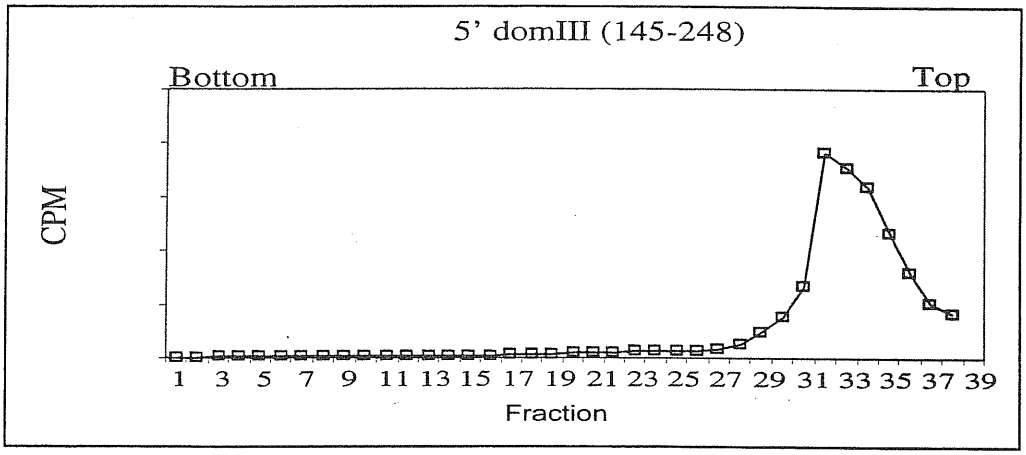


C

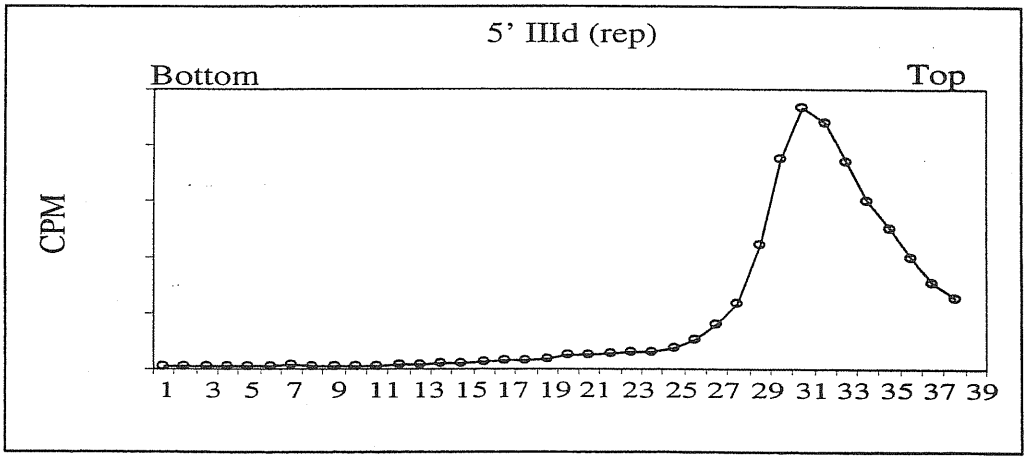


**Figure 17.** Binary IRES-40S ribosomal complex formation on HCV wild type IRES and selected mutants. Assays were performed on a 10-30% sucrose density gradient with labelled RNAs and purified 40S ribosomal subunits. Assays were done using 5'wt (A), 5'domIII(145-248) (B) and 5' IIId (rep) (C) RNAs and with 40S subunits. Sedimentation was from right to left. The position of the binary complexes is indicated by arrow.

selected regions (IIId, IIIe) have been reported to completely abolish IRES activity (Jubin et al., 2000; Psaridi et al., 1999). It was thus interesting to determine whether an analogous situation could also be found in any of the single-stranded regions of HCV domain II. Therefore, two substitutions (A54G and U63G) were inserted in the IIa and IIb bulges of domain II (mut50), as shown in Fig.18. As control, a second mutant (mut297) carrying an A297G substitution in stem-loop IIIe was used. It should been noted that this mutation was previously described to abolish IRES activity (Psaridi et al, 1999).

### 3.9 In vivo and in vitro analysis of mutants mut50 and mut297

Each mutant was then analyzed for translational ability (both *in vitro* and in a transfection assay), for complexing with the 40S ribosomal subunit, and for binding to the S9 ribosomal protein. The latter is of interest because a 25 kDa S9 is the only protein described so far whose degree of UV-crosslinking changes following mutations in the domain II region (Pestova et al, 1998b).

### 3.10 UV-crosslinking analysis of the single point mutation on the domain II

Fig.16A (left panel, lanes 1 to 3) shows a UV-crosslinking assay using a ribosomal salt wash protein extract (RSW) with each labelled RNA. The results show that UV cross-linking of the 25 kDa/S9 protein can be observed for the wild type (5'wt) and mut50 but not mut297. The same result is obtained using a purified 40S subunit preparation (40S) as shown in Fig. 19A (left panel, lanes 4 to 6). A competition analysis was also performed to confirm the specificity of this interaction: Fig. 19A, right panel, shows that in keeping with the direct binding assays only cold 5'wt and mut50 RNAs

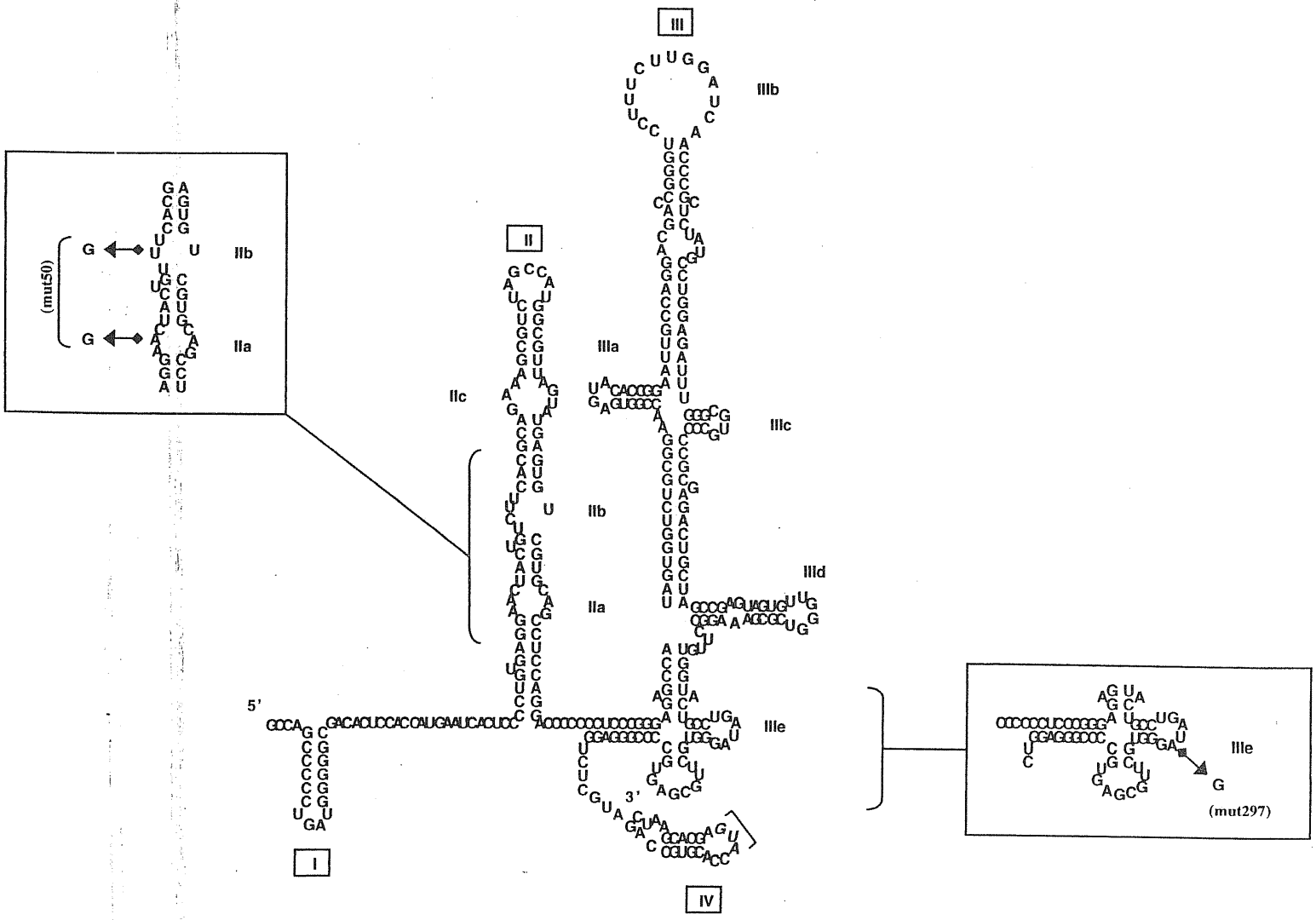


**Figure 18.** Schematic representation of the HCV 5'UTR secondary structure including part of the initiation coding sequence. The boxed regions contain the two initial mutation analysed: mut50 (A54G and U63G), and mut297 (A297G). The principal domains are indicated by roman numerals (I to IV) and single subdomains are also indicated. The translation initiator AUG is underlined.

(but not cold mut297 RNA) can compete for the binding of this protein to the HCV IRES. Both mutants were then analysed for their ability to drive IRES translation. In the case of mut297 we observed a total inhibition in the translation of the HCV core protein both *in vivo* and *in vitro* whilst mut50 showed a level of translation comparable with the wild type (Fig. 19B upper and lower panel). We then analysed by sucrose density gradient the ability of the 40S ribosomal subunit to bind to these mutant RNAs. Fig. 16C shows that mut50 binds the 40S ribosomal subunits with the same efficiency of the wild type RNA (5'wt). On the other hand, mut297 was totally incapable of binding the 40S ribosomal subunits, a result that is totally consistent with the recent crystallographic data that identify IIId/e/f as the regions which contact the 40S platform (Spahn et al., 2001).

### 3.11 Partially or complete deletion of the principal domain II bulges

Because these single-nucleotide mutations in domain II did not affect the translational ability of the HCV IRES a new set of mutants was then prepared in which all domain II bulge regions (IIa, IIb, and IIc) were partially or completely deleted. In addition, two additional mutants in the upper region of domain II were prepared to test the importance of this upper stem-loop portion. A schematic representation of all these mutants is reported in Fig. 20A.

### 3.12 UV-crosslinking and translation efficient analysis of the different domain II mutants

The degree of UV cross-linking of the S9 ribosomal protein to the HCV IRES was then tested. Fig. 20B shows that all deletions introduced in the IIa, IIb and IIc bulges

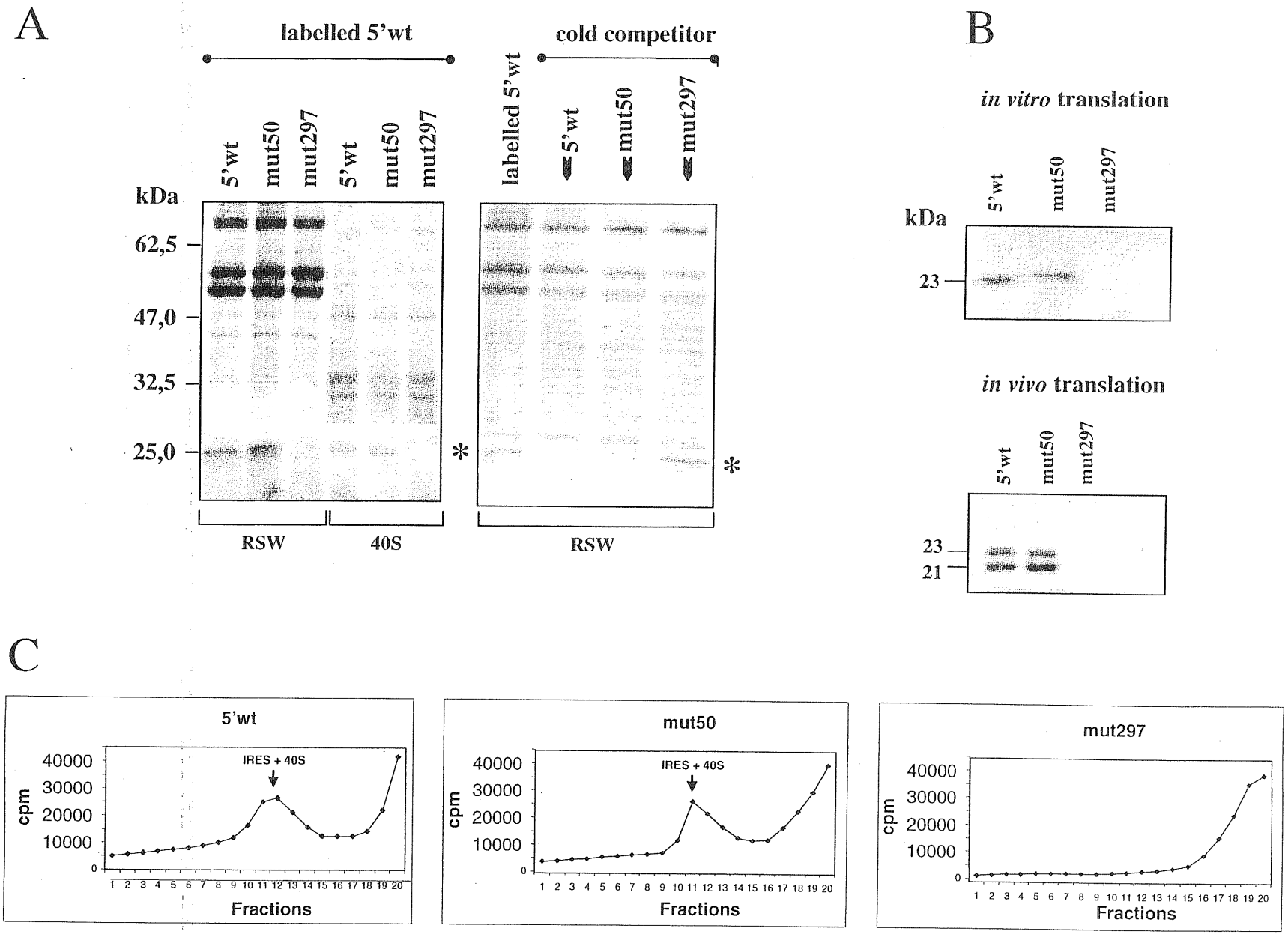
A
labelled 5'wt
cold competitor
5'wt
mut50
mut297
5'wt
mut50
mut297
labelled 5'wt
5'wt
mut50
mut297
kDa
62,5
47,0
32,5
25,0
*
*
RSW
40S
RSW
B
in vitro translation
5'wt
mut50
mut297
kDa
23
in vivo translation
5'wt
mut50
mut297
23
21
C
5'wt
IRES + 40S
cpm
40000
30000
20000
10000
0
1 2 3 4 5 6 7 8 9 10 11 12 13 14 15 16 17 18 19 20
Fractions
mut50
IRES + 40S
cpm
40000
30000
20000
10000
0
1 2 3 4 5 6 7 8 9 10 11 12 13 14 15 16 17 18 19 20
Fractions
mut297
cpm
40000
30000
20000
10000
0
1 2 3 4 5 6 7 8 9 10 11 12 13 14 15 16 17 18 19 20
Fractions

Figure 19

**Figure 19.** Fig 19A (left panel) shows a UV-crosslinking assay using COS-1 ribosomal salt wash extract (RSW lane 1-3) and a purified HeLa 40S ribosomal subunit extract (40S lanes 4-6) in the presence of labelled mut50, mut297, and 5'wt RNAs. A 25 kDa protein is observed to bind only to mut50 (lanes 2 and 5) and 5'wt(lanes 1 and lane 4) but not mut297 (lanes 3 and 6). The right panel shows a competition experiment using cold 5'wt, mut50 and mut297 RNA in the presence of labelled 5'wt and ribosomal salt wash (lane 1, no competitor). Each cold RNA was used at 5 times molar excess. The position of the 25 kDa protein is indicated by an asterisk. Fig 19B show the *in vitro* and *in vivo* IRES activity of each mutant assayed both in a rabbit reticulocyte lysate (RRL) system (upper panel) and in a transfection assay in COS-1 cells (lower panel). In the first assay only the unprocessed 35S-labelled HCV core protein is visualized by autoradiography whilst in the second assay the processed (21 kDa) and non processed (23 kDa) HCV core proteins are visualized by western blot. The two proteins were recognized using MAb B12.F8 and detected with ECL staining. Fig 19C shows an analysis of the binary IRES-40S ribosomal complex formation on 5'wt, mut50, and mut297 labelled RNAs. Assays were performed on a 10-30% sucrose density gradient with purified 40S ribosomal subunits. The position of the binary complexes is indicated by an arrow. Sedimentation was from right to left.

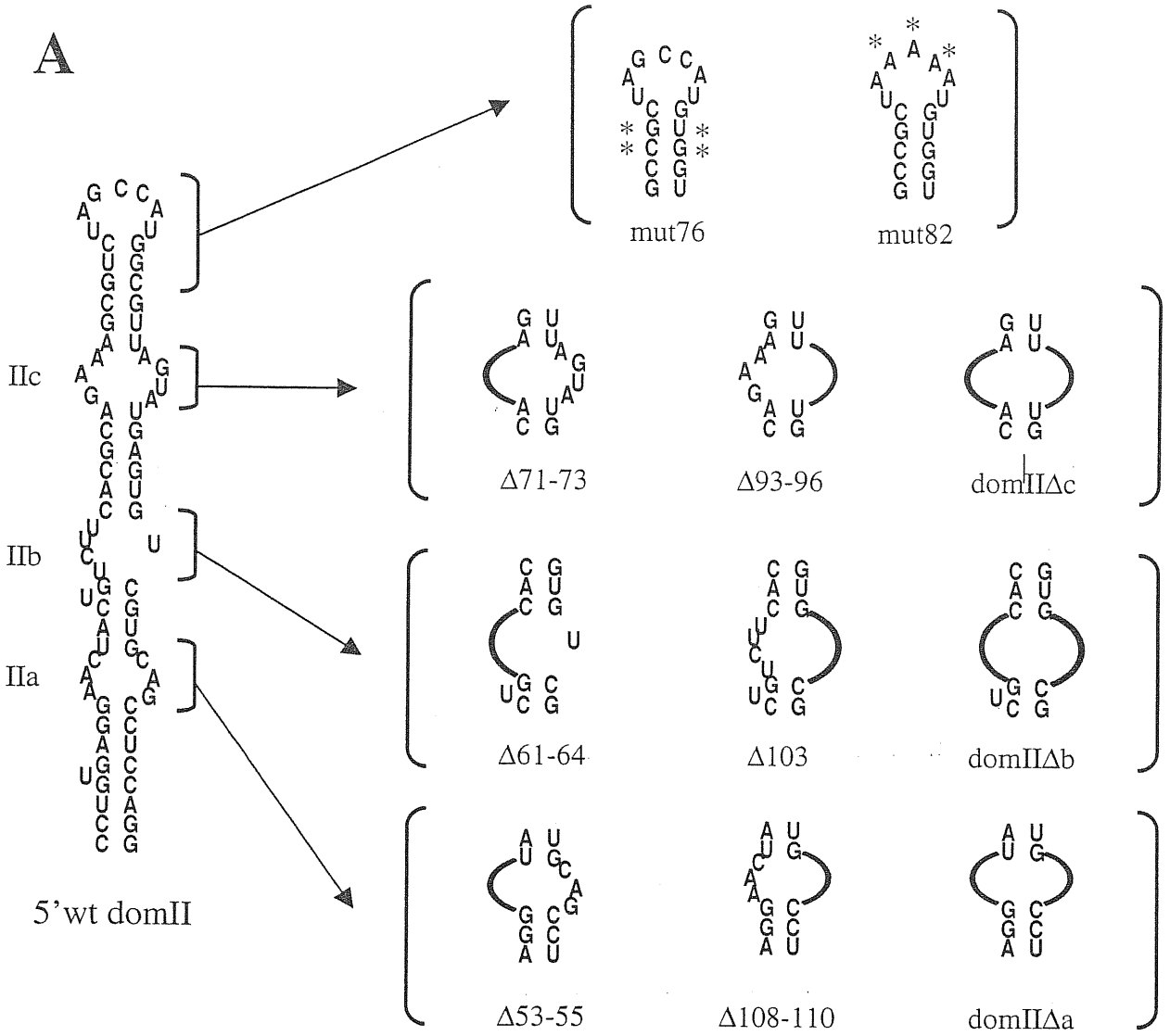
A
mut76
mut82
IIc
IIb
IIa
Δ71-73
Δ93-96
domIIΔc
Δ61-64
Δ103
domIIΔb
Δ53-55
Δ108-110
domIIΔa
5'wt domII

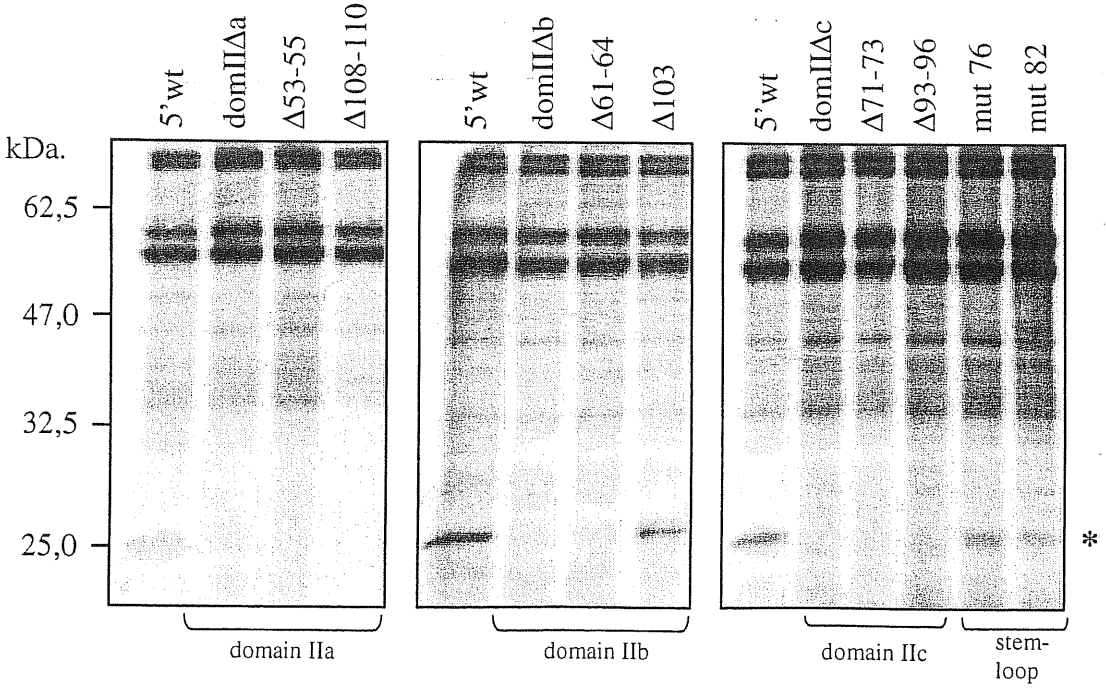
B
5'wt
domIIΔa
Δ53-55
Δ108-110
5'wt
domIIΔb
Δ61-64
Δ103
5'wt
domIIΔc
Δ71-73
Δ93-96
mut 76
mut 82
kDa.
62,5
47,0
32,5
25,0
*
domain IIa
domain IIb
domain IIc
stem-loop

Figure 20

**Figure 20.** Fig 20A shows a schematic representation of the wild type domain II of HCV 5'UTR and of the mutant structures used in this study. The arrows indicate how each series of mutants was obtained from the original 5'wt sequence by selectively deleting the three bulge regions either partially or completely. In addition, two mutants in the apical stem-loop region of domain II (mut76 and mut82) are shown. Fig 20B shows a UV-crosslinking analysis of all reported mutants in the presence of COS-1 ribosomal salt wash extract. The asterisk indicates the position of the S9 ribosomal protein.

abolished the UV cross-linking signal from the S9 ribosomal protein with the only exception of a single nucleotide deletion in bulge IIb (Δ103) and in the two upper stem-loop mutants (mut76 and mut82). In order to investigate the effect of these mutations on the efficiency of the HCV-IRES translation we transfected each mutant in COS-1 cells in the pSV GH bicistronic system (Buratti et al., 1998b), which used as reporter protein the HCV core protein itself. Figure 21A shows that the translation efficiency of these mutated IRES was variable. In particular, mutants domIIΔa, Δ53-55, and Δ93-96 showed a complete lack of IRES translation. On the other hand, mutants Δ108-110, domIIΔb, Δ61-64, domIIΔc, and Δ71-73 retained an intermediate level of IRES activity (ranging between 22 to 42%) (Fig. 21B). Finally, the mutants that showed no or little decrease in the degree of S9 crosslinking (mut76 and mut82, and mutant Δ103) showed translation efficiencies comparable to that of the 5' wt (Fig. 21B).

### 3.13 Sucrose gradient analysis of the domain II mutants

It was then tested whether this variability in IRES activity was the result of an incorrect assembly of the 40S-IRES binary complex. However, sucrose density centrifugation analysis performed by mixing labelled RNA with purified 40S subunit showed that all mutants were capable of complexing with the ribosomal subunit (Fig. 22). The similarity of all 40S-5'UTR binary complex profiles in the sucrose gradient analysis suggested that none of the mutations introduced in domain II could affect the binding of the 40S subunit to the HCV RNA, a result that is consistent with a recent study in which no changes in binding affinity of the 40S subunit were measured for an IRES with the entire domain II has been deleted (Kieft et al., 1999).

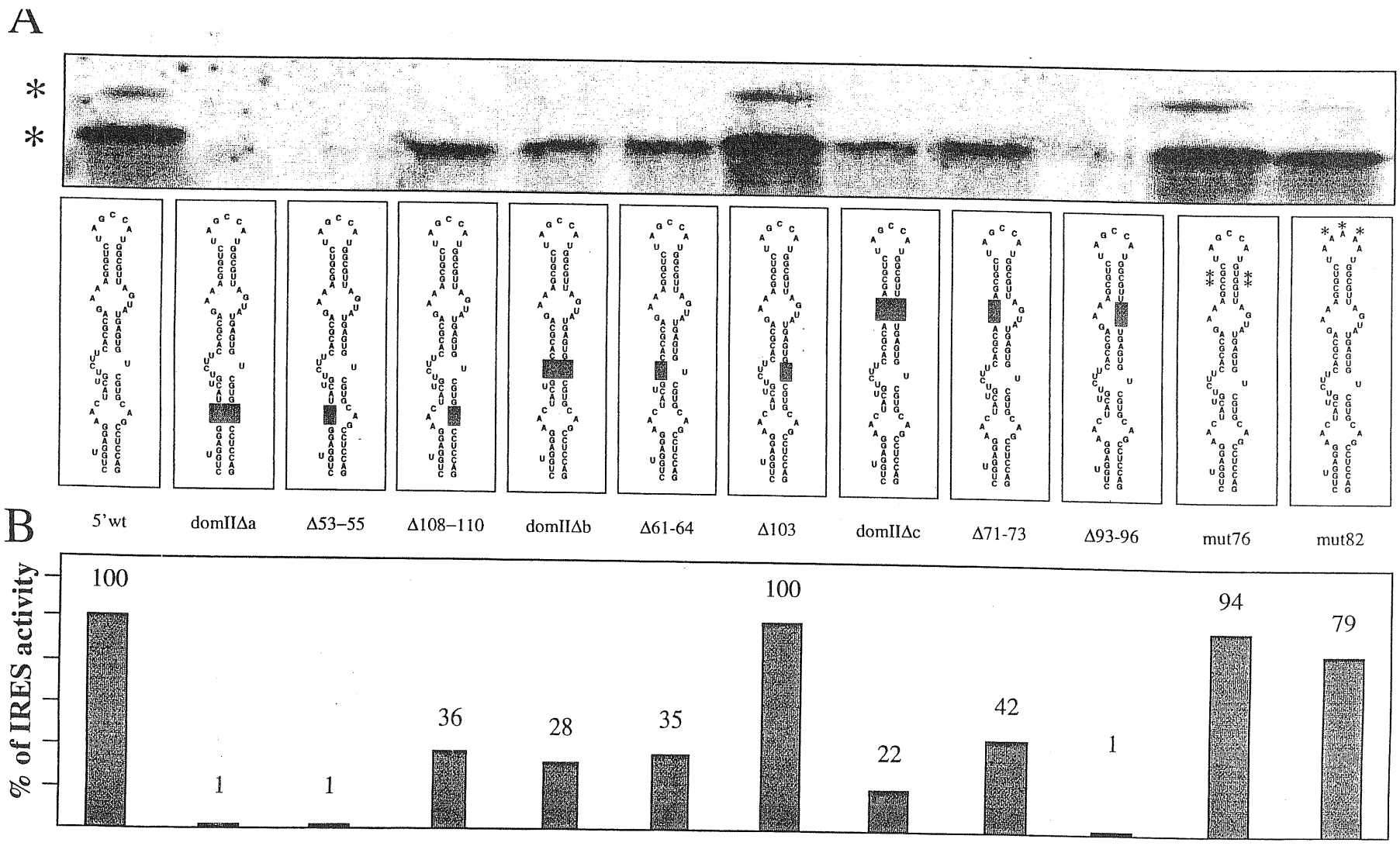


**Figure 21.** Fig 21A shows a western blot following a transfection assay in COS-1 cells of the different 5'-UTR mutants used in this study. The two bands (indicated by an asterisk) represent the processed (21 kDa) and unprocessed (23 kDa) core proteins, which were recognized using MAb B12.F8 and visualized by ECL staining. In the middle panel a schematic representation of these different domain II mutants is reported for easier reference. Fig 21B, Relative quantification of the amount of core protein produced by each mutant.

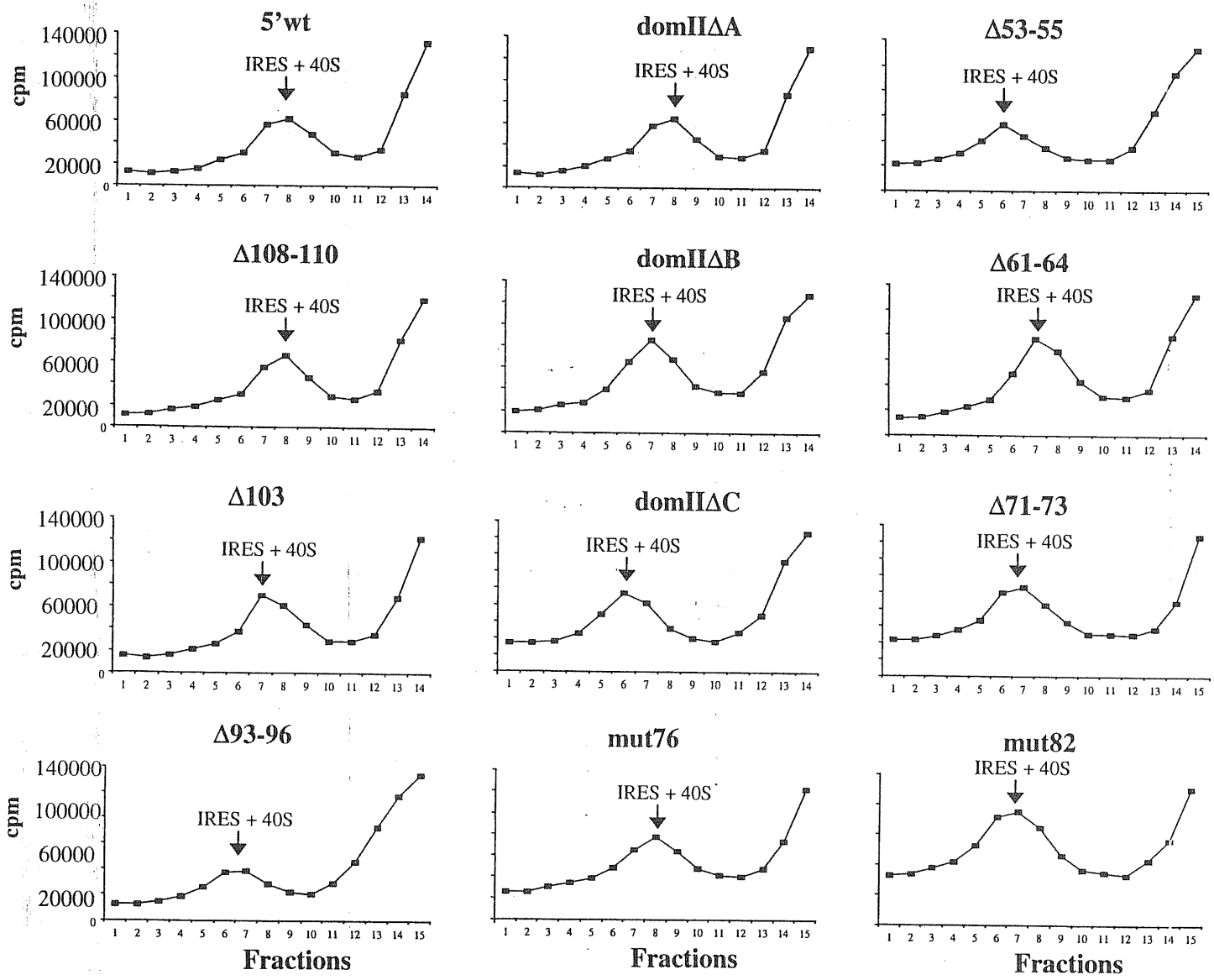


**Figure 22.** Sucrose gradient centrifugation analysis of each domain II mutant. The arrows indicate the binary IRES-40S ribosomal complexes. Assays were performed on a 10 to 30% sucrose gradient with labelled RNAs and purified 40S ribosomal subunit. Complexes were resolved by centrifugation through a 10 to 30% sucrose gradient. The radioactivity of gradient fractions was determined by Cerenkov counting. Sedimentation was from right to left.

### 3.14 Mutation of the initiator AUG and footpringting analysis

In order to rule out the existence of subtler changes in the 40S subunit positioning on the HCV IRES, footprinting analysis was performed on two representative mutants (Δ71-73 and domIIΔa) which displayed 42% and no IRES activity, respectively. The analysis, shown in Fig. 23A, demonstrates that the inhibition of RNase T1 cleavages on the IIId region (GGU-265-267) following incubation with the 40S ribosomal subunit is identical in all three IRESs, irrespective of their translational ability.

In addition, it was also checked whether a possible shift in ribosome positioning following mutations in the domain II region could be reflected in the response following mutations in the initiator AUG positioning (within the potential translation window as determined by Rijnbrand et al, 1996. For this purpose, the AUG in the wild-type IRES and the Δ71-73 mutant was shifted by 3 nucleotides in either the downstream and upstream direction and the original AUG inactivated by a AUG to AAA mutation). The Δ71-73 mutant was chosen on the basis that it displayed an intermediate level of IRES efficiency (42%) which made it ideal to detect eventual further losses (or improvements) following the shift in AUG positioning. As shown in Fig. 23B, transfection analysis of these mutant IRESs demonstrated that in all cases the ability to translate is completely abolished.

### 3.15 Secondary structure analysis of the domain II mutants Δ71-73 and ΔIIa

Finally, in order to find further differences that might correlate with the translational efficiency of these mutants the influence of these two deletions (Δ71-73 and domIIΔa) on the domain II secondary structure was measured. A secondary structure analysis of these two mutants was then performed using double-stranded (RNAse V1)

**Figure 23.** Fig 23A shows an enzymatic footpronting of the 40S-IRES complex of the 5'wt, Δ71-73 and domΔIIa. The cDNA products obtained by primer extension were run on a polyacrylamide gel to show the RNAse T1 sensitivity of these RNAs either alone (lanes 2, 5 and 8) or in the presence with the 40S subunit (lanes 3, 6 and 8). A dideoxy sequence using the same primer of the RT-extension analysis was run in parallel. The protected region (GGU-265-267) is indicated on the right. Fig 23B shows the translation efficiency of four AUG mutants (wt-aug339, wt-aug345, Δ71-73/aug339 and Δ71-73/aug345) in which the initiator AUG was mutated to AAA and a novel AUG codon (boxed in the schematic diagrams) introduced three nucleotides away either in the 5′ or the 3′ direction. The amount of reporter core protein synthesized by each mutant was determined by western blot using the B12.F8 Mab.

and single-stranded specific (RNAse T1 and S1 Nuclease) enzymes, as reported in Fig. 24. First of all, it should be noted that the control cleavages in the wild-type domain II are completely consistent with the latest structural model (Honda et al., 1999a). Most interestingly, deletion of the Δ71-73 region result in a substantially small degree of structural change. In particular, the only difference from the wild-type structure is represented by the appearance of a prominent T1 cleavage in correspondence to the G present in the other half of the IIc bulge (nt.93-96). Nonetheless, cleavage of the apical bulge (nt.80-86) in the Δ71-73 is unchanged as compared to the wild-type and the V1 cleavages are consistent with a conservation of the double-stranded wild-type regions. On the other hand, following deletion of the IIa bulge (domIIΔa) the secondary structure of domain II undergoes a drastic structural change that eliminates most of the RNAse cleavages which were obtained for the wild-type domain.

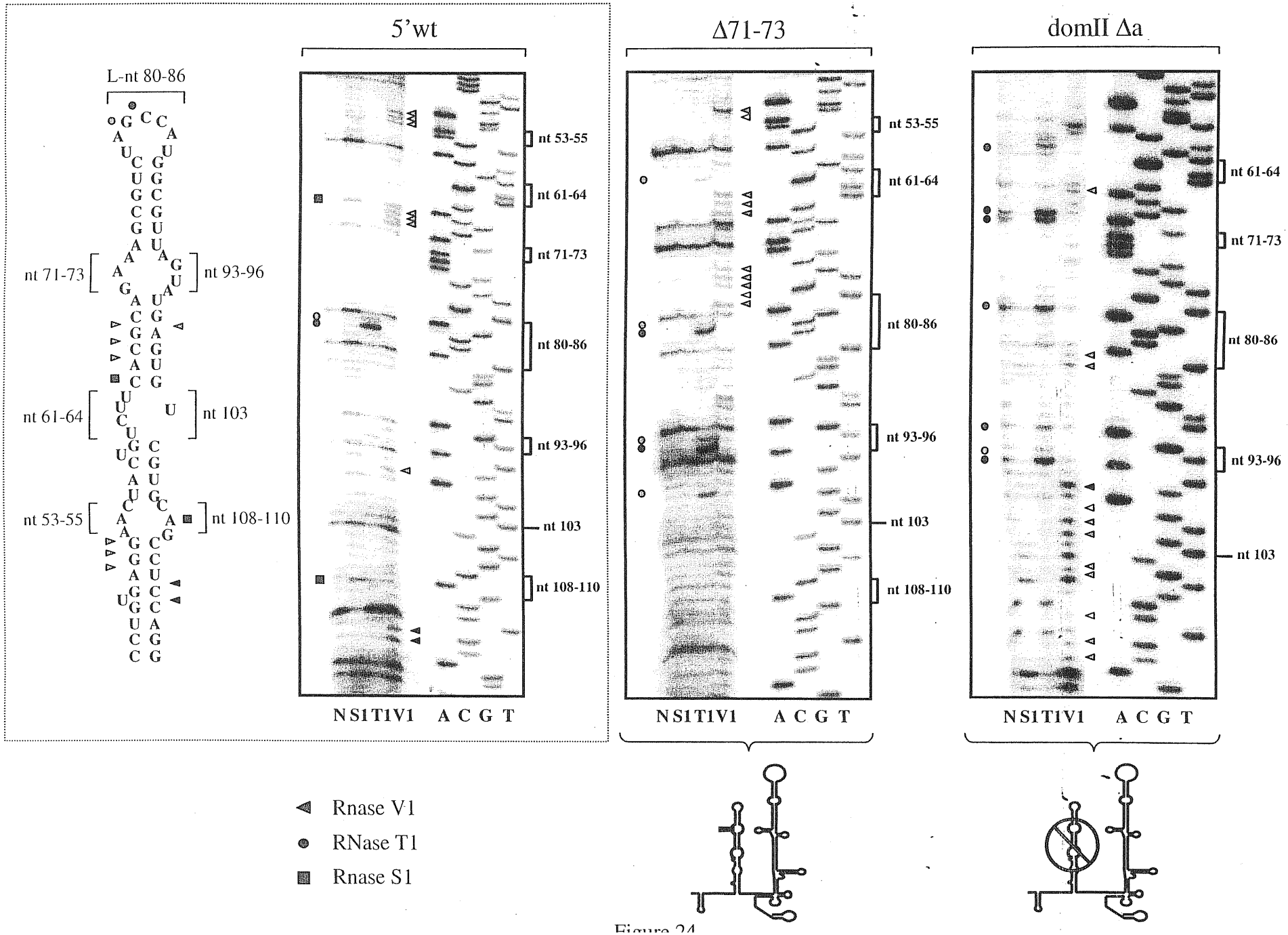
5'wt
Δ71-73
domII Δa
L-nt 80-86
nt 71-73
nt 93-96
nt 61-64
nt 103
nt 53-55
nt 108-110
nt 53-55
nt 61-64
nt 71-73
nt 80-86
nt 93-96
nt 103
nt 108-110
N S1 T1 V1 A C G T
Rnase V1
RNase T1
Rnase S1

Figure 24

**Figure 24.** Enzymatic determination of the RNA secondary structure of HCV 5'UTR domain II for the wild type sequence (5'wt) and the two mutants Δ71-73 and domIIΔa. In vitro transcribed RNA was enzymatically digested with S1 nuclease, T1 and V1 RNAses and reversly transcribed using a 5' end labelled oligo . The RT products were then separated on a 6% polyacrylamide sequencing gel. A sequencing reaction performed with the same primer was run in parallel to precisely determine the cleavage sites. Squares, circles, and triangles indicate S1 nuclease, RNAse T1 and V1 cleavage sites respectively. Black and shaded symbols indicate high and medium cleavage intensities. The vertical bars indicate the proposed bulge and loop regions of domain II. No enzyme was added to the reaction mixture in lane N. The observed cleavage sites in the wild type sequence (5'wt) are reported on the proposed schematic diagram of domain II (panel on the left).

# CHAPTER 4

## DISSCUSION

Functional and mutational studies performed on the HCV 5'UTR region coupled with data obtained from UV-crosslinking and structural analyses have allowed to gain substantial insight concerning HCV IRES function, as recently reviewed in (Hellen and Pestova, 1999; Kieft et al., 1999; Spahn et al., 2001). In particular although, several cellular factors have been found to specifically bind its structure, the HCV IRES has been recently shown to share a similarity with the mechanism of translation initiation in prokaryotes (Pestova et al., 1998b). This study has characterized in detail the binding to the HCV 5'UTR of two subunits of eukaryotic initiation factor eIF3 and of ribosomal protein S9 with regards to conservation of RNA secondary structure. In addition, we have investigated the role played by domain II and provided direct evidence that it plays an important role in HCV translation.

Concerning eIF3, the effect of secondary structure on the binding of the two subunits had already been analyzed preliminarily in a previous study in which it was shown that binding could still occur in an isolated domain III sequence and that it could be impaired by mutations which were predicted to disrupt the RNA folding of the apical stem-loop IIIb (Buratti et al., 1998b). This study showed that binding of the two previously described eIF3 subunits (p170 and p116/p110) could be achieved even when significant lower portions of domain III are missing. Moreover, it was shown that a key element in this recognition is provided by whether or not the apical stem loop RNA sequence is able to fold in the correct secondary structure. In fact, RNAse mapping of the 5'UTR secondary structure shows that nt.145-248 can fold autonomously in the

correct RNA conformation and can then bind both subunits, an observation that definitively identifies this region as possessing the minimal sequence and structural features necessary for recognition of these subunits. This result is in agreement with the footprinting data recently published by other groups (Kieft et al., 1999; Sizova et al., 1998) which not detect any protection in the HCV IRES outside the apical domain III region. It is also of particular interest the observation that mutants which contain sizable portions of the apical stem-loop sequences previously identified as important for this interaction (nt. 172 to 227 and nt. 184 to 213) were not able to bind either p170 or p116/p110. This observation was not totally expected if we consider the fact that the previously described 5'S/L mutant (in which the sequence of the apical stem-loop was inverted) had retained the ability to bind p170 but had lost the ability to bind p116/p110 (Buratti et al., 1998b). Therefore, if the recognition of p170 and p116/p110 had been predominantly dependent on the primary sequence some binding could still have taken place in the two 5'domIII (172-227) and 5'domIII (184-213) mutants. The fact that no binding occurred finds an explanation in the secondary structure of these mutants which, as opposed to the one of mutant 5'S/L, revealed that in their case the structure of the apical stem loop had not been preserved. On the other hand, the structure of the 5'S/L mutant had conserved an unexpected similarity (considering the extent of the primary nucleotide changes) to the wild type conformation). Taken together, these results show that conservation of secondary structure is a fundamental necessity to obtain protein binding and that it possesses just as great importance as the primary nucleotide sequence. In particular, the results show that conserving the one without the other (irrespectively) is not sufficient to obtain correct binding.

The fact that the correctly folded 5'domIII (145-248) mutant was not capable of IRES translation (although its binding and structural profile are most similar to those of 5'wt, even more so than those observed for the 5'S/L mutant) was also indicative that the missing lower sequence is probably involved in the binding of some other essential cellular factor. By UV-crosslinking analysis we have then identified a 25kDal protein, whose molecular weight is consistent with the molecular weight of the S9 ribosomal protein, that binds to the 5'wt sequence but which cannot be competed away by the 5'domIII (145-248) mutant. In this particular region the most prominent feature is represented by the IIId stem-loop.

Up to now, an increasing body of evidence shows that the majority of hairpins located on the HCV 5'UTR is involved in the formation of the RNA-protein interactions that allow the IRES translation to take place. In fact, hairpins IIIb (Buratti et al., 1998b), IIIc (Pestova et al., 1998b; Tang et al., 1999), and recently IIIe (Psaridi et al., 1999), have been demonstrated to be important for efficient IRES activity. Therefore, it was investigated whether the integrity of hairpin IIId was also important for IRES activity and whether its disruption affected S9 ribosomal protein binding. The results show that mutations of hairpin IIId which cause both a sequence and structural change lead to undetectable levels of IRES activity in conjunction with the loss of S9 protein binding. The analysis of IRES-40S binary ribosomal complex showed that mutant 5'domIII(145-248) and mutant 5'IIId rep. do not bind to the 40S ribosomal subunit, thus providing a functional explanation for the lack of binding. Notably, it is also indicative that mutant 5'S/L that was observed to be capable of IRES translation showed a IIId cleavage pattern similar to that of the wild-type sequence and can bind S9, providing an additional explanation of why this mutation did not affect the translational activity.

The fact that binding of the S9 ribosomal protein was already reported to be affected by deletion of hairpins IIa, and IIIc (Pestova et al., 1998b) and IIId suggested that the S9/ribosome interaction involves the tertiary folding of the RNA structure. In this respect, using small angle X-ray crystallography Kieft et al (1999) have shown that the HCV IRES possesses indeed a higher order structure of spatially organized recognition domains in the absence of cellular factors (Kieft et al., 1999). Indeed, the S9/ribosome interaction with the tertiary structure was further analyzed by studying the binding pattern in mutants already used in a previous work, where the position of wild type domain II and domain III had been inverted on a 5'UTR template without introducing mutations in their primary sequence (Buratti et al., 1998b). The UV-crosslinking analysis shows that the simple change of orientation of these domains with conservation of sequence and RNA structure can abrogate binding of the 40S ribosomal subunit.

In this respect, the recently published structural map of the HCV IRES bound to the 40S ribosome obtained using cryo-electron microscopy (Spahn et al., 2001) has increased substantially our insight on the role played in the translation mechanism by each of the IRES domains. A side from the IIId/e/f core of domain II was found to be responsible for the induction of a conformational change in the 40S subunit which could play an important role in translation initiation by holding in position the HCV coding RNA in the decoding site of the ribosome until the translational machinery is correctly assembled (Spahn et al., 2001).

It should be noted that mutational analysis has been used in the past to determine which role specific domain II nucleotide sequences played in efficient IRES translation (Fukushi et al., 1997). However, the design of these experiments were based on an

incorrect domain II structure with the stem and bulges in different positions and the results of these previous studies is of difficult interpretation, owing to the fact that the position of the stem and bulges has been considerably changed compared with the initial predictions (Brown et al., 1992; Honda et al., 1999a; Honda et al., 1996a). Therefore, a systematic mutational study concerning was performed on the latest secondary structure proposed for domain II.

Sucrose-gradient analysis of the IRES/40S complexes formed these mutants showed that all variant sequences had comparable ability to form valid complexes, a result that was confirmed by footprinting analysis on selected mutants. This conclusion is consistent with a recent study which analysed an HCV IRES mutant in which domain II had been entirely deleted and this did not result in any change of 40S binding affinity to the HCV IRES (Kieft et al., 1999). Nonetheless, almost all our deletions have the ability to decrease the degree of UV cross-linking of the S9 ribosomal protein to the HCV RNA, a possible indication that in these mutants the 40S conformational change has not taken place (Spahn et al., 2001). This decrease in IRES efficiency is particularly evident in the IIa lower region. Interestingly, in the model proposed by Spahn et al. (2001) this region is mapped near the location of the coding RNA in the mRNA binding groove. It is then tempting to speculate this result may reflect this nearness. However, correlation between loss of S9 degree of UV-crosslinking and translational ability is not complete. In fact, in several mutants where S9 UV cross-linking was abolished we have observed a small to moderate translation efficiency. Secondary structure analysis of these mutants has shown that a correlation can be established between maintenance of correct domain II secondary structure and translational ability.

The importance of secondary structure is also evident from the fact that single-point mutations in the different bulges (mut50 and Δ103) and small changes in the single-stranded region of the apical stem-loop (mut82) do not seem to affect translation ability. In this respect, it should be noted that the isolation of single-point mutations which do not appreciably affect HCV IRES activity has also been confirmed by the isolation of an HCV IRES quasispecies which contained four mutations in the bulge regions of domain II but whose translation efficiency was 80% that of the wild-type (Laporte et al., 2000). Moreover, deletions in the IIc bulge have shown a peculiar result: the double mutant domIIΔc retains a significant IRES activity (22%) whilst deletion of the right hand part of this bulge (Δ93-96) abolishes translation efficiency. This is a situation that is quite unlike what has been observed for other parts of the HCV IRES such as stem-loops IIId and IIIe (Jubin et al., 2000; Psaridi et al., 1999). A possible explanation for these observations may reside in the fact that the role played by domain II in HCV translation is, as suggested by Spahn et al, (2001) predominantly structural. Indeed, we have performed UV cross-linking analyses on these mutants using different protein extracts (S100, nuclear extracts, ribosomal salt wash, purified 40S subunit) to eventually identify cellular factors that bind domain II but to this date have not found any, a result that although not formal proof adds up to the existing evidence.

Interestingly, a recent genetic analysis (Zhao and Wimmer, 2001) of a poliovirus/HCV virus chimera has proposed that the lower region of domain II may fold in an alternative conformation to the current model (Honda et al., 1999b). The most notable difference between these two models resides in the nt.108-110 region, which in the model by Zhao et al, (2001) is in a stem position whilst in the model by Honda et al (1999a) is present in a single-stranded bulge conformation. Even though both models

are supported by phylogenetic and RNA prediction analysis our limited Nuclease S1 studies support the presence of A109 in a single-stranded status (see Fig. 10) in keeping with the structure proposed by Honda et al, (1999a). One possibility that may explain this discrepancy is that in the poliovirus/HCV chimera the lower domain II region may fold differently as opposed to our IRES constructs However, it is also tempting to speculate that both structures represent alternative foldings of domain II which may occur during the viral life-cycle. In fact, changes in tertiary conformation may have important consequences for the recruitment of trans-acting factors to IRES domains, as recently reviewed (Martinez-Salas et al., 2001).

In conclusion, the emerging picture of the HCV IRES architecture is that of a highly organized 3D structure where the binding of proteins required for translation initiation needs not only an intact domain structure but also correct spatial configuration of the domains, a clear indication of the high degree of specialization evolved by the HCV IRES to bind essential cellular factors and the 40S ribosomal subunit.

In addition, our findings support the recent model of HCV IRES/40S ribosomal subunit interaction (Spahn et al., 2001) and the structural role played therein by domain II and identify the IIa bulge region as the most efficient target for antisense inhibition of HCV translation, a promising approach in the search of HCV specific inhibitors (Di Bisceglie, 1999; Jubin et al., 2000).

REFERENCES

**Ali, N., Pruijn, G. J., Kenan, D. J., Keene, J. D., and Siddiqui, A.** (2000). Human La antigen is required for the hepatitis C virus internal ribosome entry site-mediated translation, J Biol Chem *275*, 27531-40.

**Ali, N., and Siddiqui, A.** (1997). The La antigen binds 5' noncoding region of the hepatitis C virus RNA in the context of the initiator AUG codon and stimulates internal ribosome entry site-mediated translation, Proc Natl Acad Sci U S A *94*, 2249-54.

**Ali, N., Wang, C., and Siddiqui, A.** (1995). Translation of hepatitis C virus genome, Princess Takamatsu Symp *25*, 99-110.

**Alter, H. J.** (1992). New kit on the block: evaluation of second-generation assays for detection of antibody to the hepatitis C virus, Hepatology *15*, 350-3.

**Anwar, A., Ali, N., Tanveer, R., and Siddiqui, A.** (2000). Demonstration of functional requirement of polypyrimidine tract-binding protein by SELEX RNA during hepatitis C virus internal ribosome entry site-mediated translation initiation, J Biol Chem *275*, 34231-5.

**Bartenschlager R. and Lohmann V.** (2000). Replication of hepatitis C virus, Journal of General Virology *81*, 1631-1648.

**Belsham, G. J., and Sonenberg, N.** (1996). RNA-protein interactions in regulation of picornavirus RNA translation, Microbiol Rev *60*, 499-511.

**Blyn, L. B., Towner, J. S., Semler, B. L., and Ehrenfeld, E.** (1997). Requirement of poly(rC) binding protein 2 for translation of poliovirus RNA, J Virol *71*, 6243-6.

**Botarelli, P., Brunetto, M. R., Minutello, M. A., Calvo, P., Unutmaz, D., Weiner, A. J., Choo, Q. L., Shuster, J. R., Kuo, G., Bonino, F., and et al.** (1993). T-lymphocyte response to hepatitis C virus in different clinical courses of infection, Gastroenterology *104*, 580-7.

**Brinton, M. A., and Dispoto, J. H.** (1988). Sequence and secondary structure analysis of the 5'-terminal region of flavivirus genome RNA, Virology *162*, 290-9.

**Brown, E. A., Zhang, H., Ping, L. H., and Lemon, S. M.** (1992). Secondary structure of the 5' nontranslated regions of hepatitis C virus and pestivirus genomic RNAs, Nucleic Acids Res *20*, 5041-5.

**Buratti, E., Baralle, F. E., and Tisminetzky, S. G.** (1998a). Localization of the different hepatitis C virus core gene products expressed in COS-1 cells, Cell Mol Biol (Noisy-le-grand) *44*, 505-12.

**Buratti, E., Gerotto, M., Pontisso, P., Alberti, A., Tisminetzky, S. G., and Baralle, F. E.** (1997). In vivo translational efficiency of different hepatitis C virus 5'-UTRs, FEBS Lett *411*, 275-80.

**Buratti, E., Tisminetzky, S., Zotti, M., and Baralle, F. E.** (1998b). Functional analysis of the interaction between HCV 5'UTR and putative subunits of eukaryotic translation initiation factor eIF3, Nucleic Acids Res *26*, 3179-87.

**Butcher, S. E., Dieckmann, T., and Feigon, J.** (1997). Solution structure of a GAAA tetraloop receptor RNA, Embo J *16*, 7490-9.

**Chamberlain, R. W., Adams, N. J., Taylor, L. A., Simmonds, P., and Elliott, R. M.** (1997). The complete coding sequence of hepatitis C virus genotype 5a, the predominant genotype in South Africa, Biochem Biophys Res Commun *236*, 44-9.

**Chambers, T. J., Weir, R. C., Grakoui, A., McCourt, D. W., Bazan, J. F., Fletterick, R. J., and Rice, C. M.** (1990). Evidence that the N-terminal domain of nonstructural protein NS3 from yellow fever virus is a serine protease responsible for site-specific cleavages in the viral polyprotein, Proc Natl Acad Sci U S A *87*, 8898-902.

**Chien, D. Y., Choo, Q. L., Ralston, R., Spaete, R., Tong, M., Houghton, M., and Kuo, G.** (1993). Persistence of HCV despite antibodies to both putative envelope glycoproteins, Lancet *342*, 933.

**Choo, Q. L., Kuo, G., Weiner, A. J., Overby, L. R., Bradley, D. W., and Houghton, M.** (1989). Isolation of a cDNA clone derived from a blood-borne non-A, non-B viral hepatitis genome, Science *244*, 359-62.

**Choo, Q. L., Richman, K. H., Han, J. H., Berger, K., Lee, C., Dong, C., Gallegos, C., Coit, D., Medina-Selby, R., Barr, P. J., and et al.** (1991). Genetic organization and diversity of the hepatitis C virus, Proc Natl Acad Sci U S A *88*, 2451-5.

**Collier, A. J., Tang, S., and Elliott, R. M.** (1998). Translation efficiencies of the 5' untranslated region from representatives of the six major genotypes of hepatitis C virus using a novel bicistronic reporter assay system, J Gen Virol *79*, 2359-66.

**Conte, M. R., Grune, T., Ghuman, J., Kelly, G., Ladas, A., Matthews, S., and Curry, S.** (2000). Structure of tandem RNA recognition motifs from polypyrimidine tract binding protein reveals novel features of the RRM fold, Embo J *19*, 3132-41.

**Craig, A. W., Svitkin, Y. V., Lee, H. S., Belsham, G. J., and Sonenberg, N.** (1997). The La autoantigen contains a dimerization domain that is essential for enhancing translation, Mol Cell Biol *17*, 163-9.

**Di Bisceglie, A. M.** (1999). Hepatitis C--virology and future antiviral targets, Am J Med *107*, 45S-48S.

**Dildine, S. L., and Semler, B. L.** (1992). Conservation of RNA-protein interactions among picornaviruses, J Virol *66*, 4364-76.

**Dubuisson, J., Hsu, H. H., Cheung, R. C., Greenberg, H. B., Russell, D. G., and Rice, C. M.** (1994). Formation and intracellular localization of hepatitis C virus envelope glycoprotein complexes expressed by recombinant vaccinia and Sindbis viruses, J Virol *68*, 6147-60.

**Enomoto, N., Sakuma, I., Asahina, Y., Kurosaki, M., Murakami, T., Yamamoto, C., Izumi, N., Marumo, F., and Sato, C.** (1995). Comparison of full-length sequences of interferon-sensitive and resistant hepatitis C virus 1b. Sensitivity to interferon is conferred by amino acid substitutions in the NS5A region, J Clin Invest *96*, 224-30.

**Enomoto, N., Sakuma, I., Asahina, Y., Kurosaki, M., Murakami, T., Yamamoto, C., Ogura, Y., Izumi, N., Marumo, F., and Sato, C.** (1996). Mutations in the nonstructural protein 5A gene and response to interferon in patients with chronic hepatitis C virus 1b infection, N Engl J Med *334*, 77-81.

**Failla, C., Tomei, L., and De Francesco, R.** (1994). Both NS3 and NS4A are required for proteolytic processing of hepatitis C virus nonstructural proteins, J Virol *68*, 3753-60.

**Fong, T. L., Shindo, M., Feinstone, S. M., Hoofnagle, J. H., and Di Bisceglie, A. M.** (1991). Detection of replicative intermediates of hepatitis C viral RNA in liver and serum of patients with chronic hepatitis C, J Clin Invest *88*, 1058-60.

**Frangeul, L., Cresta, P., Perrin, M., Duverlie, G., Khorsi, H., Musset, L., Opolon, P., Huraux, J. M., and Lunel, F.** (1998). Pattern of HCV antibodies with special reference to NS5A reactivity in HCV-infected patients: relation to viral genotype, cryoglobulinemia and response to interferon, J Hepatol *28*, 538-43.

**Fukushi, S., Katayama, K., Kurihara, C., Ishiyama, N., Hoshino, F. B., Ando, T., and Oya, A.** (1994). Complete 5' noncoding region is necessary for the efficient internal initiation of hepatitis C virus RNA, Biochem Biophys Res Commun *199*, 425-32.

**Fukushi, S., Kurihara, C., Ishiyama, N., Hoshino, F. B., Oya, A., and Katayama, K.** (1997). The sequence element of the internal ribosome entry site and a 25- kilodalton cellular protein contribute to efficient internal initiation of translation of hepatitis C virus RNA, J Virol *71*, 1662-6.

**Goodier, J. L., Fan, H., and Maraia, R. J.** (1997). A carboxy-terminal basic region controls RNA polymerase III transcription factor activity of human La protein, Mol Cell Biol *17*, 5823-32.

**Gosert, R., Chang, K. H., Rijnbrand, R., Yi, M., Sangar, D. V., and Lemon, S. M.** (2000). Transient expression of cellular polypyrimidine-tract binding protein stimulates cap-independent translation directed by both picornaviral and flaviviral internal ribosome entry sites In vivo, Mol Cell Biol *20*, 1583-95.

**Grakoui, A., McCourt, D. W., Wychowski, C., Feinstone, S. M., and Rice, C. M.** (1993a). A second hepatitis C virus-encoded proteinase, Proc Natl Acad Sci U S A *90*, 10583-7.

**Grakoui, A., Wychowski, C., Lin, C., Feinstone, S. M., and Rice, C. M.** (1993b). Expression and identification of hepatitis C virus polyprotein cleavage products, J Virol *67*, 1385-95.

**Hahm, B., Kim, Y. K., Kim, J. H., Kim, T. Y., and Jang, S. K.** (1998). Heterogeneous nuclear ribonucleoprotein L interacts with the 3' border of the internal ribosomal entry site of hepatitis C virus, J Virol *72*, 8782-8.

**Han, J. H., Shyamala, V., Richman, K. H., Brauer, M. J., Irvine, B., Urdea, M. S., Tekamp-Olson, P., Kuo, G., Choo, Q. L., and Houghton, M.** (1991). Characterization of the terminal regions of hepatitis C viral RNA: identification of conserved sequences in the 5' untranslated region and poly(A) tails at the 3' end, Proc Natl Acad Sci U S A *88*, 1711-5.

**Heinz, F. X.** (1992). Comparative molecular biology of flaviviruses and hepatitis C virus, Arch Virol Suppl *4*, 163-71.

**Hellen, C. U., and Pestova, T. V.** (1999). Translation of hepatitis C virus RNA, J Viral Hepat *6*, 79-87.

**Hellen, C. U., Witherell, G. W., Schmid, M., Shin, S. H., Pestova, T. V., Gil, A., and Wimmer, E.** (1993). A cytoplasmic 57-kDa protein that is required for translation of picornavirus RNA by internal ribosomal entry is identical to the nuclear pyrimidine tract-binding protein, Proc Natl Acad Sci U S A *90*, 7642-6.

**Hershey, J. W., Asano, K., Naranda, T., Vornlocher, H. P., Hanachi, P., and Merrick, W. C.** (1996). Conservation and diversity in the structure of translation initiation factor EIF3 from humans and yeast, Biochimie *78*, 903-7.

**Heus, H. A., and Pardi, A.** (1991). Structural features that give rise to the unusual stability of RNA hairpins containing GNRA loops, Science *253*, 191-4.

**Hijikata, M., Kato, N., Ootsuyama, Y., Nakagawa, M., and Shimotohno, K.** (1991). Gene mapping of the putative structural region of the hepatitis C virus genome by in vitro processing analysis, Proc Natl Acad Sci U S A *88*, 5547-51.

**Hijikata, M., Mizushima, H., Akagi, T., Mori, S., Kakiuchi, N., Kato, N., Tanaka, T., Kimura, K., and Shimotohno, K.** (1993). Two distinct proteinase activities required for the processing of a putative nonstructural precursor protein of hepatitis C virus, J Virol *67*, 4665-75.

**Honda, M., Beard, M. R., Ping, L. H., and Lemon, S. M.** (1999a). A phylogenetically conserved stem-loop structure at the 5' border of the internal ribosome entry site of hepatitis C virus is required for cap-independent viral translation, J Virol *73*, 1165-74.

**Honda, M., Brown, E. A., and Lemon, S. M.** (1996a). Stability of a stem-loop involving the initiator AUG controls the efficiency of internal initiation of translation on hepatitis C virus RNA, Rna *2*, 955-68.

**Honda, M., Ping, L. H., Rijnbrand, R. C., Amphlett, E., Clarke, B., Rowlands, D., and Lemon, S. M.** (1996b). Structural requirements for initiation of translation by internal ribosome entry within genome-length hepatitis C virus RNA, Virology *222*, 31-42.

**Honda, M., Rijnbrand, R., Abell, G., Kim, D., and Lemon, S. M.** (1999b). Natural variation in translational activities of the 5' nontranslated RNAs of hepatitis C virus genotypes 1a and 1b: evidence for a long- range RNA-RNA interaction outside of the internal ribosomal entry site, J Virol *73*, 4941-51.

**Ina, Y., Mizokami, M., Ohba, K., and Gojobori, T.** (1994). Reduction of synonymous substitutions in the core protein gene of hepatitis C virus, J Mol Evol *38*, 50-6.

**Ito, T., and Lai, M. M.** (1997). Determination of the secondary structure of and cellular protein binding to the 3'-untranslated region of the hepatitis C virus RNA genome, J Virol *71*, 8698-706.

**Ito, T., Tahara, S. M., and Lai, M. M.** (1998). The 3'-untranslated region of hepatitis C virus RNA enhances translation from an internal ribosomal entry site, J Virol *72*, 8789-96.

**Ito, T., and Lai, M. M.** (1999). An internal polypyrimidine-tract-binding protein-binding site in the hepatitis C virus RNA attenuates translation, which is relieved by the 3'-untranslated sequence, Virology *254*, 288-96.

**Jackson, R. J., Howell, M. T., and Kaminski, A.** (1990). The novel mechanism of initiation of picornavirus RNA translation, Trends Biochem Sci *15*, 477-83.

**Jackson, R. J., and Kaminski, A.** (1995). Internal initiation of translation in eukaryotes: the picornavirus paradigm and beyond, Rna *1*, 985-1000.

**Jang, S. K., Krausslich, H. G., Nicklin, M. J., Duke, G. M., Palmenberg, A. C., and Wimmer, E.** (1988). A segment of the 5' nontranslated region of encephalomyocarditis virus RNA directs internal entry of ribosomes during in vitro translation, J Virol *62*, 2636-43.

**Jubin, R., Vantuno, N. E., Kieft, J. S., Murray, M. G., Doudna, J. A., Lau, J. Y., and Baroudy, B. M.** (2000). Hepatitis C virus internal ribosome entry site (IRES) stem loop IIId contains a phylogenetically conserved GGG triplet essential for translation and IRES folding [In Process Citation], J Virol *74*, 10430-7.

**Kaminski, A., Hunt, S. L., Patton, J. G., and Jackson, R. J.** (1995). Direct evidence that polypyrimidine tract binding protein (PTB) is essential for internal initiation of translation of encephalomyocarditis virus RNA, Rna *1*, 924-38.

**Kamoshita, N., Tsukiyama-Kohara, K., Kohara, M., and Nomoto, A.** (1997). Genetic analysis of internal ribosomal entry site on hepatitis C virus RNA: implication for involvement of the highly ordered structure and cell type-specific transacting factors, Virology *233*, 9-18.

**Kato, N., Hijikata, M., Ootsuyama, Y., Nakagawa, M., Ohkoshi, S., Sugimura, T., and Shimotohno, K.** (1990). Molecular cloning of the human hepatitis C virus genome from Japanese patients with non-A, non-B hepatitis, Proc Natl Acad Sci U S A *87*, 9524-8.

**Kato, N., Ootsuyama, Y., Ohkoshi, S., Nakazawa, T., Sekiya, H., Hijikata, M., and Shimotohno, K.** (1992). Characterization of hypervariable regions in the putative envelope protein of hepatitis C virus, Biochem Biophys Res Commun *189*, 119-27.

**Kato, N., Sekiya, H., Ootsuyama, Y., Nakazawa, T., Hijikata, M., Ohkoshi, S., and Shimotohno, K.** (1993). Humoral immune response to hypervariable region 1 of the putative envelope glycoprotein (gp70) of hepatitis C virus, J Virol *67*, 3923-30.

**Kenan, D. J., Query, C. C., and Keene, J. D.** (1991). RNA recognition: towards identifying determinants of specificity, Trends Biochem Sci *16*, 214-20.

**Kieft, J. S., Zhou, K., Jubin, R., Murray, M. G., Lau, J. Y., and Doudna, J. A.** (1999). The hepatitis C virus internal ribosome entry site adopts an ion- dependent tertiary fold, J Mol Biol *292*, 513-29.

**Kohara, M., Tanaka, T., Tsukiyama-Kohara, K., Tanaka, S., Mizokami, M., Lau, J. Y., and Hattori, N.** (1995). Hepatitis C virus genotypes 1 and 2 respond to interferon-alpha with different virologic kinetics, J Infect Dis *172*, 934-8.

**Kolupaeva, V. G., Pestova, T. V., and Hellen, C. U.** (2000). An enzymatic footprinting analysis of the interaction of 40S ribosomal subunits with the internal ribosomal entry site of hepatitis C virus, J Virol *74*, 6242-50.

**Kolupaeva, V. G., Pestova, T. V., Hellen, C. U., and Shatsky, I. N.** (1998). Translation eukaryotic initiation factor 4G recognizes a specific structural element within the internal ribosome entry site of encephalomyocarditis virus RNA, J Biol Chem *273*, 18599-604.

**Kolykhalov, A. A., Feinstone, S. M., and Rice, C. M.** (1996). Identification of a highly conserved sequence element at the 3' terminus of hepatitis C virus genome RNA, J Virol *70*, 3363-71.

**Komoda, Y., Hijikata, M., Sato, S., Asabe, S., Kimura, K., and Shimotohno, K.** (1994). Substrate requirements of hepatitis C virus serine proteinase for intermolecular polypeptide cleavage in Escherichia coli, J Virol *68*, 7351-7.

**Kozak, M.** (1989). The scanning model for translation: an update, J Cell Biol *108*, 229-41.

**Kozak, M.** (1992). Regulation of translation in eukaryotic systems, Annu Rev Cell Biol *8*, 197-225.

**Lanford, R. E., Notvall, L., Chavez, D., White, R., Frenzel, G., Simonsen, C., and Kim, J.** (1993). Analysis of hepatitis C virus capsid, E1, and E2/NS1 proteins expressed in insect cells, Virology *197*, 225-35.

**Laporte, J., Malet, I., Andrieu, T., Thibault, V., Toulme, J. J., Wychowski, C., Pawlotsky, J. M., Huraux, J. M., Agut, H., and Cahour, A.** (2000). Comparative analysis of translation efficiencies of hepatitis C virus 5' untranslated regions among intraindividual quasispecies present in chronic infection: opposite behaviors depending on cell type [In Process Citation], J Virol *74*, 10827-33.

**Le, S. Y., and Maizel, J. V., Jr.** (1998). Evolution of a common structural core in the internal ribosome entry sites of picornavirus, Virus Genes *16*, 25-38.

**Le, S. Y., Siddiqui, A., and Maizel, J. V., Jr.** (1996). A common structural core in the internal ribosome entry sites of picornavirus, hepatitis C virus, and pestivirus, Virus Genes *12*, 135-47.

**Leffers, H., Dejgaard, K., and Celis, J. E.** (1995). Characterisation of two major cellular poly(rC)-binding human proteins, each containing three K-homologous (KH) domains, Eur J Biochem *230*, 447-53.

**Lin, C., Lindenbach, B. D., Pragai, B. M., McCourt, D. W., and Rice, C. M.** (1994). Processing in the hepatitis C virus E2-NS2 region: identification of p7 and two distinct E2-specific products with different C termini, J Virol *68*, 5063-73.

**Lu, H. H., and Wimmer, E.** (1996). Poliovirus chimeras replicating under the translational control of genetic elements of hepatitis C virus reveal unusual properties of the internal ribosomal entry site of hepatitis C virus, Proc Natl Acad Sci U S A *93*, 1412-7.

**Lutsch, G., Bielka, H., Enzmann, G., and Noll, F.** (1983). Electron microscopic investigations on the location of rat liver ribosomal proteins S3a, S5, S6, S7 and S9 by means of antibody labeling, Biomed Biochim Acta *42*, 705-23.

**Maitra, U., Stringer, E. A., and Chaudhuri, A.** (1982). Initiation factors in protein biosynthesis, Annu Rev Biochem *51*, 869-900.

**Martinez-Salas, E., Ramos, R., Lafuente, E., and Lopez De Quinto, S.** (2001). Functional interactions in internal translation initiation directed by viral and cellular IRES elements, J Gen Virol *82*, 973-84.

**Meerovitch, K., Svitkin, Y. V., Lee, H. S., Lejbkowicz, F., Kenan, D. J., Chan, E. K., Agol, V. I., Keene, J. D., and Sonenberg, N.** (1993). La autoantigen enhances and corrects aberrant translation of poliovirus RNA in reticulocyte lysate, J Virol *67*, 3798-807.

**Merrick, W. C.** (1992). Mechanism and regulation of eukaryotic protein synthesis, Microbiol Rev *56*, 291-315.

**Miyamura, T., and Matsuura, Y.** (1993). Structural proteins of hepatitis C virus, Trends Microbiol *1*, 229-31.

**Mizushima, H., Hijikata, M., Asabe, S., Hirota, M., Kimura, K., and Shimotohno, K.** (1994). Two hepatitis C virus glycoprotein E2 products with different C termini, J Virol *68*, 6215-22.

**Odreman-Macchioli, F. E., Tisminetzky, S. G., Zotti, M., Baralle, F. E., and Buratti, E.** (2000). Influence of correct secondary and tertiary RNA folding on the binding of cellular factors to the HCV IRES, Nucleic Acids Res *28*, 875-85.

**Okamoto, H., Okada, S., Sugiyama, Y., Kurai, K., Iizuka, H., Machida, A., Miyakawa, Y., and Mayumi, M.** (1991). Nucleotide sequence of the genomic RNA of hepatitis C virus isolated from a human carrier: comparison with reported isolates for conserved and divergent regions, J Gen Virol *72*, 2697-704.

**Pause, A., Methot, N., Svitkin, Y., Merrick, W. C., and Sonenberg, N.** (1994). Dominant negative mutants of mammalian translation initiation factor eIF-4A define a critical role for eIF-4F in cap-dependent and cap- independent initiation of translation, Embo J *13*, 1205-15.

**Pelletier, J., and Sonenberg, N.** (1988). Internal initiation of translation of eukaryotic mRNA directed by a sequence derived from poliovirus RNA, Nature *334*, 320-5.

**Perez, I., McAfee, J. G., and Patton, J. G.** (1997). Multiple RRMs contribute to RNA binding specificity and affinity for polypyrimidine tract binding protein, Biochemistry *36*, 11881-90.

**Pestova, T. V., Borukhov, S. I., and Hellen, C. U.** (1998a). Eukaryotic ribosomes require initiation factors 1 and 1A to locate initiation codons [see comments], Nature *394*, 854-9.

**Pestova, T. V., Hellen, C. U., and Shatsky, I. N.** (1996). Canonical eukaryotic initiation factors determine initiation of translation by internal ribosomal entry, Mol Cell Biol *16*, 6859-69.

**Pestova, T. V., Shatsky, I. N., Fletcher, S. P., Jackson, R. J., and Hellen, C. U.** (1998b). A prokaryotic-like mode of cytoplasmic eukaryotic ribosome binding to the initiation codon during internal translation initiation of hepatitis C and classical swine fever virus RNAs, Genes Dev *12*, 67-83.

**Pinol-Roma, S., Swanson, M. S., Gall, J. G., and Dreyfuss, G.** (1989). A novel heterogeneous nuclear RNP protein with a unique distribution on nascent transcripts, J Cell Biol *109*, 2575-87.

**Poole, T. L., Wang, C., Popp, R. A., Potgieter, L. N., Siddiqui, A., and Collett, M. S.** (1995). Pestivirus translation initiation occurs by internal ribosome entry, Virology *206*, 750-4.

**Psaridi, L., Georgopoulou, U., Varaklioti, A., and Mavromara, P.** (1999). Mutational analysis of a conserved tetraloop in the 5' untranslated region of hepatitis C virus identifies a novel RNA element essential for the internal ribosome entry site function, FEBS Lett *453*, 49-53.

**Reed, K. E., Grakoui, A., and Rice, C. M.** (1995). Hepatitis C virus-encoded NS2-3 protease: cleavage-site mutagenesis and requirements for bimolecular cleavage, J Virol *69*, 4127-36.

**Reynolds, J. E., Kaminski, A., Carroll, A. R., Clarke, B. E., Rowlands, D. J., and Jackson, R. J.** (1996). Internal initiation of translation of hepatitis C virus RNA: the ribosome entry site is at the authentic initiation codon, Rna *2*, 867-78.

**Reynolds, J. E., Kaminski, A., Kettinen, H. J., Grace, K., Clarke, B. E., Carroll, A. R., Rowlands, D. J., and Jackson, R. J.** (1995). Unique features of internal initiation of hepatitis C virus RNA translation, Embo J *14*, 6010-20.

**Rijnbrand, R., Bredenbeek, P., van der Straaten, T., Whetter, L., Inchauspe, G., Lemon, S., and Spaan, W.** (1995). Almost the entire 5' non-translated region of hepatitis C virus is required for cap-independent translation, FEBS Lett *365*, 115-9.

**Rijnbrand, R. C., Abbink, T. E., Haasnoot, P. C., Spaan, W. J., and Bredenbeek, P. J.** (1996). The influence of AUG codons in the hepatitis C virus 5' nontranslated region on translation and mapping of the translation initiation window, Virology *226*, 47-56.

**Saito, I., Miyamura, T., Ohbayashi, A., Harada, H., Katayama, T., Kikuchi, S., Watanabe, Y., Koi, S., Onji, M., Ohta, Y., and et al.** (1990). Hepatitis C virus infection is associated with the development of hepatocellular carcinoma, Proc Natl Acad Sci U S A *87*, 6547-9.

**Santolini, E., Migliaccio, G., and La Monica, N.** (1994). Biosynthesis and biochemical properties of the hepatitis C virus core protein, J Virol *68*, 3631-41.

**Seeff, L. B., Miller, R. N., Rabkin, C. S., Buskell-Bales, Z., Straley-Eason, K. D., Smoak, B. L., Johnson, L. D., Lee, S. R., and Kaplan, E. L.** (2000). 45-year follow-up of hepatitis C virus infection in healthy young adults, Ann Intern Med *132*, 105-11.

**Selby, M. J., Glazer, E., Masiarz, F., and Houghton, M.** (1994). Complex processing and protein:protein interactions in the E2:NS2 region of HCV, Virology *204*, 114-22.

**Shine, J., and Dalgarno, L.** (1974). The 3'-terminal sequence of Escherichia coli 16S ribosomal RNA: complementarity to nonsense triplets and ribosome binding sites, Proc Natl Acad Sci U S A *71*, 1342-6.

**Sickinger, S., and Schweizer, M.** (1999). A high affinity binding site for the polypyrimidine tract binding protein (PTB) is located in the 5'-untranslated region of the rat proteinase alpha1-inhibitor 3 variant I gene, Biol Chem *380*, 1217-23.

**Simmonds, P.** (1995). Variability of hepatitis C virus, Hepatology *21*, 570-83.

**Simmonds, P.** (2001). The origin and evolution of hepatitis viruses in humans, J Gen Virol *82*, 693-712.

**Simmonds, P., Alberti, A., Alter, H. J., Bonino, F., Bradley, D. W., Brechot, C., Brouwer, J. T., Chan, S. W., Chayama, K., Chen, D. S., and et al.** (1994). A proposed system for the nomenclature of hepatitis C viral genotypes, Hepatology *19*, 1321-4.

**Singh, R., Valcarcel, J., and Green, M. R.** (1995). Distinct binding specificities and functions of higher eukaryotic polypyrimidine tract-binding proteins, Science *268*, 1173-6.

**Siomi, H., Matunis, M. J., Michael, W. M., and Dreyfuss, G.** (1993). The pre-mRNA binding K protein contains a novel evolutionarily conserved motif, Nucleic Acids Res *21*, 1193-8.

**Sizova, D. V., Kolupaeva, V. G., Pestova, T. V., Shatsky, I. N., and Hellen, C. U.** (1998). Specific interaction of eukaryotic translation initiation factor 3 with the 5' nontranslated regions of hepatitis C virus and classical swine fever virus RNAs, J Virol *72*, 4775-82.

**Smith, D. B., Mellor, J., Jarvis, L. M., Davidson, F., Kolberg, J., Urdea, M., Yap, P. L., and Simmonds, P.** (1995). Variation of the hepatitis C virus 5' non-coding region: implications for secondary structure, virus detection and typing. The International HCV Collaborative Study Group, J Gen Virol *76*, 1749-61.

**Spaete, R. R., Alexander, D., Rugroden, M. E., Choo, Q. L., Berger, K., Crawford, K., Kuo, C., Leng, S., Lee, C., Ralston, R., and et al.** (1992). Characterization of the hepatitis C virus E2/NS1 gene product expressed in mammalian cells, Virology *188*, 819-30.

**Spahn, C. M., Kieft, J. S., Grassucci, R. A., Penczek, P. A., Zhou, K., Doudna, J. A., and Frank, J.** (2001). Hepatitis C virus IRES RNA-induced changes in the conformation of the 40s ribosomal subunit, Science *291*, 1959-62.

**Spangberg, K., and Schwartz, S.** (1999). Poly(C)-binding protein interacts with the hepatitis C virus 5' untranslated region, J Gen Virol *80*, 1371-6.

**Spangberg, K., Wiklund, L., and Schwartz, S.** (2001). Binding of the La autoantigen to the hepatitis C virus 3' untranslated region protects the RNA from rapid degradation in vitro, J Gen Virol *82*, 113-20.

**Svitkin, Y. V., Pause, A., and Sonenberg, N.** (1994). La autoantigen alleviates translational repression by the 5' leader sequence of the human immunodeficiency virus type 1 mRNA, J Virol *68*, 7001-7.

**Tan, E. M.** (1989). Antinuclear antibodies: diagnostic markers for autoimmune diseases and probes for cell biology, Adv Immunol *44*, 93-151.

**Tanaka, T., Kato, N., Cho, M. J., and Shimotohno, K.** (1995). A novel sequence found at the 3' terminus of hepatitis C virus genome, Biochem Biophys Res Commun *215*, 744-9.

**Tanaka, T., Kato, N., Cho, M. J., Sugiyama, K., and Shimotohno, K.** (1996). Structure of the 3' terminus of the hepatitis C virus genome, J Virol *70*, 3307-12.

**Tang, S., Collier, A. J., and Elliott, R. M.** (1999). Alterations to both the primary and predicted secondary structure of stem-loop IIIc of the hepatitis C virus 1b 5' untranslated region (5'UTR) lead to mutants severely defective in translation which cannot be complemented in trans by the wild-type 5'UTR sequence, J Virol *73*, 2359-64.

**Taniguchi, S., Okamoto, H., Sakamoto, M., Kojima, M., Tsuda, F., Tanaka, T., Munekata, E., Muchmore, E. E., Peterson, D. A., and Mishiro, S.** (1993). A structurally flexible and antigenically variable N-terminal domain of the hepatitis C virus E2/NS1 protein: implication for an escape from antibody, Virology *195*, 297-301.

**Tanji, Y., Hijikata, M., Hirowatari, Y., and Shimotohno, K.** (1994). Hepatitis C virus polyprotein processing: kinetics and mutagenic analysis of serine proteinase-dependent cleavage, J Virol *68*, 8418-22.

**Tomei, L., Failla, C., Santolini, E., De Francesco, R., and La Monica, N.** (1993). NS3 is a serine protease required for processing of hepatitis C virus polyprotein, J Virol *67*, 4017-26.

**Tsukiyama-Kohara, K., Iizuka, N., Kohara, M., and Nomoto, A.** (1992). Internal ribosome entry site within hepatitis C virus RNA, J Virol *66*, 1476-83.

**Varani, G.** (1995). Exceptionally stable nucleic acid hairpins, Annu Rev Biophys Biomol Struct *24*, 379-404.

**Wang, C., Le, S. Y., Ali, N., and Siddiqui, A.** (1995). An RNA pseudoknot is an essential structural element of the internal ribosome entry site located within the hepatitis C virus 5' noncoding region, Rna *1*, 526-37.

**Wang, C., Sarnow, P., and Siddiqui, A.** (1993). Translation of human hepatitis C virus RNA in cultured cells is mediated by an internal ribosome-binding mechanism, J Virol *67*, 3338-44.

**Wang, C., Sarnow, P., and Siddiqui, A.** (1994). A conserved helical element is essential for internal initiation of translation of hepatitis C virus RNA, J Virol *68*, 7301-7.

**Weiner, A. J., Christopherson, C., Hall, J. E., Bonino, F., Saracco, G., Brunetto, M. R., Crawford, K., Marion, C. D., Crawford, K. A., Venkatakrishna, S., and et al.** (1991). Sequence variation in hepatitis C viral isolates, J Hepatol *13*, S6-14.

**Weiner, A. J., Geysen, H. M., Christopherson, C., Hall, J. E., Mason, T. J., Saracco, G., Bonino, F., Crawford, K., Marion, C. D., Crawford, K. A., and et al.** (1992). Evidence for immune selection of hepatitis C virus (HCV) putative envelope glycoprotein variants: potential role in chronic HCV infections, Proc Natl Acad Sci U S A *89*, 3468-72.

**Woese, C. R., Winker, S., and Gutell, R. R.** (1990). Architecture of ribosomal RNA: constraints on the sequence of "tetra- loops", Proc Natl Acad Sci U S A *87*, 8467-71.

**Xiao, Q., Sharp, T. V., Jeffrey, I. W., James, M. C., Pruijn, G. J., van Venrooij, W. J., and Clemens, M. J.** (1994). The La antigen inhibits the activation of the interferon-inducible protein kinase PKR by sequestering and unwinding double-stranded RNA, Nucleic Acids Res *22*, 2512-8.

**Yamada, N., Tanihara, K., Takada, A., Yorihuzi, T., Tsutsumi, M., Shimomura, H., Tsuji, T., and Date, T.** (1996). Genetic organization and diversity of the 3' noncoding region of the hepatitis C virus genome, Virology *223*, 255-61.

**Yoo, B. J., Spaete, R. R., Geballe, A. P., Selby, M., Houghton, M., and Han, J. H.** (1992). 5' end-dependent translation initiation of hepatitis C viral RNA and the presence of putative positive and negative translational control elements within the 5' untranslated region, Virology *191*, 889-99.

**Zein, N. N., and Persing, D. H.** (1996). Hepatitis C genotypes: current trends and future implications, Mayo Clin Proc *71*, 458-62.

**Zemel, R., Gerechet, S., Greif, H., Bachmatove, L., Birk, Y., Golan-Goldhirsh, A., Kunin, M., Berdichevsky, Y., Benhar, I., and Tur-Kaspa, R.** (2001). Cell transformation induced by hepatitis C virus NS3 serine protease, J Viral Hepat *8*, 96-102.

**Zhao, W. D., and Wimmer, E.** (2001). Genetic analysis of a poliovirus/hepatitis C virus chimera: new structure for domain II of the internal ribosomal entry site of hepatitis C virus, J Virol *75*, 3719-30.

**Zignego, A. L., Macchia, D., Monti, M., Thiers, V., Mazzetti, M., Foschi, M., Maggi, E., Romagnani, S., Gentilini, P., and Brechot, C.** (1992). Infection of peripheral mononuclear blood cells by hepatitis C virus, J Hepatol *15*, 382-6.